

**UNIVERSITY OF SOUTHAMPTON**

**FACULTY OF MEDICINE, HEALTH AND BIOLOGICAL SCIENCES**

**School of Medicine**

**Immunological Effects of Extracellular Calreticulin**

**Vivien Watson**

Thesis for the degree of Doctor of Philosophy

December 2005

UNIVERSITY OF SOUTHAMPTON  
ABSTRACT  
FACULTY OF MEDICINE, HEALTH AND BIOLOGICAL SCIENCES  
SCHOOL OF MEDICINE  
Doctor of Philosophy  
IMMUNOLOGICAL EFFECTS OF EXTRACELLULAR CALRETICULIN  
Vivien Watson

A number of stress proteins, including hsp70, hsp90, gp96 and calreticulin (CRT), have been shown to elicit protective immune responses against their tumour of origin. This effect appears to be due to their ability to act as chaperones, delivering bound peptides to antigen presenting cells (APCs) for cross-presentation on MHC class I, and also to direct activation of APCs by HSPs. Hsp70 and gp96 have been particularly well studied. In this study, I have investigated the antigen chaperoning and APC activating functions of the ER-resident chaperone CRT.

I have purified CRT from a murine mastocytoma cell line and removed contaminating endotoxin from this and my model antigen ovalbumin (OVA). Immunisation of mice with this CRT results in a degree of protection from challenge with the source tumour, P815. *In vivo* co-administration of CRT with OVA results in proliferation of adoptively transferred OVA-specific CD8<sup>+</sup>, but not CD4<sup>+</sup> T cells. *In vitro*, incubation of CRT with autologous, bone marrow-derived dendritic cells (DCs) does not induce expression of activation markers or production of pro-inflammatory cytokines. CRT also had no effect on phagocytosis of latex beads by a DC line. Investigations into the effect of CRT on the ability of OVA-pulsed DCs to prime naïve OVA-specific transgenic T cells *in vitro* indicated that it does not enhance their ability to prime MHC Class II-restricted OVA specific T cells. However, some IL-2 production by Class I-restricted OVA-specific T cells was observed.

I have also demonstrated that CRT binds specifically to receptors on DCs and macrophages and is subsequently internalised. Preliminary data indicate that CRT can be complexed to peptides *in vitro* and deliver these to DCs for processing and presentation to T cells.

# Table of Contents

<b>ABSTRACT.....</b>	<b>1</b>
<b>TABLE OF CONTENTS.....</b>	<b>2</b>
<b>LIST OF FIGURES AND TABLES.....</b>	<b>6</b>
<b>DECLARATION.....</b>	<b>9</b>
<b>ACKNOWLEDGEMENTS.....</b>	<b>10</b>
<b>ABBREVIATIONS.....</b>	<b>11</b>
<b>CHAPTER 1: INTRODUCTION.....</b>	<b>15</b>
1.1 THE IMMUNE RESPONSE.....	15
1.1.1 Components of the immune response.....	15
1.1.2 Dendritic cells at the centre of the immune response – a network of subsets.....	15
1.1.3 Antigen capture and processing by dendritic cells.....	19
1.1.4 MHC Class II loading.....	20
1.1.5 MHC Class I loading.....	21
1.1.6 Cross-presentation of exogenous antigens on MHC Class I...22	
1.1.7 Activation and maturation of dendritic cells.....	27
1.2 HEAT SHOCK PROTEINS.....	33
1.2.1 The heat shock response.....	33
1.2.2 HSPs – ubiquitous and abundant soluble intracellular proteins.....	34
1.2.3 Heat shock proteins in the immune response.....	35
1.2.4 Heat shock protein receptors.....	39
1.2.5 The endotoxin debate.....	46
1.2.6 Trafficking of heat shock proteins and chaperoned peptides within APCs.....	48
1.3 CALRETICULIN.....	50
1.3.1 The structure of CRT.....	50
1.3.2 Homeostatic functions of CRT.....	51
1.3.3 Extracellular functions of CRT.....	53
1.3.4 Cellular localisation of CRT.....	56
1.4 CALRETICULIN AS AN IMMUNOSTIMULATORY HSP.....	58

<b>CHAPTER 2: MATERIALS AND METHODS.....</b>	<b>60</b>
2.1 MICE.....	60
2.2 REAGENTS.....	60
2.3 TISSUE CULTURE AND CELL BIOLOGY.....	61
2.3.1 Cell lines and tissue culture.....	61
2.3.2 Purification and culture of bone marrow-derived dendritic cells.....	61
2.3.3 Isolation of splenic dendritic cells.....	62
2.3.4 T cell purification.....	62
2.4 DENDRITIC CELL ACTIVATION AND ANTIGEN PRESENTATION ASSAYS.....	63
2.4.1 DC assay setup.....	63
2.4.2 Flow cytometry and antibodies.....	63
2.4.3 Cytokine ELISAs.....	64
2.5 PURIFICATION OF CRT.....	65
2.5.1 Purification of CRT from P815.....	65
2.5.2 SDS-PAGE and Western Blot.....	66
2.5.3 Protein quantification.....	67
2.5.4 Endotoxin testing.....	67
2.5.5 Endotoxin removal from OVA and CRT.....	68
2.6 PHAGOCYTOSIS ASSAYS.....	69
2.6.1 Phagocytosis assay setup.....	69
2.6.2 FACS analysis of phagocytosis assays.....	69
2.6.3 Antigen presentation assays.....	70
2.7 ASSESSMENT OF CRT BINDING TO CELLS.....	71
2.7.1 Alexa-488 labelling of CRT.....	71
2.7.2 Assessment of CRT binding to APCs – FACS.....	71
2.7.3 Assessment of CRT binding and internalisation to BMDCs – confocal microscopy.....	71
2.8 COMPLEXING CRT TO SIINFEKL.....	72
2.9 <i>IN VIVO</i> PROLIFERATION OF CFSE-LABELLED T CELLS.....	72
2.10 <i>IN VIVO</i> TUMOUR PROTECTION.....	73

<b>CHAPTER 3: PREPARATION OF CALRETICULIN AND OVALBUMIN....</b>	<b>74</b>
3.1 INTRODUCTION.....	74
3.2 RESULTS.....	76
3.2.1 Purification of murine CRT from the mastocytoma cell line P815.....	76
3.2.2 Endotoxin contamination leads to significant experimental artefact.....	84
3.2.3 Removal of endotoxin contamination from ovalbumin and calreticulin.....	84
3.2.4 Is the calreticulin functional?.....	88
3.3 DISCUSSION.....	89
3.3.1 Experimental artefact due to endotoxin contamination.....	89
3.3.2 Structure and functionality of CRT.....	90
<b>CHAPTER 4: CALRETICULIN DOES NOT HAVE AN ADJUVANT EFFECT ON ANTIGEN PRESENTING CELLS.....</b>	<b>92</b>
4.1 INTRODUCTION.....	92
4.2 RESULTS.....	93
4.2.1 BMDCs upregulate cell surface markers in response to various activation stimuli, but not in response to calreticulin.....	93
4.2.2 Freshly isolated splenic DCs upregulate cell surface markers in response to LPS, but not in response to calreticulin.....	97
4.2.3 DCs produce IL-12 and IL-2 in response to LPS and CpG DNA, but not in response to calreticulin or hsp70.....	99
4.2.4 Stimulation with LPS, TNF $\alpha$ or CpG DNA enables OVA- pulsed DCs to prime naïve CD4 <sup>+</sup> transgenic T cells, whereas CRT and hsp70 do not.....	102
4.2.5 Calreticulin does not affect IL-2 production by transgenic CD4 <sup>+</sup> T cells in response to LPS- or TNF $\alpha$ -activated OVA- pulsed DCs.....	103
4.2.6 Effect of CRT on priming CD8 <sup>+</sup> T cells <i>in vitro</i> .....	104
4.2.7 Calreticulin does not enhance phagocytosis of latex beads by DC2.4 cells, whereas LPS does.....	107
4.2.8 CRT stimulates proliferation of CD8 <sup>+</sup> but not CD4 <sup>+</sup> T cells <i>in</i> <i>vivo</i> .....	111

4.3 DISCUSSION.....	113
4.3.1 Autologous CRT and hsp70 do not activate DCs.....	113
4.3.2 Relevance of tested concentrations of CRT and hsp70.....	115
4.3.3 An immunosuppressive role for CRT?.....	115
4.3.4 CRT and phagocytosis.....	117
4.3.5 Preferential activation of CD8 <sup>+</sup> T cells.....	117
4.3.6 Where does the activation signal come from?.....	118
<b>CHAPTER 5: RECEPTOR-MEDIATED BINDING OF CALRETICULIN TO ANTIGEN PRESENTING CELLS AND CHAPERONING FUNCTION.....</b>	<b>119</b>
5.1 INTRODUCTION.....	119
5.2 RESULTS.....	120
5.2.1 Labelling of CRT with Alexa-Fluor.....	120
5.2.2 CRT specifically binds to APCs.....	120
5.2.3 BMDCs internalise CRT <i>in vitro</i> .....	123
5.2.4 Chaperoning of peptides by CRT for presentation by APCs.....	127
5.3 DISCUSSION.....	129
5.3.1 CRT binding to APCs.....	129
5.3.2 CRT internalisation and trafficking.....	130
5.3.3 Chaperoning function of CRT.....	130
<b>CHAPTER 6: GENERAL DISCUSSION.....</b>	<b>132</b>
6.1 SUMMARY OF FINDINGS.....	132
6.2 DISCUSSION AND FUTURE WORK.....	134
6.2.1 Effects of CRT on different cell types.....	134
6.2.2 A separate danger signal <i>in vivo</i> ?.....	135
6.2.3 CRT as an immune suppressor?.....	135
6.2.4 Differential effects of autologous vs foreign HSPs.....	136
6.2.5 CRT and Ag delivery.....	137
<b>REFERENCES.....</b>	<b>139</b>

## List of Figures and Tables

Figure 1.1	The life cycle of dendritic cells – “The Langerhans cell paradigm”...16
Table 1.1	Murine DC subsets.....17
Figure 1.2	The MHC class I and class II processing pathways in DCs.....20
Figure 1.3	The peptide-loading complex.....22
Figure 1.4	The phagosome-to-cytosol pathway of cross-presentation of antigen.24
Figure 1.5	The vacuolar pathway of cross-presentation of antigen.....26
Figure 1.6	Toll-like receptors and their ligands.....28
Figure 1.7	TLR structure and signalling.....31
Table 1.2	The main families of heat shock proteins.....34
Figure 1.8	Innate and adaptive effects of interaction of HSPs with their receptors on APCs.....38
Table 1.3	Summary of data on HSP receptors.....39
Figure 1.9	HSP-APC interactions integrate innate and adaptive immune responses.....45
Figure 1.10	The structure of bacterial LPS.....46
Figure 1.11	Linear representation of CRT domains and model of 3D structure...50
Figure 3.1	Representative chromatogram from running 5ml filtered, dialysed P815 lysate on DEAE column controlled by AKTA Prime system...78
Figure 3.2	Coomassie blue staining and calregulin western blot of fractions from DEAE columns.....79
Figure 3.3	Representative chromatogram from running 10ml pooled, concentrated DEAE fractions on Resource Q column controlled by AKTA Prime system.....80
Figure 3.4	Coomassie blue staining and calregulin western blot of fractions from Resource Q column.....81
Figure 3.5	Representative chromatogram from running pooled, concentrated CRT-containing Resource Q fractions on HiLoad 26/60 Superdex 200 prep grade column controlled by AKTA Prime system.....82
Figure 3.6	Coomassie blue staining and calregulin western blot of fractions from gel filtration column.....83

Figure 3.7	Protein concentration and endotoxin contamination levels of fractions obtained by loading 1ml 100mg/ml OVA in PBS onto a 5ml Polymyxin B-agarose column.....	85
Table 3.1	Values used to prepare graphs in figure 3.7.....	85
Figure 3.8	Protein concentration and endotoxin contamination levels of fractions obtained by running CRT on 2ml Polymyxin B-agarose column.....	86
Table 3.2	Values used to prepare graphs in figure 3.8.....	86
Figure 3.9	Coomassie blue staining of pooled, concentrated fractions from Polymyxin B treatment of CRT.....	86
Figure 3.10	Low-endotoxin OVA does not activate DCs in the absence of external stimulation.....	87
Figure 3.11	DCs pulsed with low endotoxin OVA do not prime naïve OTII T cells in the absence of external stimulation.....	87
Figure 3.12	Protective effect of CRT.....	88
Figure 4.1	LPS and CpG DNA enhance DC expression of cell surface activation markers.....	94
Figure 4.2	LPS and TNF $\alpha$ enhance DC expression of cell surface activation markers, whereas CRT does not.....	94
Figure 4.3	LPS and CpG DNA enhance DC expression of cell surface activation markers, whereas CRT and hsp70 do not.....	95
Figure 4.4	CRT at concentrations up to 200 $\mu$ g/ml fails to induce any upregulation of DC surface activation markers.....	96
Figure 4.5	LPS induces upregulation of CD86 by splenic DCs, whereas CRT does not.....	97
Figure 4.6	Splenic DCs incubated with LPS increase their expression of surface markers more than those incubated with CRT.....	98
Figure 4.7	Effect of CRT on DC surface marker expression induced by LPS.....	99
Figure 4.8	LPS and CpG DNA induce production of IL-2 and IL-12, but not IL-10 or IFN $\gamma$ , from DCs in a concentration-dependent manner.....	100
Figure 4.9	Neither CRT nor hsp70 induce production of IL-2 or IL-12 by DCs.....	101
Figure 4.10	Concentrations of CRT up to 200 $\mu$ g/ml do not induce IL-2 or IL-12 production by DCs.....	101




Figure 4.11	LPS, TNF $\alpha$ and CpG DNA enable OVA-pulsed DCs to induce IL-2 production from naïve T cells, whereas CRT does not.....	102
Figure 4.12	CpG DNA, but not CRT or hsp70, enables OVA-pulsed DCs to induce IL-2 production from naïve CD4 <sup>+</sup> T cells.....	103
Figure 4.13	CRT has no effect on response of OTII T cells to LPS- or TNF $\alpha$ -activated, OVA-pulsed DCs.....	104
Figure 4.14	Effects of CRT and LPS on priming of naïve OVA-specific CD8 <sup>+</sup> T cells.....	105
Figure 4.15	Representative FACS histogram plot showing the peaks of LB uptake at 37°C with no LPS pre-exposure, 4 hours LPS pre-exposure and 48 hours LPS pre-exposure by cells that were not quenched by TB.....	108
Figure 4.16	Total LB uptake increases with pre-exposure to LPS, but not CRT..	108
Figure 4.17	Pre-exposure to LPS, but not CRT, leads to increase in the number of beads internalised per cell.....	109
Figure 4.18	Pre-exposure to LPS, but not CRT, leads to enhanced CD80 expression by DC2.4 cells.....	110
Figure 4.19	Change in antigen presentation by DC2.4 to B3Z T cells.....	110
Figure 4.20	Co-administration of CRT with OVA results in proliferation of CFSE-labelled CD8 <sup>+</sup> T cells.....	112
Table 4.1	Proliferation of OTI T cells <i>in vivo</i> .....	112
Figure 5.1	Alexa-CRT binding to APCs.....	121
Figure 5.2	Binding of Alexa-CRT to APCs.....	122
Figure 5.3	Binding of Alexa-CRT to APCs following pre-incubation with inhibitors.....	122
Figure 5.4	Alexa-CRT binds to BMDCs and is internalised.....	124
Figure 5.5	SIINFEKL complexed to CRT induces a stronger response from transgenic T cells than free SIINFEKL.....	128

## DECLARATION OF AUTHORSHIP

I declare that the thesis entitled 'Immunological effects of extracellular calreticulin' and the work presented in it are my own. I confirm that:

- this work was done wholly while in candidature for a research degree at this University;
- where I have consulted the published work of others, this is always clearly attributed;
- where I have quoted from the work of others, the source is always given. With the exception of such quotations, this thesis is entirely my own work;
- I have acknowledged all main sources of help;
- where the thesis is based on work done by myself jointly with others, I have made clear exactly what was done by others and what I have contributed myself;
- none of this work has been published before submission.

Signed: .....  .....

Date: ..... 7/3/06 .....

## Acknowledgements

I would like to thank my supervisor Professor Tim Elliott for his guidance and support throughout my project. Tim is a real inspiration, and meetings with him always result in lots of ideas for new and exciting experiments. When things are tough, Tim's enthusiasm is infectious, and soon things don't look as bad!

I would also particularly like to thank and acknowledge Tara Walford for all the hard work she has put in on the phagocytosis experiments described in section 4.2.7, she really went above and beyond the call of duty for a medical student in the lab and her endless enthusiasm and giggles really brightened up the lab. Thanks are also due to Dr. Catherine Bryant for her help and advice with the *in vivo* work, and to Dr. Alexandra Mant for her constant advice on the phagocytosis assays and microscopy, and to both for displaying the patience of saints when faced with the 500<sup>th</sup> question of the day. Thanks also to Dr Anton Page for technical assistance and training with confocal microscopy.

I owe a huge debt to everybody else in the Elliott lab, particularly Fay, Chris, Rachel, Denise and Nasia, for their constant support in all matters, lab-related and not. They have all helped to keep me (relatively) sane and made my time in Southampton really enjoyable. Thanks are due to everyone for putting up with me, particularly on the bad days, when I can be not the easiest person in the world to work with!

Last, but by no means least, I would like to thank my family, who have all been really supportive and encouraged me in all I have done, throughout my life and particularly in the last four years. Their faith in me has been a constant source of strength and inspiration. This thesis is dedicated to them all.

This work was funded by Cancer Research UK.

## Abbreviations

$\alpha 2M$	$\alpha 2$ -macroglobulin
AcLDL	acetylated low density lipoprotein
Ag	antigen
APC	antigen presenting cell
$\beta_2m$	$\beta_2$ microglobulin
BCA	bicinchoninic acid
BM	bone marrow
BMDC	bone marrow-derived dendritic cell
BSA	bovine serum albumin
CAM	chorioallantoic membrane
CD	cluster of differentiation
CFSE	Carboxy-fluorescein succinimidyl ester
CHO	chinese hamster ovary
CLIP	MHC class II-associated Ii peptides
CNX	calnexin
CPRG	chlorophenol red $\beta$ -galactosidase
CRT	calreticulin
CTL	cytotoxic T lymphocyte
CTLA	cytotoxic T lymphocyte-associated protein
DC	dendritic cell
DN	double negative
DNA	deoxyribonucleic acid
DRiP	defective ribosomal product
ds	double stranded
EDTA	ethylenediaminetetraacetic acid
ELISA	enzyme-linked immunosorbent assay
ER	endoplasmic reticulum
ERAD	ER-associated degradation
ERAP	ER-associated aminopeptidase
ERp57	ER protein 57
EtOH	ethanol
EU	endotoxin units

Fc	fragment crystallisable
FCS	foetal calf serum
FcR	Fc receptor
FITC	fluorescein isothiocyanate
GITR	glucocorticoid-induced TNF-receptor-related protein
GM-CSF	granulocyte macrophage-colony stimulating factor
gp96	glycoprotein 96
grp	glucose regulated protein
GST	glutathione S-transferase
HBSS	Hanks buffered saline solution
HEK	human embryonic kidney
HI	heat-inactivated
His	histidine
HIV	human immunodeficiency virus
HRP	horseradish peroxidase
HSPs	heat shock proteins
hsp70	heat shock protein 70
hsp90	heat shock protein 90
IFN	interferon
Ig	immunoglobulin
Ii	Invariant chain
I $\kappa$ B	inhibitor of NF- $\kappa$ B
IKK	inhibitor of NF- $\kappa$ B kinase
IL	interleukin
IL-1R	interleukin-1 receptor
iNOS	inducible nitric oxide synthase
IRAK	IL-1 receptor-associated kinase
IRF	IFN-regulatory factor
IU	international units
JIA	juvenile idiopathic arthritis
KDa/kD	kilodaltons
L	ligand
LAL	limulus amebocyte lysate
LAMP	lysosomal associated membrane protein

LB	latex bead
LDL	low density lipoprotein
LOX-1	lectin-like oxidised LDL receptor
LPS	lipopolysaccharides
LRP	LDL-receptor related protein
LRR	leucine-rich repeat
M	molar
MAPK	mitogen activated protein kinase
MBL	mannose binding lectin
mAb	monoclonal antibody
m $\Phi$	macrophage
MACS	magnetic cell separation
mBSA	maleylated bovine serum albumin
MCP	monocyte chemoattractant protein
MDP	muramyl dipeptide
MHC	major histocompatibility complex
MIIC	MHC Class II-rich compartment
MIP	macrophage inflammatory protein
Mtb	mycobacterial
MyD88	myeloid differentiation factor 88
NEAA	non-essential amino acids
NF- $\kappa$ B	nuclear factor $\kappa$ B
NK	natural killer
NKT cell	natural killer T cell
NO	nitric oxide
OST	oligosaccharyl transferase
OVA	ovalbumin
pDC	plasmacytoid dendritic cell
PAGE	polyacrylamide gel electrophoresis
PAMP	pathogen-associated molecular pattern
PBMC	peripheral blood mononuclear cell
PBS	phosphate buffered saline
PE	phycoerythrin
PFA	paraformaldehyde

PLGA	poly(lactic-co-glycolic acid)
pNPP	p-nitrophenyl phosphate
PRR	pattern recognition receptor
RA	rheumatoid arthritis
RANTES	regulated upon activation, normal T cells expressed and secreted
RAP	receptor associated protein
RIP	receptor interacting protein
RME	receptor-mediated endocytosis
RNA	ribonucleic acid
RPMI	Roswell Park Memorial Institute
SDS	sodium dodecyl sulphate
SERCA	sarco-endoplasmic reticulum Ca <sup>2+</sup> -ATPase
siRNA	small interfering RNA
SIRP	signal regulatory protein
SLE	systemic lupus erythematosus
SR	scavenger receptor
SREC	scavenger receptor expressed by endothelial cell
TAB	TAK1-binding protein
TAK	TGF- $\beta$ -activated kinase
TAP	transporter associated with antigen processing
TcR	T cell receptor
TGF	transforming growth factor
TIR	Toll/interleukin-1 receptor
TIRAP	Toll-IL-1R domain-containing adaptor protein
TLR	Toll-like receptor
TNF	tumour necrosis factor
TNF-R	tumour necrosis factor receptor
TRADD	TNF-receptor-associated death domain
TRAF	TNF-receptor-associated factor
TRAM	TRIF-related adapter molecule
Treg	regulatory T cell
TRIF	TIR domain-containing adapter inducing IFN-beta
US6	unique short segment 6
UGGT	UDP-glucose:glycoprotein transferase

# **1. Introduction**

## **1.1 The Immune Response**

### **1.1.1 Components of the immune response**

The immune system exists to protect the body from infection and maintain a healthy state. In order to achieve this, the immune system must respond quickly to remove any potential threats, such as invading microorganisms, without responding to and damaging normal, healthy tissues. The immune system is composed of two main arms: innate, antigen (Ag)-nonspecific, and adaptive, Ag-specific, immunity. The innate immune system is composed of phagocytic cells, natural killer (NK) cells, complement and interferons (IFNs) and is able to rapidly recognise danger signals such as pathogens and damaged tissue through a number of pattern recognition receptors (PRRs). The adaptive immune system is composed of B and T lymphocytes and activation of this component of the immune system results in immunoglobulin (Ig) gene rearrangement and high affinity antibody production by B cells, development of effector T cells and subsequently immunological memory. In order to generate an effective immune response, these two arms of the immune system must be linked, and this is achieved by antigen presenting cells (APCs). APCs are of crucial importance for generation of adaptive immune responses- although B cells can recognise antigen directly through surface Ig receptors, T cells require antigens to be processed by APC and presented as peptide fragments in the context of major histocompatibility complex (MHC) class I (CD8<sup>+</sup> T cells) or class II (CD4<sup>+</sup> T cells) molecules. MHC class I molecules are expressed by all nucleated cells and generally present fragments of intracellular pathogens such as viruses, whereas class II molecules are normally only expressed by APCs, such as B cells, macrophages and dendritic cells (DCs) and present fragments of extracellular antigens that have been captured by the APC.

### **1.1.2 Dendritic cells at the centre of the immune response – a network of subsets**

DCs are the most potent APCs, and the only ones capable of inducing primary immune responses. DCs are highly specialised for capturing Ags and processing and presenting these to T and B cells. A number of subsets of DCs in both mouse and human have been identified, which may help to account for the great plasticity of



these cells. This section shall focus on the mouse dendritic cell network, as the work described in this thesis has been carried out exclusively in a murine system. A comprehensive review of human dendritic cell subtypes can be found in [1]. The traditional model of the DC lifecycle was based on studies carried out on Langerhans cells (the DC type found in the epidermis) in the 1980s and is as follows: DC progenitors originate in the bone marrow, and give rise to precursor cells that migrate to the tissues, where they reside as immature cells specialised for antigen capture, with a high phagocytic capacity but low expression of costimulatory molecules and MHC class II molecules required to activate an adaptive immune response. When these immature DCs encounter “danger” signals, such as bacterial products or inflammatory mediators, they downregulate Ag capture and upregulate processing and presentation of captured Ag as well as increasing expression of costimulatory molecules. They migrate to the lymphoid organs (spleen and lymph nodes), where they encounter rare Ag-specific T cells, thus initiating the adaptive immune response (reviewed in [2, 3]). Figure 1.1 (adapted from [3]) shows the so called “Langerhans cells paradigm”.

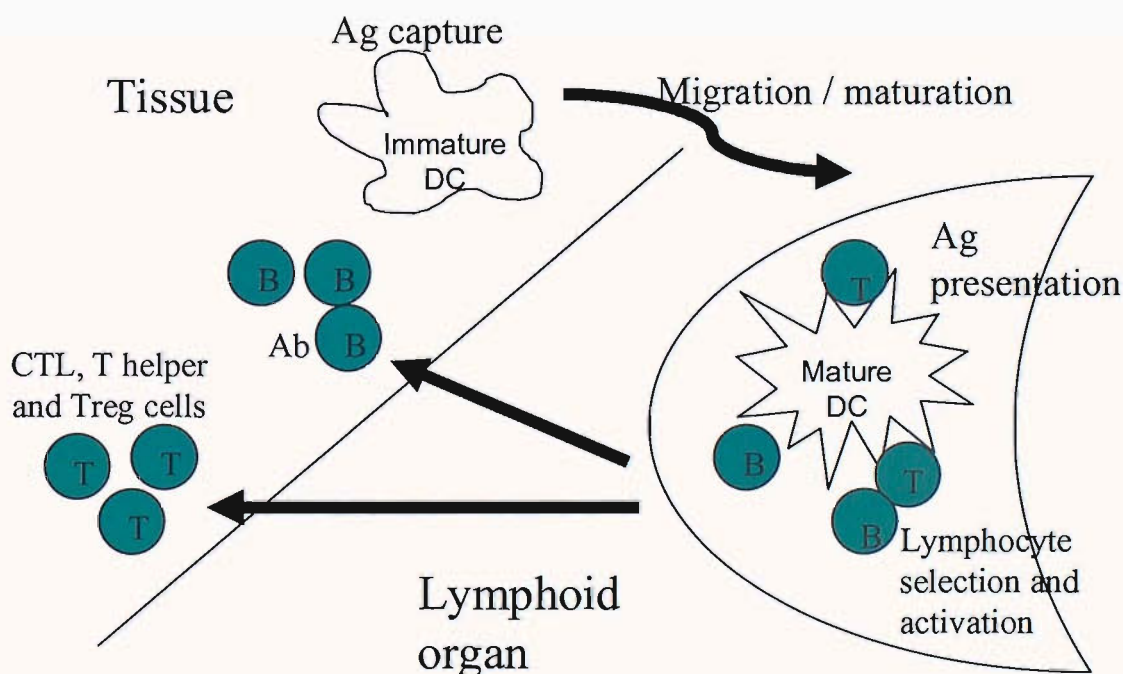


**Figure 1.1** The life cycle of dendritic cells – “The Langerhans cell paradigm”

However, subsequent studies involving isolation of dendritic cells from tissues such as spleen and lymph nodes, as well as improved methods of *in vitro* DC culture, and analysis of an increasing variety of cell surface markers, has revealed a heterogeneity among DCs, leading to the recognition of DCs as a network of subsets with distinct functions, origins and migratory properties rather than a single population of cells.

	Surface phenotype							
DC type	CD11c	CD8	CD4	CD205	CD11b	CD45RA	Derivation	Distinguishing properties
CD8 DC	+	+	–	+	–	–	Blood	High IL-12 Cross-presentation of cellular antigen Cross-priming Cross-tolerance
CD4 DC	+	–	+	–	+	–	Blood	Most numerous DCs in spleen
CD4CD8 DC	+	–	–	–	+	–	Blood	High IFN- $\gamma$
Langerhans' cell	+	– /low	–	Very high	+	–	Skin epithelia	Traffic to lymph node from skin Present contact sensitizing antigens
Dermal/interstitial DC	+	–	–	+	±	–	Tissue	In all tissues Traffic to draining lymph nodes Prime CD4 T-cell immunity to tissue infections
Plasmacytoid DC	Low	±	±	–	–	+	Blood/tissues	High IFN- $\alpha$ , do not look like DCs until stimulated

DC, dendritic cell; IFN, interferon; IL-12, interleukin-12.

**Table 1.1** Murine DC subsets

Table 1.1, adapted from [4], summarises the main DC subsets thus far identified in the mouse, their surface phenotype and main functions. The first major subdivision is between plasmacytoid and conventional DCs. Plasmacytoid DCs (pDCs) are so called because of their morphological similarity to plasma cells, and are distinguished from conventional DC subsets by their expression of CD45RA and lower levels of CD11c. pDCs are poor antigen presenting cells, but are the main producers of type I interferons (IFNs) – i.e. IFN- $\alpha$  and  $-\beta$ , thus playing a key role in early anti-viral immune responses, and may also be involved in activating other DC subtypes, as well

as other immune cells including NK cells. A detailed review of pDCs can be found in [5].

The so-called conventional DCs can be further subdivided into blood- and tissue-derived DCs. The three blood-derived DC subsets, which are found in all lymph nodes and in the spleen, can be distinguished by their expression of CD4 and CD8 $\alpha$  – one set expresses CD8 but not CD4 (CD8 DCs), another CD4 not CD8 (CD4 DCs), and the third expresses neither (double negative (DN) DCs). These DCs do not appear to traffic through peripheral tissues before reaching the secondary lymphoid organs, but rather to derive from precursors that traffic to spleen and lymph nodes directly from the bone marrow via the blood. The CD8 DCs are found in the T cell areas of the lymphoid organs, whereas the other blood-derived DC subsets are located in the marginal zones [4, 6]. The two subtypes of tissue-derived DCs are not found in the spleen, but are found in peripheral tissues, from where they traffic to local draining lymph nodes, apparently constitutively rather than in response to inflammatory stimuli as described in the Langerhans cell paradigm. Interstitial/dermal DCs are found in many tissues, and thus in most lymph nodes, and are characterised by expression of CD11b and DEC-205. Langerhans cells, as previously mentioned, are restricted to the epidermis and so are found only in subcutaneous lymph nodes and characterised by expression of CD11b, high levels of DEC-205 and low to no CD8 [4, 6]. All of these subsets appear to be distinct lineages arising from independent precursors, as opposed to from a single precursor depending on environmental factors [1, 4].

Studies have also been carried out to investigate the maturational state of DC subsets *in vivo* (reviewed in [6]). When DC subsets are purified from lymph nodes, the tissue-derived DCs appear as classically mature DCs – i.e. expressing high levels of surface MHC class II and the co-stimulatory molecules CD80, CD86 and CD40 and with the capability to prime naïve T cells, but present newly encountered Ag very poorly. Blood-derived DCs, however, appear immature - expressing low levels of surface MHC II, CD80, CD86 and CD40 and incapable of activating naïve T cells, but with high levels of intracellular MHC II and efficient Ag processing and presentation. These cells can be stimulated by inflammatory stimuli or even *in vitro* culture to undergo the maturation process [6]. Thus, whereas tissue-derived DCs follow a life

cycle similar to that originally described for Langerhans cells, blood-derived DCs are found in an immature state in the lymphoid organs, and respond to activation signals and mature in situ. These differences should be taken into account when considering the functions of the different DC subtypes. Some of these functions are described as appropriate in the following sections, although not all shall be discussed here, and are summarised in table 1.1. Detailed reviews can be found in [1, 4, 6].

### **1.1.3 Antigen capture and processing by dendritic cells**

As has been mentioned, immature DCs are highly efficient at Ag capture. DCs can capture Ag by a number of methods, outlined below.

#### *i) Receptor-Mediated Endocytosis*

Receptor-mediated endocytosis (RME) involves binding of extracellular Ags to receptors on the DC cell surface, which are then internalised through formation of clathrin-coated pits. On binding of ligand to the receptor, a signal is initiated in the cytoplasmic tail of the receptor, resulting in recruitment of adaptor molecules, which in turn recruit clathrin and initiate formation of coated pits. A number of receptors are involved in RME by DCs, including scavenger receptors (SRs), C-type lectin receptors (mannose receptor, DEC-205, DC-SIGN) and Fc $\gamma$  receptor type I (CD64), II (CD32) and III (CD16) [7].

#### *ii) Phagocytosis and Macropinocytosis*

Phagocytosis and macropinocytosis are methods by which DCs internalise particulate and soluble Ag, respectively [7]. Both processes are actin-dependent.

Macropinocytosis is constitutive in immature DCs, and allows the DCs to rapidly and constantly sample their extracellular environment by taking up large amounts of surrounding fluid. Phagocytosis is generally a receptor-mediated process. Binding of ligand to the receptor induces a signalling cascade, which results in rearrangement of the actin cytoskeleton and extension of membrane pseudopodia to surround and capture particles such as apoptotic or necrotic cell fragments, viruses, bacteria, intracellular parasites and also latex beads in experimental systems (reviewed in [2, 3, 8, 9]). The receptors involved in phagocytosis are generally similar to those involved in RME.

DCs present Ags to T cells on MHC molecules. As previously mentioned, internal Ags are normally presented on MHC class I molecules, and extracellular Ags are

normally presented on MHC class II molecules. In order to be expressed on the cell surface in the context of MHC molecules, Ags must first be processed to generate short peptides or epitopes (reviewed in [2, 3]). Figure 1.2 (adapted from [3]) shows an outline of the MHC class I and II processing pathways, described below.

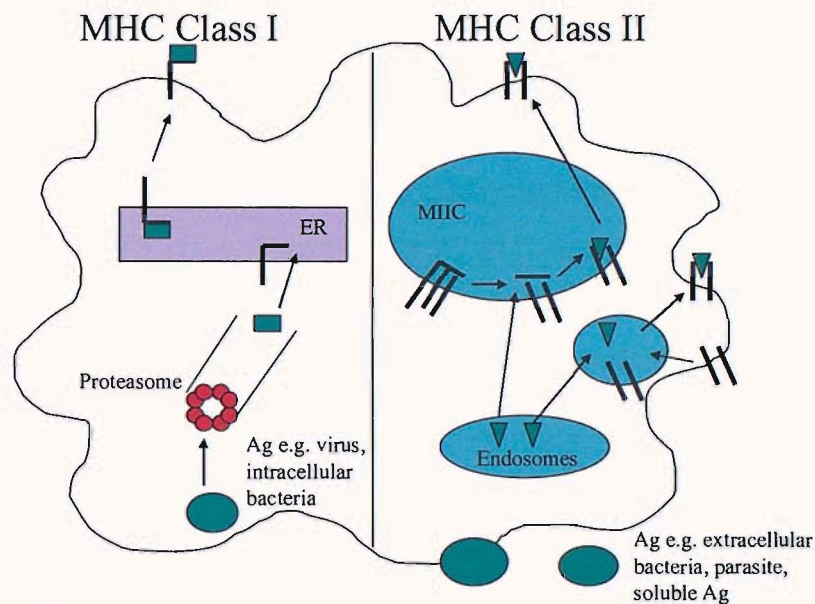


**Figure 1.2** The MHC class I and class II processing pathways in DCs.

#### 1.1.4 MHC Class II loading

Ags captured by immature DCs are targeted to lysosome-related intracellular compartments, which accumulate MHC class II molecules. These compartments are known as MHC class II-rich compartments (MIICs) and contain all the components required to generate MHC class II-peptide complexes. Newly synthesised MHC class II molecules associate with the invariant chain (Ii) chaperone in the ER, which has a fragment, CLIP, that inserts into the peptide binding groove, stabilising the class II molecule and protecting the binding groove from other peptides. These MHC II-Ii complexes move from the ER to early endosomes and then to MIICs via late endosomes. In these compartments, the class II molecules encounter antigenic peptides resulting from degradation of endocytosed proteins (the original source for which can have been extra- or intra-cellular). In order for Ag to gain access to the peptide-binding groove, CLIP needs to be removed, a process which requires several factors - low pH (encouraging an open conformation of class II), the chaperone DM (that stabilises the open conformation of class II), and proteolytic degradation of the regions of Ii surrounding CLIP. A number of proteases are believed to be involved in this degradation, although the only clearly defined step is the final one, which



converts Iip10 into CLIP, and is carried out by cathepsin S. This step also removes a retention signal present in the cytoplasmic tail of Ii, which prevents the class II-Ii complex from trafficking to the cell surface. Following the cathepsin S degradation, CLIP can be displaced from the peptide binding groove with higher affinity peptides. The activity of cathepsin S is regulated by its endogenous inhibitor cystatin C, which limits degradation of Ii and thus class II loading and export to the cell surface in immature DC. Upon DC activation, cystatin C is downregulated and cathepsin S activity increases, allowing Ii degradation and export of peptide-loaded MHC class II molecules to the cell surface. A more detailed review can be found in Villadangos et al [10]. In some cases, extracellular Ags gain access to the MHC class I processing and presentation pathway, a process known as cross-presentation, which is discussed later, and is reviewed in [11, 12].

#### **1.1.5 MHC Class I loading**

MHC class I processing and presentation results in the display of an array of peptides at the cell surface that have been generated within the cell. This immunopeptidome provides a “snapshot” of the physiological state of the cell, and is scanned by CTLs and NK cells to detect any abnormalities arising from, for example, virus infection or tumour mutations. As MHC class I molecules bind 8-10mer peptides of specific sequences, protein antigens must undergo a process of degradation and selection in order to be loaded onto class I. The first step in this pathway is poly-ubiquitination of cytosolic proteins, which targets them to the proteasome, which cleaves the proteins into peptides that can range in size from 2-3 to >20 amino acids. Much of the material targeted for proteasomal degradation is known as defective ribosomal products, or DRiPs [13] – these are newly synthesised proteins that may be non-functional due to errors in protein synthesis or are the result of post-translational mistakes such as misfolding. Up to 30% of newly synthesised proteins are ubiquitinated and degraded by the proteasome soon after synthesis. The oligopeptides generated by the proteasome are then selectively transported from the cytosol into the ER via the transporter associated with antigen processing (TAP), where they are further trimmed into 8-10mers if necessary by an ER-associated aminopeptidase (ERAP-1) and loaded onto newly synthesised MHC class I molecules in a process controlled by the peptide-loading complex, shown below.

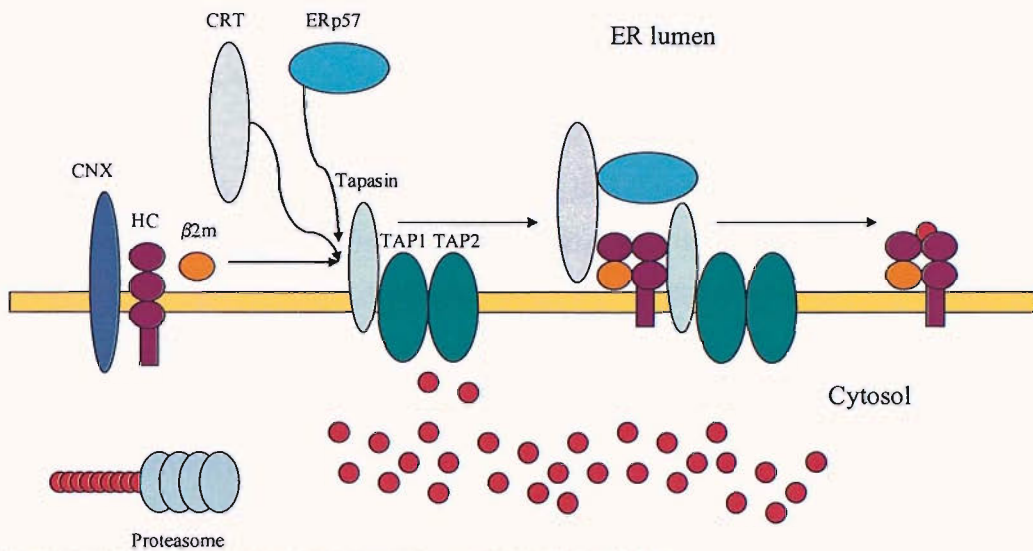


**Figure 1.3** The peptide-loading complex. Adapted from [14].

In the peptide-loading complex, tapasin associates with TAP via its transmembrane domain and stabilizes the TAP1/TAP2 heterodimer. Tapasin also associates with ERp57, apparently via a structural disulfide bond. Newly synthesised MHC Class I heavy chains bind to calnexin (CNX), a membrane-bound ER chaperone that assists in Class I folding and disulfide bond formation. After dissociation from CNX, heavy chain binds  $\beta_2$  microglobulin ( $\beta_2m$ ) and associates with CRT via a monoglucosylated glycan. Interactions between class I heavy chain and tapasin and between CRT and Erp57 complete the peptide-loading complex. Peptides of the appropriate sequence can then bind to class I, resulting in dissociation of class I from the peptide loading complex. Fully assembled, stable class I can then leave the ER and travel to the plasma membrane via the Golgi apparatus. This subject has been reviewed in depth in [14], where original papers are cited, unless otherwise indicated. The role of CRT in the peptide-loading complex is discussed more fully in section 1.3.

### 1.1.6 Cross-presentation of exogenous antigens on MHC Class I

A problem with the traditional paradigm of antigen processing and presentation, i.e. that endogenous Ags are presented on MHC class I and exogenous Ags on MHC class II molecules arises from the fact that only professional APCs, such as DCs, expressing both MHC-Ag complexes and appropriate costimulation are capable of priming naïve T cells. How, then, can CTL responses be primed to viruses, intracellular pathogens or tumours that do not infect bone-marrow derived APCs? It is now clear that professional APCs, in particular DCs, are capable of acquiring Ag from other cells and presenting this exogenously acquired Ag on MHC class I

molecules, a process termed cross-presentation. The resulting induction of an effector CTL response is known as cross-priming.

The phenomenon of cross-presentation was first identified in 1976 by Bevan [15], who observed that mice immunised with allogeneic cells, which differed at all MHC and minor Ags from the host, generated CTLs specific for minor Ags from the graft presented on host MHC I molecules. This indicated that minor Ags must be transferred from donor cells to host APCs. The sources of Ag and mechanisms of cross-presentation remained a mystery for some time, but answers to these questions are now emerging. It has been demonstrated that soluble protein Ag is cross-presented much less efficiently ( $\sim 10^4$  fold) than particulate or cell-associated Ag [16-18]. HSP-peptide complexes also appear to be cross-presented both *in vitro* and *in vivo* (discussed in more detail in section 1.2), as does protein generated following DNA or RNA immunisation. Recent studies (reviewed in [12]) suggest that cellular proteins represent the predominant form of cross-presented Ag *in vivo*. These differences appear to be linked to the route of Ag uptake – particulate and cell-associated Ag is generally internalised by phagocytosis, and Ag taken up by this route has been shown to be cross-presented far more efficiently than endocytosed Ag [12]. This may relate to the relative accessibility of cross-presentation pathways from different intracellular compartments – as described below, phagosomes and macropinosomes appear to be particularly suited to directing Ag for cross-presentation.

DCs and macrophages have been identified by numerous studies as being capable of carrying out cross-presentation (reviewed in [4, 12]). There is some evidence that B cells and neutrophils are capable of cross-presentation *in vitro*, but these cells appear to play little or no role in cross-priming *in vivo*. *In vivo*, the CD8 $\alpha^+$  subset of DCs appears to be the main cell population involved in cross-priming (and indeed in cross-tolerance) [4]. It is still unclear whether this ability of the CD8 DCs to cross-present is due to a difference in Ag uptake by different DC subsets, or to differences in the cross-presentation machinery within the cells. Some studies have observed that CD8 DCs preferentially capture apoptotic cells and cross-present derived Ags to CD8 T cells, suggesting that it is the ability to capture Ag that dictates whether or not cross-presentation occurs. However, other work has demonstrated that, *in vitro*, all 3



splenic DC subsets could take up cellular Ag and present this to CD4<sup>+</sup> T cells, but only the CD8 DCs could cross-present to CD8<sup>+</sup> T cells, indicating fundamental differences in the cross-presentation machinery between the different subsets (reviewed and cited in [4]).

This leads us to the important issue of how exogenously acquired Ags come to be displayed on the cell surface in the context of MHC class I, rather than class II molecules. Two main pathways have been proposed, the phagosome-to-cytosol pathway and the vacuolar pathway. Each pathway shall be described briefly, along with evidence for their roles in cross-presentation of different Ags (reviewed in [4, 12, 14]).

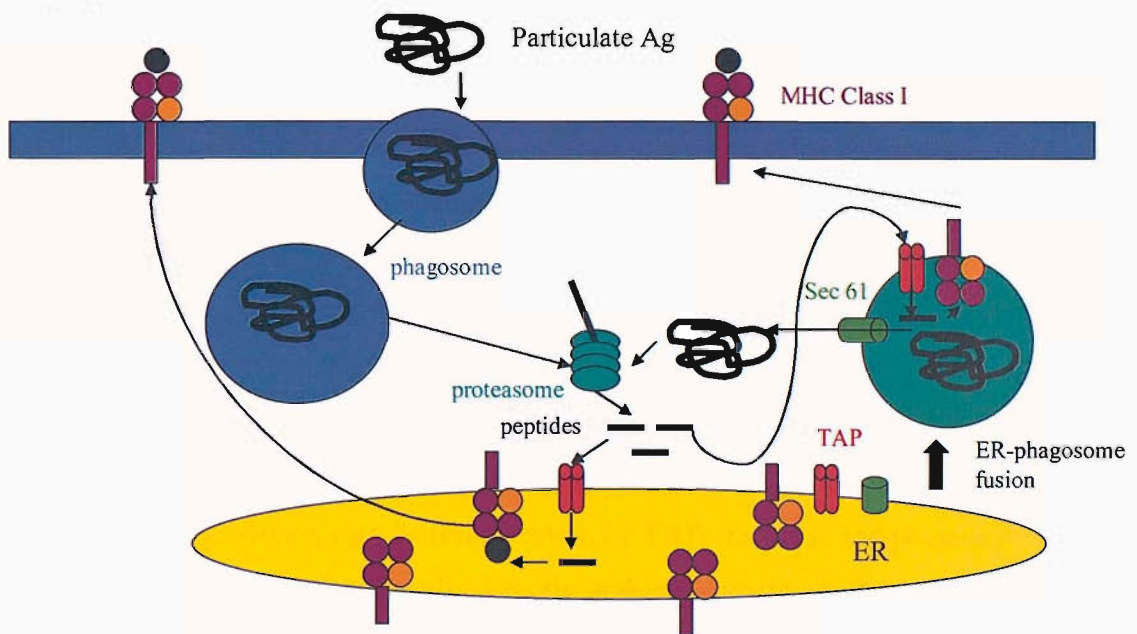


**Figure 1.4** The phagosome-to-cytosol pathway of cross-presentation of antigen. Adapted from [12].

In the phagosome-to-cytosol pathway of cross-presentation (fig. 1.4), Ag that is internalised into a phagosome or macropinosome is subsequently transferred to the cytosol, where it is degraded by the proteasome into oligopeptides which are then transported by TAP and loaded onto MHC class I. This theory is supported by evidence that cross-presentation of Ag bound to iron oxide or polystyrene beads is blocked by proteasome inhibitors and that TAP-deficient macrophages and DCs cannot cross-present such Ag. As proteasomes are only found in the cytosol and nucleus of cells, and not in endocytic compartments, and as TAP functions to transport peptides from the cytosol across membranes, these findings indicate that

peptides must be generated in the cytosol, but how does the Ag gain access to the cytosol from the phagosome? The answer to this was suggested by work from Desjardins, who found that ER proteins were present in early phagosomes, possibly as a result of ER membrane donation during phagocytosis [19]. In the ER, a process known as ER-associated degradation (ERAD) exists, which is used for the degradation of misfolded ER proteins, and involves retrotranslocation of these misfolded proteins from the ER to the cytosol for proteasomal degradation [19]. It therefore seems likely that the same mechanism used for export of misfolded proteins from the ER could be used to transfer particulate Ag from the phagosome to the cytosol. It has been suggested that Sec-61, a multicomponent channel involved in import and export of proteins from the ER, may also be involved in this process [4, 12, 14]. Another candidate is Derlin-1, a protein that has been shown to associate with MHC Class I heavy chains associated with the human cytomegalovirus protein US2, which targets class I for retrotranslocation to the cytosol and degradation [14]. Components of both channels have been found associated with phagosomes. While the precise identity of the channel involved is as yet unclear, it seems extremely likely that such a transporter is transferred to the phagosome with ER membrane, providing a route for egress of Ag from the phagosome to the cytosol. The presence of ER components in phagosomes, including TAP, the components of the peptide loading complex, and ERAP, has raised the possibility that some peptides derived from proteasomal degradation may be translocated, by TAP, back into the phagosome and loaded onto MHC Class I molecules directly in this compartment. TAP associated with phagosomes has been shown to be active, and it has also been demonstrated that MHC class I-peptide complexes can form in phagosomes [14]. Peptides from the proteasome probably gain access both to the ER and to phagosomes via TAP, and so will be loaded onto class I in both locations, although the relative contribution of each *in vivo* is not yet clear.

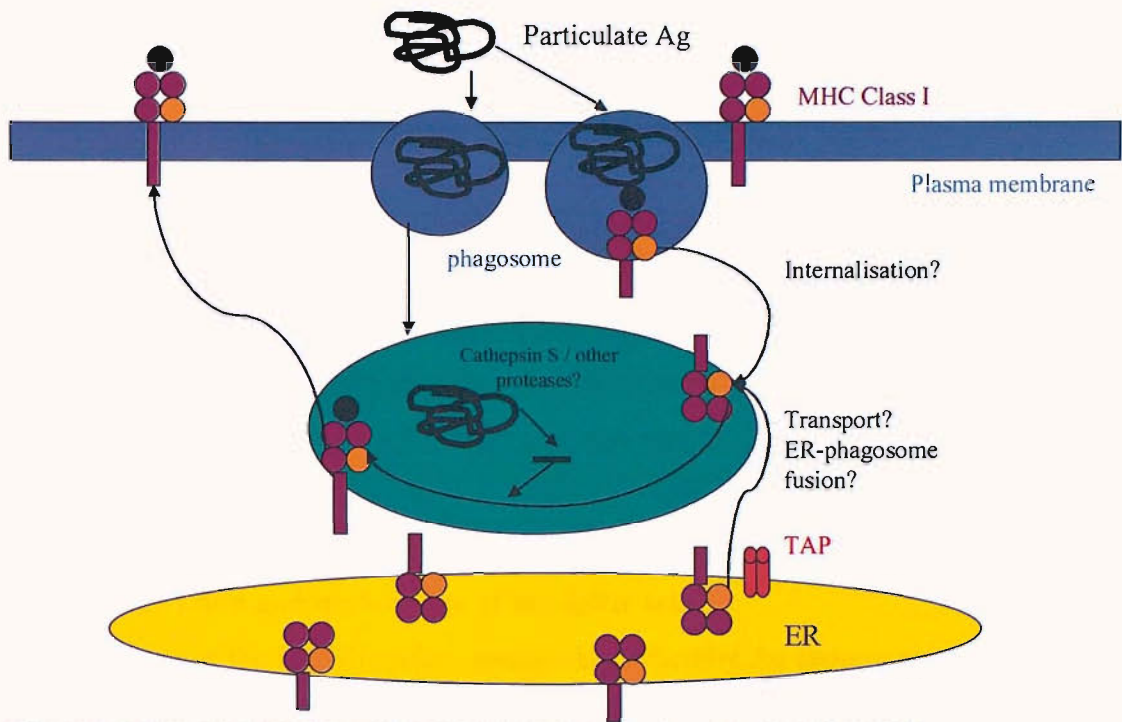


**Figure 1.5** The vacuolar pathway of cross-presentation of antigen. Adapted from [12].

Evidence for a second pathway of cross-presentation came from observations that cross-presentation of certain Ags, including *E. coli*-associated proteins, PLGA beads, soluble proteins or viral proteins or virus-like particles, was TAP- and proteasome-independent. This indicates that the peptides presented on MHC class I are not generated in the cytosol by this pathway, but within a distinct subcellular compartment, subsequently identified as an endocytic vacuole (reviewed in [12]). The mechanisms of this pathway have been less well studied than those of the phagosome-to-cytosol pathway, and so are not as well understood, although some details are emerging. All data reported here are reviewed and cited in [12]. Cathepsin S appears to play a key role in the degradation of Ag, as cathepsin S-deficient macrophages or DCs cannot present OVA by this pathway. Other cathepsins are unable to compensate for loss of cathepsin S in this system. Although the reasons for this are unclear it may involve the ability of cathepsin S to be active at neutral pH suitable for MHC class I loading, or it may be that cathepsin S traffics preferentially to these subcellular compartments. It is also currently unknown how empty MHC class I molecules traffic to the vacuolar compartments – possibilities include incorporation of surface class I from the plasma membrane during phagosome formation and trafficking of newly-synthesised class I from the ER, potentially via ER membrane donation. It cannot be ruled out that peptides generated in the vacuole

are subsequently transported into the ER, or another subcellular compartment, for loading.

Why certain Ags are presented specifically by one pathway or the other remains unclear. It may be that the ability of the different proteases present in each compartment to generate the appropriate peptides is important. However, a key factor appears to be the physical form of the Ag – different kinds of particles localize to different compartments following internalisation, and this may ultimately determine which pathway they enter.

### **1.1.7 Activation and maturation of dendritic cells**

A key process in the DC lifecycle is maturation, whereby Ag capture is downregulated and processing and presentation of captured Ag is enhanced. Mature DCs also express high levels of co-stimulatory molecules CD80, CD86 and CD40 as well as other molecules involved in DC-T cell interactions on their surface and produce pro-inflammatory cytokines such as IL-2 and IL-12, enabling them to prime naïve T cells and drive the development of the immune response. This process is crucial for development of an immune response, as there is now a range of evidence that recognition of Ag on immature DCs by T cells leads to the development of tolerance.

There are two main types of stimulus that can induce DC maturation. These are exogenous danger signals – i.e. microbial products such as LPS, non-methylated bacterial DNA sequences (CpG DNA), double stranded (ds)RNA and flagellin – and endogenous danger signals such as type I IFNs, HSPs and uric acid. Five types of surface receptors have been reported to induce DC maturation [7]: (i) Toll-like receptors (TLRs), (ii) cytokine receptors, (iii) TNF-receptor (TNF-R) family members (including CD40, OX40 and Fas), (iv) FcRs, and (v) sensors of cell death. It is unlikely that these pathways are redundant; they may act synergistically or may result in functionally distinct DC populations.

The phenotypic and functional changes induced by DC maturation are reviewed in [2, 3]. These effects are mediated by a number of intracellular signalling pathways, depending on the receptors engaged. Toll-like receptors (TLRs) are an example of



pattern recognition receptors (PRRs). PRRs are key components of the innate immune system, which recognise conserved molecular patterns known as pathogen-associated molecular patterns, or PAMPs. These are substances such as Lipid A of LPS, which is highly conserved between all Gram-negative bacteria, and thus enables the immune system to recognise an extremely wide range of pathogens through relatively few receptors. Figure 1.6 (adapted from [20]) shows the range of mammalian toll-like receptors and their ligands. The balance between pro- and anti-inflammatory mediators, such as TNF, IL-1, IL-6, IL-10, TGF- $\beta$ , and prostaglandins in the local microenvironment also plays an important role in DC activation and maturation, as do T cell-derived signals, particularly CD40-CD40L interaction, and interactions with NK cells.

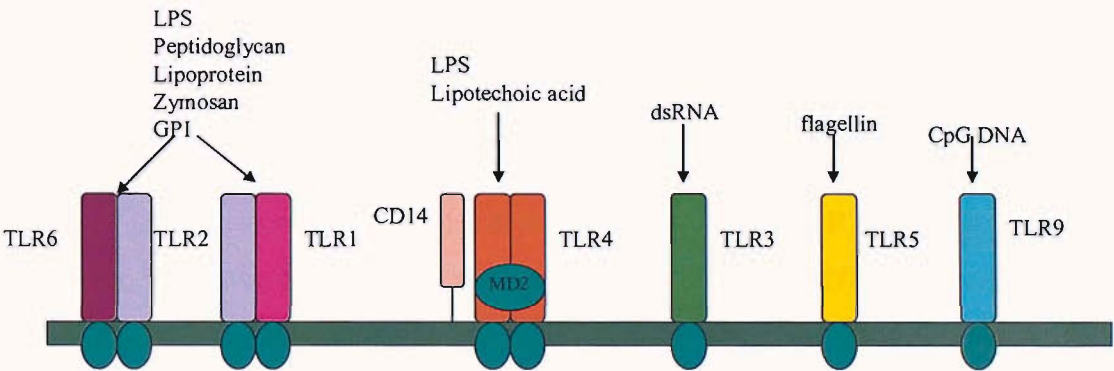


**Figure 1.6** Toll-like receptors and their ligands.

I shall not describe in detail here all of the different signalling pathways involved in DC activation, but the signalling pathways utilised by TLRs shall be summarised as an example.

The TLRs are type I integral membrane glycoproteins and are members of a large superfamily that includes the IL-1 receptors (IL-1Rs). While the extracellular domains of the TLRs and IL-1Rs are markedly different, with IL-1Rs containing 3 Ig-like domains whereas TLRs contain leucine-rich repeat (LRR) motifs, the cytoplasmic tails of these molecules contain a conserved region known as the Toll/IL-1R (TIR) domain. TIR domains show amino acid sequence conservation of 20-30%, and the homologous regions make up 3 boxes, which are essential for signalling (fig. 1.7a). Ligand binding to TLRs induces receptor dimerisation, which results in recruitment of downstream signalling molecules (fig. 1.7b). These include the adaptor

proteins MyD88, IL-1 receptor-associated kinases (IRAKs), TGF- $\beta$ -activated kinase (TAK1), TAK1-binding protein 1 (TAB1), TAB2 and TNF-receptor-associated factor 6 (TRAF6). Recruitment and activation of adaptor proteins in turn leads to recruitment and activation of inhibitor of NF- $\kappa$ B (I $\kappa$ B) kinases (IKKs), which phosphorylate I $\kappa$ Bs. This leads to degradation of I $\kappa$ B and subsequent release and nuclear translocation of NF- $\kappa$ B. Activated TAK1 also phosphorylates mitogen-activated protein kinases (MAPKs), including JNK. The ultimate product of this cascade is the activation of various genes by the transcription factors, resulting in cytokine production and DC maturation. This pathway, referred to as the MyD88-dependent pathway, is utilised by all the TLRs, with the possible exception of TLR3, and also by all members of the IL-1R family.

Studies on MyD88-deficient mice and cells indicated that another, MyD88-independent, signalling pathway may be induced by at least some TLRs. MyD88-deficient mice are incapable of producing pro-inflammatory cytokines such as TNF $\alpha$ , IL-1 $\beta$  or IL-6 in response to ligands of TLR2, TLR4, TLR5, TLR7 or TLR9. However, while MyD88-deficient macrophages do not activate NF- $\kappa$ B in response to TLR2 ligand, this activation does occur in response to the TLR4 ligand, LPS. Although the MyD88-deficient macrophages cannot produce pro-inflammatory cytokines, they do express a number of IFN-inducible genes and this expression is abolished in TLR4-deficient mice, indicating signalling through a TLR4-dependent, MyD88-independent pathway (fig. 1.7c). Activation of this pathway has also been shown to result in maturation of bone marrow-derived DCs as measured by upregulation of co-stimulatory molecules CD80, CD86 and CD40, and the ability to induce proliferation of T cells, apparently as a consequence of IFN- $\beta$  production. TLR3 appears to signal mainly through this pathway, while TLR4 can signal through both MyD88-dependent and -independent pathways. The MyD88-independent signalling cascade is dependent on another adaptor protein, TRIF. TRIF associates with TRAF6 and TBK1 through its N-terminal region, mediating activation of NF- $\kappa$ B and IFN-regulatory factor 3 (IRF-3) respectively. Activation of both of these contributes to activation of the *IFN- $\beta$*  gene. TRIF can also associate with receptor-interacting protein 1 (RIP1) through its C-terminal domain and this is thought to be involved with NF- $\kappa$ B activation.

The identification of the MyD88-independent pathway of TLR signalling also began to shed light on one of the mysteries of the TLR system – if all the receptors signal through the same pathway, how do they generate the varying patterns of gene expression induced by different TLR ligands? This can be at least partially explained by the use of different adaptor proteins by the different TLRs. As well as MyD88 (essential for all TLR-mediated inflammatory cytokine production) and TRIF (essential for MyD88-independent IFN- $\alpha/\beta$  production via TLRs 3 and 4), other adaptors include TIRAP, essential for MyD88-dependent signalling through TLRs 2 and 4, and TRAM, which appears to be specifically involved in MyD88-independent signalling through TLR4. Engagement of different adaptor proteins by receptors can therefore influence the subsequent signalling pathway and transcription factors activated. A detailed discussion on this issue can be found in [21], where the TLR signalling pathways are reviewed in detail.

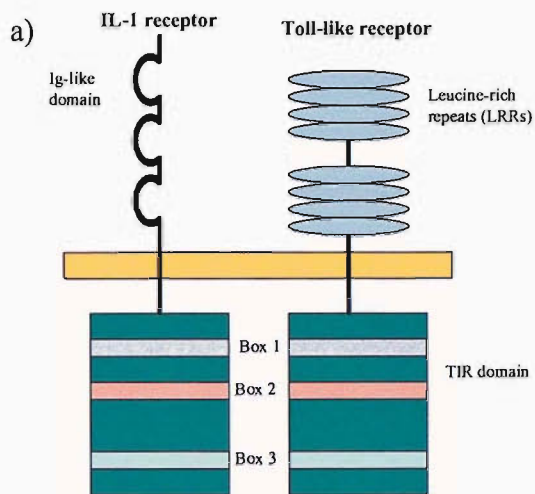
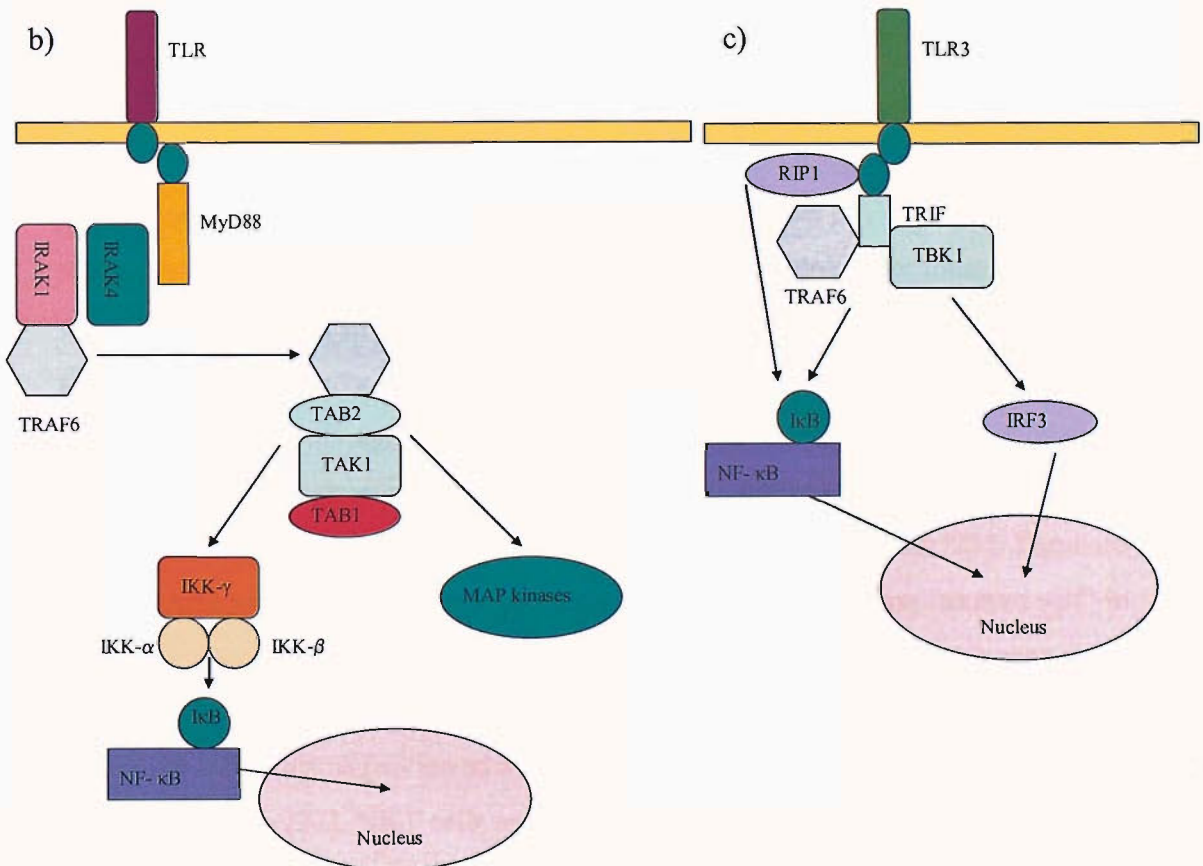


**Figure 1.7** TLR structure and signalling.  
a) TLRs and IL-1Rs share conserved cytoplasmic TIR domain, containing highly homologous box regions, but their extracellular domains are very different.  
b) Outline of the MyD88-dependent signalling cascade.  
c) Outline of TRIF-dependent, MyD88-independent signalling pathway.  
Adapted from [11].





DC activation is crucial for the development of the adaptive immune response. In order for full T cell activation to occur, the T cell needs to receive two signals. Signal 1 is delivered by recognition of specific Ag in the context of MHC by the T cell receptor (TcR). The second signal required for full T cell activation is delivered by interaction of co-stimulatory molecules on mature DCs (such as CD80/86 and CD40) with their ligands on the surface of T cells (CD28, CTLA-4 and CD40L). Delivery of signal 1 in the absence of signal 2 does not signal T cell activation, and can lead to induction of T cell anergy or deletion. Only DCs that have undergone the maturation process express sufficient levels of co-stimulatory molecules to deliver signal 2. No other APCs express sufficient levels of co-stimulation to deliver this signal. Thus DCs play a crucial role in linking the innate and adaptive arms of the immune response – activation by innate mechanisms leads to priming of an adaptive immune response.

The role of CD40 in T cell priming by DC is a subject of great interest, as CD40 ligation is thought to be important for full maturation of DCs and also for DC-T cell interactions and T cell priming. Steinman's group [22] have published an elegant study, demonstrating that upregulation of CD80/86 and cytokine production by DCs could be induced by cytokines, independently of CD40 ligation, but that this was not sufficient to prime naïve T cells in the absence of the CD40-CD40L interaction. Thus CD40 may act as a 3<sup>rd</sup> signal for T cell activation. Another topic of great interest and investigation at this time is the so-called “cross-talk” between DCs and other cells of the innate immune system, such as NK and NKT cells and  $\gamma\delta$  T cells [23]. These cells can also be activated by microbial products and also by recognising “altered self” in the form of tumour products or stress proteins and all 3 populations have been shown to induce DC maturation, apparently by a mixture of cytokine- and cell contact-dependent mechanisms (reviewed in [23]). In the study by Steinman's group mentioned above [22], NKT cells induced the CD40-CD40L interaction required for T cell priming by DCs. As mature DCs also stimulate these innate immune cells, the cross-talk between DCs and innate lymphocytes may be crucial for the development of a full immune response, both by augmenting and sustaining the initial innate response and by priming the adaptive immune response.

## 1.2 Heat shock proteins

### 1.2.1 The heat shock response

As happens so often in science, the discovery of the genes encoding heat shock proteins (HSPs) occurred completely by accident when the temperature of an incubator full of fruit flies was inadvertently increased [24, 25]. Ferruccio Ritossa was studying gene activity in *Drosophila* salivary glands, which at that time could be observed under the light microscope as chromosomal puffing, in an effort to resolve a controversy over the type of nucleic acid produced in these puffs. Following the increase in temperature of the incubator by a colleague, Ritossa noticed a different puffing pattern than was usual for that stage of larval development. When these experiments were carried out with proper controls, this pattern was found to be reproducible, and it was also noted that RNA synthesis occurred extremely rapidly, within 2-3 minutes of temperature increase. This was the first observation of the heat shock response.

The heat shock response is the most conserved genetic system known, and exists in all organisms in which it has been looked for, from archaebacteria to plants and animals [26]. This is a process whereby organisms respond to heat or other stressful conditions by producing HSPs. This response is designed to protect cells from the toxic effects of stresses and is induced in a very rapid and intense manner.

Interestingly, the temperature at which the heat shock response is induced varies between organisms, to reflect the different temperatures encountered by these organisms in their natural environments. In *Drosophila*, for example, induction occurs at 33-37°C, a temperature that could be encountered on a warm summer day. Thermophilic bacteria, which grow at 50°C, induce the heat shock response at 60°C, and arctic fish that live in around 0°C temperatures induce HSPs at 5-10°C. These observations, along with the discovery of a strong relationship between HSP induction and thermotolerance, led to the theory that HSPs are induced by moderate, non-lethal, stresses and subsequently protect the organism from more severe and potentially lethal stresses. However, this is not the whole story, as HSPs have also been shown to be constitutively expressed in cells and to play important roles in normal cellular function.

### 1.2.2 HSPs – ubiquitous and abundant soluble intracellular proteins

There are ten families of HSPs, each containing one to five members (see Table 1.2, adapted from [27]). Family members are closely related, but there is little amino acid homology between families.

HSP family	Members	Intracellular location
Small HSPs	hsp10, GROES, hsp16, $\alpha$ -crystallin, hsp20, hsp25, hsp26, hsp27	Cytosol
HSP40	hsp40, DNAJ, SIS1	Cytosol
HSP47	hsp47	Endoplasmic reticulum
Calreticulin	CRT, calnexin	Endoplasmic reticulum
HSP60	hsp60, hsp65, GROEL	Cytosol and mitochondria
HSP70	hsp70, hsc70, hsp110, DNAK SSC1, SSQ1, ECM10 BiP, grp170	Cytosol Mitochondria Endoplasmic reticulum
HSP90	hsc84, hsp96, HTPG gp96	Cytosol Endoplasmic reticulum
HSP100	hsp104, hsp110 hsp78	Cytosol Mitochondria

**Table 1.2** The main families of heat shock proteins.

HSPs are found in a variety of intracellular locations, including the cytosol of prokaryotes, and the cytosol, nuclei, endoplasmic reticulum (ER), mitochondria and chloroplasts of eukaryotes [28]. As mentioned above, HSPs are constitutively expressed in cells - indeed they constitute the most abundant group of proteins inside cells, suggesting that they play important roles in normal cell metabolism. A number of diverse functions have been attributed to HSPs: as well as thermotolerance [26], which has already been mentioned, HSPs are involved in protein folding and unfolding [29], protein degradation [30], assembly of multi-subunit complexes [31], and buffering the expression of mutations [32]. The involvement of HSP family members in protein folding by binding partially folded intermediates has led them to be often referred to as molecular chaperones. HSP expression is upregulated in response to many stresses such as high temperatures, toxins, oxidative conditions and glucose deprivation, during which their normal cellular function is amplified in order to prevent the intracellular precipitation of unfolded proteins, which is toxic to cells. These functions of HSPs shall not be reviewed in detail here – for detailed reviews see [28-30].

### 1.2.3 Heat shock proteins in the immune response

The search for the tumour-specific antigens of the Meth A sarcoma led to the identification of gp96 as a potent tumour antigen [33-35]. Subsequently, a number of chaperones, including calreticulin, hsp70, hsp90, hsp110 and grp170 were demonstrated to elicit anti-tumour responses in both prophylactic and therapeutic settings against tumours of diverse histological origins [36-39]. It was observed that protective immunity elicited by HSPs isolated from a particular cancer was specific to that cancer and that HSPs derived from normal tissues did not elicit protective immunity to any of the cancers tested. These findings initially suggested that HSPs would display somatic polymorphism and so would differ between cancers and normal tissues and also from one cancer to another. However, sequencing studies revealed the HSPs to be non-polymorphic, indicating that there must be another explanation for the specificity of immunogenicity (reviewed in [40, 41]).

Further studies demonstrated the association of a large collection of peptides with apparently homogeneous gp96 preparations, supporting a new hypothesis that the specificity of immunogenicity of HSP preparations was due to their association with low molecular weight substances undetectable by polyacrylamide gel electrophoresis (reviewed in [40, 41]). This was confirmed when it was shown that tumour-protective hsp70 preparations were rendered ineffective by the removal of peptides [36]. Many laboratories are now working on identifying the structural basis of HSP-peptide interaction. A peptide-binding pocket has been identified in bacterial hsp70 by Zhu et al. [42] and work is ongoing to establish the precise nature of the peptide binding sites of hsp90 and gp96 [43, 44].

Several independent observations have supported the idea that HSPs act as chaperones of antigenic peptides. Immunisation with gp96 preparations from cells expressing  $\beta$ -galactosidase or minor histocompatibility antigens has been shown to elicit specific CTL responses against the particular antigens [45, 46]. Various groups have demonstrated the association of viral epitopes with gp96 purified from infected, but not non-infected cells (reviewed in [40]). Blachere et al. [47] have shown that complexes of various peptides with hsp70 and gp96 can be generated *in vitro* and that, while gp96 and hsp70 are non-immunogenic alone, peptides associated with

these molecules could elicit specific CTL responses. This report also demonstrated that very small amounts of peptide were required to be associated with gp96 for immunogenicity (~1-2ng) and that peptides complexed with mouse serum albumin, another peptide binding protein, were unable to induce CTLs, suggesting that this ability is unique to HSP-chaperoned peptides. These findings are supported by later work from Binder et al. [48], who introduced antigenic peptides into the cytosol of cells either alone or bound to hsp90, gp96, hsp70 or serum albumin. Free peptides or those bound to serum albumin were presented on MHC class I at much lower efficiency than those bound to HSPs. It was also observed that deoxyspergualin, a drug that binds specifically to hsp90 and hsp70 and sequesters the HSPs, abrogated this presentation. The same group have recently proposed that HSP-chaperoned peptides are a necessary and sufficient source of Ag for cross-priming of CTLs [49], demonstrating that while depletion from EG7.OVA lysates of gp96, CRT, hsp70 or hsp90 had no effect on the response of transgenic, OVA-specific T cells, depletion of all of these together resulted in complete abrogation of the response. Reconstitution of the lysate with any of gp96, hsp70 or hsp90 individually restored the response. It is difficult to reconcile these results with the wealth of data supporting whole protein as the major source of Ag for cross-presentation, discussed in section 1.1.6, but they do provide further evidence of HSPs as chaperones for antigenic peptides into the cross-presentation pathway.

Although the initial focus was on induction of CD8<sup>+</sup> cytotoxic T cell (CTL) responses, it has also now been demonstrated that HSPs can chaperone peptides into the MHC class II processing and presentation pathway and thereby induce CD4<sup>+</sup> T cell responses. Doody et al. [50] compared the ability of gp96 to prime CD4<sup>+</sup> and CD8<sup>+</sup> T cell responses using adoptive transfer models. Administration of soluble gp96-peptide complexes resulted in generation of both class I- and class II-restricted epitopes and induced proliferation of both CD4<sup>+</sup> and CD8<sup>+</sup> T cells. However, only the CD8<sup>+</sup> T cells developed effector function. The authors therefore concluded that gp96 selectively primed CD8<sup>+</sup> effector function. These findings were contradicted, however, by a report from Palliser and colleagues [51], who demonstrated that a heat shock protein-OVA fusion protein resulted in generation of class I- and class II-restricted epitopes, but that far more class II-peptide complexes than class I-peptide complexes were displayed at the DC cell surface and the resulting CD4<sup>+</sup> T cell

response was much more vigorous than the CD8<sup>+</sup> T cell response. These findings would make sense in the context of the known Ag processing and presentation pathways. It seems unlikely that all of an endocytosed antigen would gain access to the class I presentation pathway. Bearing this in mind, it could also be expected that both CD4<sup>+</sup> and CD8<sup>+</sup> T cells would be activated in order to induce the most effective immune response, as CD4<sup>+</sup> T cell help is generally required to generate an optimal CD8<sup>+</sup> response, and this is an avenue that will be further explored in this project.

In the study of re-presentation of HSP-peptide complexes by APCs, another interesting aspect of the interaction between HSPs and APCs was revealed. It was found that not only could HSPs act as chaperones, delivering peptides to APCs, but that they could also interact directly with APCs, inducing APC activation. Exposure of APCs to HSPs has been observed to induce a number of peptide-independent effects. These include secretion of inflammatory cytokines TNF $\alpha$ , IL-1 $\beta$ , IL-12 and GM-CSF by macrophages [52, 53]; induction of inducible nitric oxide synthase (iNOS) and production of nitric oxide (NO) by macrophages and DCs [54]; secretion of chemokines, e.g. monocyte chemoattractant protein-1 (MCP-1), macrophage inflammatory protein-2 (MIP-2) and regulated upon activation, normal T cells expressed and secreted (RANTES) by T cells [55, 56]; upregulation by DCs of MHC class II, CD86, and CD40 [53, 57-59]; migration of CD11c<sup>+</sup> cells from the site of gp96 immunisation to the draining lymph nodes [60]; and translocation of NF- $\kappa$ B into the nuclei of macrophages and DCs [52, 53].

These observations have suggested a key role for HSPs in the activation of immune responses. Of key importance are studies demonstrating that necrotic, but not apoptotic, cell death leads to release of HSPs and to maturation of DCs by activation of NF $\kappa$ B [53]. This appears to be a primitive defence mechanism: since HSPs are the most abundant soluble molecules in cells they would be reliable messengers of cell lysis, suggesting stress or disease. Srivastava and Amato [40] suggest that the immunogenicity of cells, infectious agents and tumours depends to a significant degree upon the extent to which cell death leads to induction and extracellular release of HSPs and subsequent interaction between HSPs and APCs.

These findings suggest a dual role for HSPs in the induction of immune responses by delivering antigenic peptides to APCs, which can then be processed and presented on MHC molecules to T cells, and also by acting as “danger signals” to APCs, resulting in APC activation characterised by upregulation of cell surface activation markers and production of pro-inflammatory cytokines, enabling DCs to effectively prime naïve CD4<sup>+</sup> and CD8<sup>+</sup> T cells. This is supported by much research demonstrating both qualities of HSPs in addition to those described previously, particularly in anti-tumour responses [61-64]. Recently, MacAry et al. [65] utilised peptide binding mutants of mycobacterial hsp70 to separate these two functions. They demonstrated that mutant hsp70 unable to bind peptide was able to induce cytokine and chemokine secretion by human DCs, but that peptide binding to hsp70 was essential for efficient generation of CTL responses. The data described here are reviewed in detail in [27, 41, 66, 67]. Figure 1.8 (adapted from [68]) illustrates the potential innate and adaptive outcomes of engagement of HSPs with receptors on APCs.

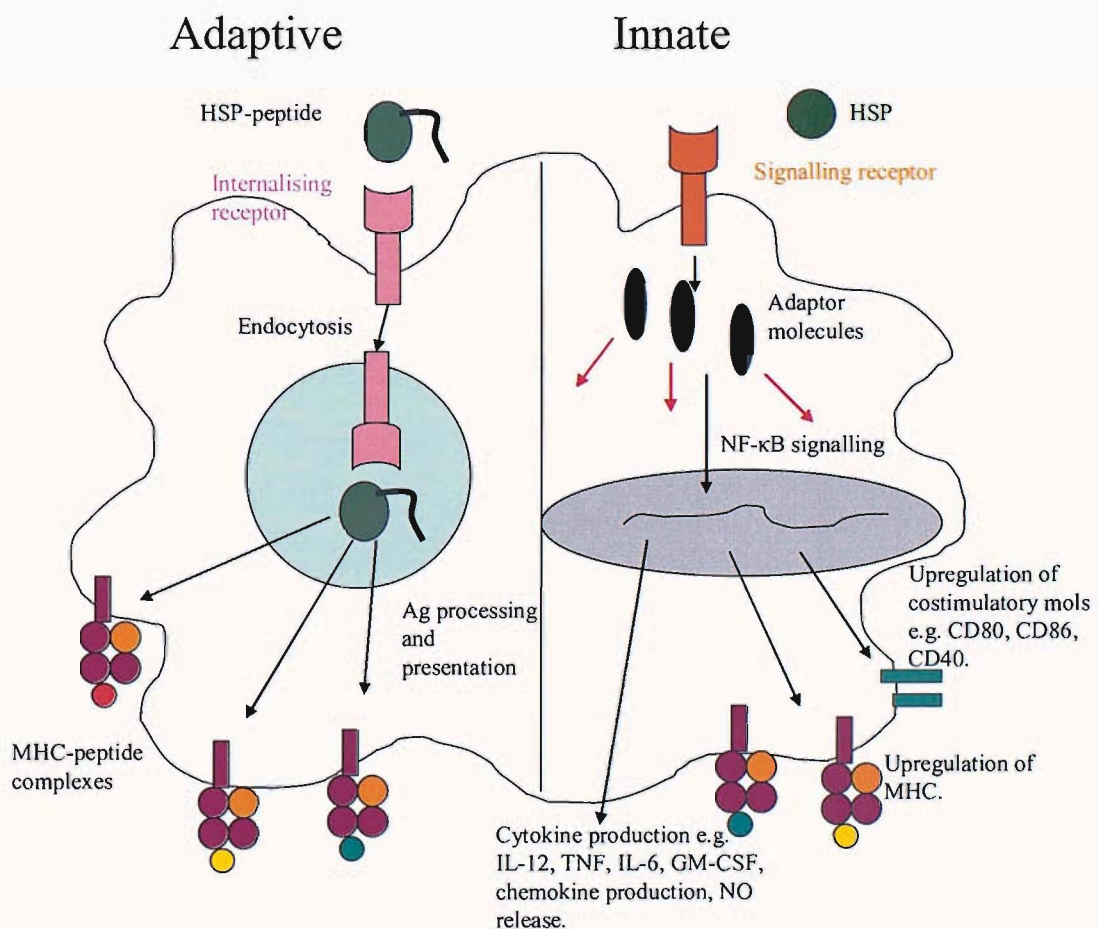


**Figure 1.8** Innate and adaptive effects of interaction of HSPs with their receptors on APCs.



### 1.2.4 Heat shock protein receptors

The highly efficient uptake and re-presentation of HSP-peptide complexes by APCs led to suggestions that HSPs and any associated peptides enter APCs by receptor-mediated endocytosis [69]. The ability of HSPs to directly activate APCs also indicates that APCs bear receptors for HSPs. The identification of such receptors has progressed rapidly in the last few years.

**Table 1.3** Summary of data on hsp receptors

<b>Receptor</b>	<b>HSP and cells</b>	<b>Effect</b>	<b>Ref</b>
CD91	gp96 (murine) RAW264.7 mΦ (macrophage) and peritoneal mΦ (murine)	Uptake – Ab and α2M inhibit re-presentation of gp96-chaperoned peptide.	[70]
	gp96, hsp90, hsp70, CRT (all murine) RAW264.7 mΦ, peritoneal mΦ, BMDC (murine)	Uptake – binding of FITC-HSP. Free HSPs compete re-presentation of gp96-chaperoned peptide. α2M inhibits re-presentation of HSP-chaperoned peptides, as does anti-CD91.	[71]
	gp96 (porcine) Peritoneal mΦ (murine), RAW264.7, CHO.	None - no co-localisation of gp96 and CD91 internally. No positive correlation between CD91 expression and gp96 binding. α2M does not compete for binding or inhibit re-presentation of gp96-chaperoned peptide.	[72]
	gp96 (murine) RAW264.7	Uptake – RAP and α2M compete with gp96 for binding and inhibit re-presentation of gp96-chaperoned peptide. α2M and anti-CD91 inhibit in vivo re-presentation. si-RNA knockout of CD91 abrogates gp96 binding. Anti-CD91 prevents rejection of Meth A fibrosarcoma induced by immunisation with Meth A-derived gp96.	[73]
	E. coli DnaK, Mtb hsp70 Peritoneal mΦ (murine).	Uptake – anti-CD91 inhibits re-presentation of HSP-complexed peptides.	[74]
	CRT (murine) Peritoneal mΦ, DC2.4, CRT+ and - fibroblasts	None – no correlation between CD91 expression and CRT-APC interaction. CD91 expression does not confer CRT association. No difference between ability of CD91 <sup>+/+</sup> and CD91 <sup>-/-</sup> fibroblasts to traffic CRT. CRT trafficking does not parallel that of Pseudomonas exotoxin-A, an obligate CD91 ligand.	[75]



CD40	Mtb hsp70, NOT human Human monocytes and DC	Signalling – deletion of CD40 cytoplasmic tail abolishes, and anti-CD40 inhibits Mtb hsp70-induced production of CC-chemokines. Specific binding demonstrated.	[76]
	Hsp70 (murine) Murine mΦ line	Uptake and signalling – hsp70 (alone or pep-bound) binds CD40. Binding enhanced by LPS stimulation of cells, which enhances CD40 expression. hsp70 binds HEK293 cells transfected with human hsp70 and induces p38 signalling and peptide uptake.	[77]
LOX-1	Hsp70 (human?) Human DC and mΦ	Uptake – anti-LOX-1 inhibits hsp70 binding to human DC and mΦ (partially, total block with mBSA suggests involvement of other SRs). Anti-LOX-1 prevents in vitro hsp70-mediated re-presentation of OVA. Not gp96 receptor.	[78]
SR-A	gp96 and CRT (porcine) peritoneal mΦ (murine)	Uptake – SR-A inhibitory ligand fucoidin inhibits binding and uptake of gp96 and CRT and re-presentation of gp96-chaperoned peptide. SR-A expression in HEK293 cells is sufficient for gp96 and CRT binding and internalisation. MΦ from SR-A knockout mice are deficient in gp96 and CRT binding. Noted only ~50% deficiency, possibly indicating involvement of another SR.	[79]
SREC-1	CRT (human) and gp96 (porcine) Murine mΦ and DC	Uptake – SR ligand AcLDL competes for endocytosis of CRT. Expression of SREC-1 in CHO cells confers ability to bind and endocytose CRT and gp96. SREC-1 mediates endocytosis of CRT in mΦ.	[80]
CD14	Hsp70 (human) Human astrocytoma cells and HEK293 cells	Signalling – transfection of human astrocytoma cells with CD14 enhances TNFα production in response to hsp70. Transfection of HEK293 cells with CD14 enhances NF-κB transcription in response to hsp70. Also saw CD14-independent pathway.	[52, 81]
TLRs	Hsp70 (Human?) Human DC	Signalling – transfection of HEK293 cells – TLR-4 and CD14 required for optimal NF-κB activation by hsp70. IL-1R not used, but expression of both TLR-2 and TLR-4 resulted in synergistic NF-κB activation in a CD14-dependent, MyD88-independent manner. TLR-2, -4 and CD14 required for potent IL-6 production.	[82]



Hsp70 (human) Murine BMDC	Signalling – IL-12p40 and TNF $\alpha$ production by BMDC in response to hsp70 impaired in MyD88 knockout mice. Transfection of 293T cells with TLR-2 or TLR-4 and MD-2 leads to large increase in NF- $\kappa$ B signalling. Diminished IL-12p40 and TNF $\alpha$ production by TLR-4, but not TLR-2, knockout BMDC.	[83]
Gp96 (source not indicated) Murine BMDC	Signalling – gp96-induced IL-12 production and CD86 upregulation by BMDC abrogated in TLR-4 knockout mice, and more so in TLR-2 and -4 double knockout, but not in TLR-2 knockout. Activation required endocytosis of gp96.	[84]
Hsp70 (human) Murine m $\Phi$ Human monocytes	Signalling – m $\Phi$ from TLR-4-deficient mice did not produce TNF $\alpha$ in response to hsp70, those from normal mice did. Production of IL-6 by human monocytes was blocked by anti-TLR-4 or anti-CD14.	[85]
Hsp60 (human and chlamydial) Murine m $\Phi$	Signalling – hsp60 activates JNK1/2, p38, IKK, NF- $\kappa$ B and ERK1/2. JNK and IKK activation signalling abrogated by knocking out MyD88 or TRAF6. Transfection of 293T cells with TLR-2 or TLR-4 and MD-2 enabled them to activate NF- $\kappa$ B in response to hsp60. Signalling dependent on endocytosis of hsp60.	[86]
Hsp60 (human) Murine m $\Phi$	Signalling – TNF $\alpha$ and NO production by m $\Phi$ in response to hsp60 abrogated in TLR-4-deficient mice.	[87]

Table 1.3 summarises the main publications to date on HSP receptors, both endocytic and signalling. Binder et al [70] initially identified CD91 ( $\alpha$ 2-macroglobulin receptor, LDL-related protein) as a cell surface receptor for gp96, on the basis of isolation and sequencing of the p80 fragment of CD91 from plasma membrane extracts from cells which had bound gp96. The natural ligand for CD91,  $\alpha$ 2-macroglobulin ( $\alpha$ 2M), was also demonstrated to inhibit re-presentation of a gp96-chaperoned antigenic peptide. Basu et al [71] subsequently reported that CD91 acts as a receptor for hsp70, CRT and hsp90, facilitating uptake and re-presentation of peptides complexed to these HSPs.

However, Berwin et al [72] have since shown that  $\alpha$ 2M and receptor-associated protein (RAP), an antagonist of all known CD91 ligands, did not affect cell surface

binding, receptor-mediated endocytosis or peptide re-presentation of gp96. This study also demonstrated that CD91 and its ligand, *Pseudomonas* exotoxin, segregated from receptor-internalised gp96 in early compartments of the endocytic pathway. These data suggest a primary, CD91-independent re-presentation pathway for gp96-associated peptides in APCs, but have been disputed by Binder et al. [73], who used siRNA for CD91 to demonstrate that a decline in the cross-presenting ability of APCs corresponded to the decline in CD91 expression. As receptor expression recovered, so did the ability of the cells to cross-present gp96- or  $\alpha 2M$ -chaperoned peptides. *In vivo* experiments were also performed, and demonstrated that protective tumour immunity elicited by tumour-derived gp96-peptide complexes was abrogated by co-administration of anti-CD91 antisera. Further support for the role of CD91 comes from Stebbing et al. [88], who reported that APCs pulsed with lysates of cells infected with HIV stimulated PBMCs of patients with Kaposi's sarcoma, and that this stimulation could be inhibiting by blockade with anti-CD91.

Together with Walters, Berwin has now extended the findings of CD91-independent interaction of APC with gp96 [72] to CRT-APC interactions [75]. CD91 expression did not correlate with the ability of peritoneal macrophages and DC2.4 cells to bind and internalise fluorescently labelled CRT, with both cell types taking up similar amounts of CRT despite the macrophages expressing >10-fold greater levels of CD91 than DC2.4. The authors also observed that CD91 expression did not confer the ability to associate CRT, nor did CD91-deficient and CD91-expressing cells differ in their ability to traffic CRT. CRT trafficking within the cell was demonstrated by cell-type specificity, CD91 dependence and endocytic localisation not to parallel that of an obligate CD91 ligand, *Pseudomonas* exotoxin A, all indicating that CRT binding, uptake and trafficking is not CD91-dependent.

The evidence described above indicates that CD91 plays a role as a receptor for heat shock proteins, however the extent of this role is disputed, and it is also clear that CD91 is unlikely to be the only HSP receptor. Numerous studies have identified a number of other receptors involved in HSP uptake or signalling. In 2001, CD40 was identified as a signalling receptor for mycobacterial, but not mammalian, hsp70 on the basis of direct binding studies and also the ability of anti-CD40 antibodies to inhibit chemokine secretion by macrophages stimulated with mycobacterial hsp70

[76]. Becker et al. [77] subsequently reported that CD40 acts as an endocytic receptor for murine hsp70. It was observed that GST-tagged CD40 associated with hsp70 in cell lysates, and that binding of hsp70 to APCs was enhanced following LPS stimulation, a condition that enhances expression of CD40 by APCs. Hsp70-facilitated uptake of peptides by CD40 was also demonstrated.

LOX-1, a scavenger receptor from the same superfamily as CD91, was identified as an endocytic receptor for hsp70-peptide complexes on human DCs by Delneste et al. [78]. Comparison of human macrophages and DCs revealed that the CD91 ligand  $\alpha$ 2M competed efficiently with hsp70 for binding to macrophages, but poorly for binding to DCs. Anti-LOX-1 antibodies and the LOX-1 ligand acetylated albumin competed with hsp70 for binding to DCs and also inhibited cross-presentation of an hsp70-chaperoned protein. These data raised considerable interest in the role of scavenger receptors as HSP receptors, which has been confirmed by the identification of 2 further scavenger receptors, scavenger receptor-A (SR-A) and scavenger receptor expressed by endothelial cell-1 (SREC-1) as HSP receptors.

Following their initial report of a CD91-independent representation pathway for gp96-chaperoned peptides [72], Berwin and colleagues identified SR-A as a receptor mediating internalisation of gp96 and CRT by APCs [79]. They observed that gp96 internalisation and cross-presentation of associated peptides were inhibited by fucoidin, an SR-A inhibitory ligand. It was also demonstrated that macrophages from SR-A<sup>-/-</sup> mice were impaired in gp96 binding and uptake, and that transfection of SR-A into HEK 293 cells conferred these cells with the ability to recognise and take up gp96.

In the SR-A study [79], it was noted that fucoidin competed uptake of gp96 and CRT beyond levels accounted for by SR-A, leading the authors to believe that another scavenger receptor could be involved in binding HSPs. Further studies [80] demonstrated that, while SR-A accounted for ~50% cell-surface CRT binding capacity as determined in experiments using SR-A<sup>-/-</sup> macrophages, the scavenger receptor ligand acetylated-LDL (AcLDL) competed this residual uptake. SREC-1-transfected CHO cells were shown to bind and internalise CRT and gp96, and this was competed by fucoidin and AcLDL. Also worth noting in this study is the finding

that not all scavenger receptors that bound AcLDL bound CRT or gp96. Notably LOX-1-transfected CHO cells did not bind CRT, nor did CD36-transfected cells, although CD36 has been reported to be a receptor for gp96 [89].

CD14 molecules were shown to be involved in HSP binding by studies into the stimulatory effects of hsp60 and hsp70 on endothelial cells and macrophages [90]. Asea et al. [52] observed that transfection of human astrocytoma cells with CD14 enhanced TNF $\alpha$  production by these cells in response to hsp70. The same authors also demonstrated that transfection of HEK293 cells with CD14 enhanced NF- $\kappa$ B transcription in response to hsp70 [81]. This group suggested that CD14 is not essential for hsp70 signalling, but could enhance it.

Toll-like receptors (TLRs) are key components of the innate immune system, and also play a key role in linking the innate and adaptive arms of the immune system via their stimulatory effects on DCs, as described in section 1.1.7. A large amount of evidence has been gathered to implicate TLRs in induction of signalling pathways in APCs in response to HSPs. Asea and colleagues demonstrated that recombinant hsp70 could signal through TLR-2 and TLR-4 with the involvement of CD14 [82]. Vabulas et al. observed that IL-12p40 production by RAW264.7 macrophages in response to hsp70 was partially abrogated by knocking out MyD88 and TRAF6, components of the downstream TLR-4 signalling cascade. Transfection of 293T cells with TLR-2 alone or with TLR-4 and its co-receptor MD-2 led to a large increase in NF- $\kappa$ B signalling. Diminished IL-12p40 and TNF $\alpha$  production from TLR-4, but not TLR-2, knockout mice provided further support for TLR-4 mediated signalling by hsp70 [83]. These authors have also described a role for TLR-2 and TLR-4 in gp96-mediated activation of DCs, and that this activation is dependent on endocytosis of gp96 [84]. Further evidence of a role for TLR-4 in hsp70 signalling came from Dybdahl et al. [85], who demonstrated that macrophages from mice deficient in TLR-4 did not produce TNF $\alpha$  in response to recombinant human hsp70, whereas macrophages from normal mice did. These authors also noted that antibodies against CD14 or TLR-4 blocked production of IL-6 by human monocytes in response to hsp70.

TLRs have also been implicated in interactions between APCs and human hsp60. Vabulas et al. [86] demonstrated that human hsp60 led to NF- $\kappa$ B and TNF $\alpha$



production by 293T cells transfected with TLR-2 or TLR-4 and MD-2. Hsp60 also activated JNK and IKK kinase signalling and TNF $\alpha$  production by RAW264.7 macrophages. This effect was partially abrogated by knocking out MyD88 or TRAF6. Ohashi et al. [87] used mice deficient in TLR-4 to demonstrate that TNF $\alpha$  and IL-6 production by mouse macrophages in response to human hsp60 was dependent on TLR-4.

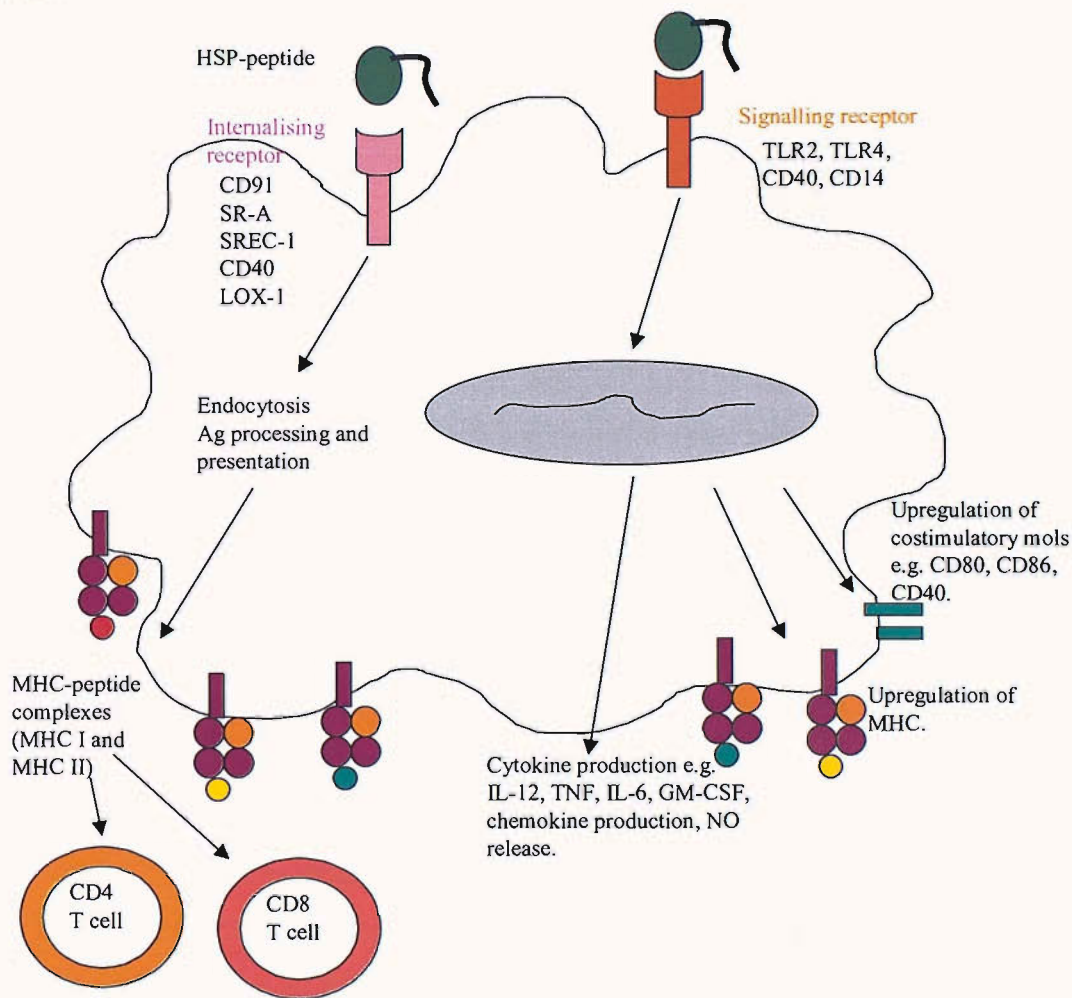


**Figure 1.9** HSP-APC interactions integrate innate and adaptive immune responses.

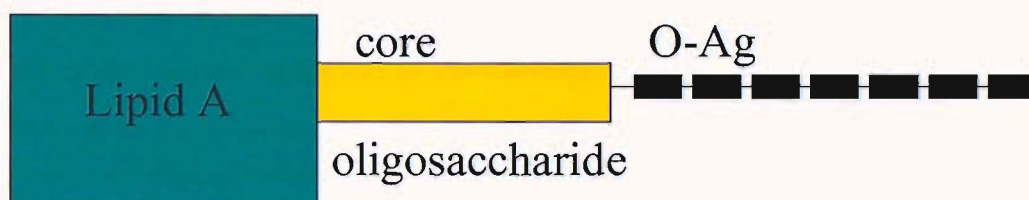
Thus, a number of receptors involved in signalling by HSPs and in HSP uptake by APCs have been identified. A summary of these data are shown in figure 1.9 (adapted from [27]), and a comprehensive review can be found in [68].

The precise roles of each of the described receptors remains unclear, but it seems likely that HSPs exert their effects on APCs through a combination of various receptors. Uptake seems to be mainly mediated by SRs, such as CD91, SR-A and SREC-1. Activation may be mediated by TLRs, CD14 or CD40, as none of the

uptake receptors are known to be signalling receptors. Our knowledge of other innate immune activators suggests a level of redundancy is likely to maximise the likelihood of an appropriate response being generated.

### 1.2.5 The endotoxin debate

As HSP receptors were identified, it did not escape notice that many of these receptors were already known as receptors for bacterial products, particularly LPS,



which is known to bind CD14 and TLR-2 and -4.

**Figure 1.10** The structure of bacterial LPS. LPS is composed of a polar heteropolysaccharide chain covalently linked to a non-polar lipid moiety, Lipid A. Lipid A anchors the LPS into the outer bacterial membrane, and is highly conserved between different genera of bacteria, while the core polysaccharide and O-antigen are exposed to the surrounding solution. The O-antigen consists of repeating oligosaccharide units, specific for each bacterial strain – this determines the serological identity of the bacterium.

The term endotoxin was coined by Pfeiffer to describe the class of lipopolysaccharides, which, in conjunction with proteins and phospholipids, constitute the outer membrane of Gram-negative bacteria and are also extremely common contaminants of protein solutions. Endotoxins are integral components of the bacterial cell wall, essential for bacterial growth and viability. They play a vital role in the organisation, stability and barrier function of the outer membrane and protect bacteria against antibiotics, phages, proteases and complement factors.

The structure of bacterial LPS is shown in figure 1.10. All endotoxin variants are composed of a polar heteropolysaccharide chain covalently linked to a non-polar lipid moiety, lipid A, which anchors the endotoxin into the outer membrane of bacteria. The heteropolysaccharide, composed of a core oligosaccharide and an O antigen (O-Ag), is exposed to the surrounding solution and determines the serological identity of the bacterium. The O-Ag is made up of repeating oligosaccharide units, which are specific for each bacterial strain, and are completely absent in some strains. The characteristic chemical structures of the core oligosaccharide are 2 saccharides only

found in bacterial LPS, 2-keto-3-deoxyoctonic acid and L-glycero-D-manno-heptose. Lipid A is the most conservative part of endotoxins from different bacterial genera, and consists of a  $\beta$ ,1-6 linked disaccharide of glucosamine, covalently linked to 3-hydroxy-acyl substituents with 12-16 carbon atoms via amide and ester bonds, which may be further esterified with simple fatty acids. The core region close to lipid A, and lipid A itself, are partially phosphorylated, thus causing endotoxin molecules to exhibit a net negative charge at neutral pH.

The endotoxin content of solutions is measured by Limulus Amebocyte Lysate (LAL) assay and its activity measured in international units per ml (IU/ml) or endotoxin units per ml (EU/ml). Levels of endotoxin contamination in protein solutions are commonly given as EU/mg protein. Even very small levels of endotoxin in protein solutions can have dramatic effects on APCs, so it is important to remove as much contamination as possible. This is achieved using Polymyxin B, a cyclic antibiotic that binds to LPS with high affinity, either by adding Polymyxin B directly to culture medium, or by running contaminated proteins over columns of Polymyxin B conjugated to agarose beads.

Attempts have recently been made to determine whether the reported immunostimulatory effects of HSPs are real or merely an artefact caused by endotoxin contamination of HSP preparations. Gao and Tsan [91] compared the effects of recombinant human hsp70 with the same preparation that had been run over a Polymyxin B-agarose column to remove contaminating LPS. Although both hsp70 preparations appeared identical by SDS-PAGE and western blot, and were both functional, as assessed by their ability to uncoat clathrin; the untreated hsp70 induced TNF $\alpha$  production by monocytes and macrophages in a manner similar to LPS, whereas the low-endotoxin hsp70 did not. TNF $\alpha$  stimulation by the untreated hsp70 could be abrogated by addition of Polymyxin B to cultures. In another study, Bausinger et al. [92] compared recombinant human hsp70 with three levels of endotoxin contamination. Untreated hsp70 (400-4500 IU/mg endotoxin) induced maturation of human monocyte-derived DC at a concentration of 3 $\mu$ g/ml, which could be abrogated by addition of polymyxin B, whereas low endotoxin hsp70 (56 IU/mg) did not enhance CD83 expression but did produce low levels of IL-6, which could be enhanced by addition of CD14. Very low endotoxin hsp70 (<10 IU/mg) did



not induce CD83 expression, IL-6 production or MAPK signalling, even in the presence of CD14. Both low and very low endotoxin hsp70 preparations were, however, able to mediate cross-presentation of an ovalbumin-derived peptide. These results suggest that, in the absence of contaminating endotoxin, hsp70 does not activate APCs, but does still act as a chaperone.

Reed et al. [93] subsequently investigated the role of endotoxin in gp96-elicited macrophage activation. The authors found that gp96 bound to endotoxin in a high-affinity, saturable and specific manner and subsequently generated low endotoxin gp96 and CRT. Low endotoxin gp96 retained its native conformation, ligand binding activity, and *in vitro* chaperone function, but was unable to activate NF- $\kappa$ B signalling, nitric oxide production or inducible nitric oxide synthase production by macrophages, all of which are potently induced by LPS. Both low endotoxin gp96 and CRT did, however, elicit a marked increase in ERK phosphorylation. These results indicated that CRT and gp96 do have some effects on APCs, but that some of the reported effects might be caused by endotoxin.

Taken together, these studies are cause for concern over the role of endotoxin contamination in the reported immunostimulatory properties of HSPs. Further studies are required to fully elucidate the role of endotoxin in APC activation by HSPs, and the possibility of contamination should be considered when interpreting results of previous work. Great care is now being taken by all groups working on the effects of HSPs to use pure preparations, which have been thoroughly tested and treated to remove all traces of endotoxin, and it should be mentioned that some studies using stringent controls to rule out endotoxin contamination have still demonstrated APC activation. An evaluation of the signalling receptor data with regard to endotoxin contamination indicate that the TLR data are fairly robust and well controlled to account for endotoxin contamination. As CD14 can act in concert with TLRs this may explain its reported involvement.

### **1.2.6 Trafficking of heat shock proteins and chaperoned peptides within APCs**

The results previously described demonstrate that exogenously delivered HSP-peptide complexes can elicit MHC Class I-restricted CD8<sup>+</sup> T cell responses. This presentation of HSP-chaperoned peptides on MHC Class I molecules is an example

of cross-presentation, a process described in section 1.1.6 of this thesis. As discussed in that section, there appear to be 2 mechanisms by which exogenous Ags can gain access to the MHC class I presentation pathway, the phagosome-to-cyotsol pathway and the vacuolar pathway, and a number of groups have carried out studies to elucidate the pathway(s) utilised by HSP-chaperoned peptides.

It has been demonstrated that only macrophages and dendritic cells are capable of re-presentation of HSP-chaperoned peptides; non-professional APCs such as fibroblasts and B cells do not re-present these peptides [94]. It has also been demonstrated that re-presentation is sensitive to brefeldin A and does not occur by transfer of peptides from HSPs to Class I on the cell surface [94]. In 1999, Arnold-Schild et al. [69] demonstrated that endocytosed gp96-peptide complexes enter an endosomal compartment, further demonstrated by Suto and Srivastava to be non-acidic [94]. Basu et al. showed that processing of the peptides associated with gp96 was TAP- and proteasome-dependent, thus suggesting involvement of the cytosolic processing pathway, although a mechanism for peptide entry to the cytosol was not identified [71]. Work from Castellino and colleagues demonstrated that, following receptor mediated endocytosis of hsp70-peptide complexes, peptide processing and presentation on MHC Class I molecules could occur by either TAP-dependent or – independent mechanisms, depending on the structure of the peptide [95]. More recently, Tobian et al. [74] investigated cross-presentation of peptides chaperoned by bacterial HSPs, and found that this occurred by cytosolic (TAP-dependent) mechanisms in DCs, but by vacuolar (TAP-independent) mechanisms in macrophages. In both cases, cross-presentation was CD91-dependent. Part of these findings were supported by work from Palliser et al. [51], who demonstrated that only a small fraction of peptides from soluble heat shock fusion proteins that entered DCs by RME were cross-presented, and that this occurred in a proteasome- and TAP-dependent manner. Thus, the majority of work seems to support a cytosolic mechanism for processing of HSP-chaperoned peptides, although how the peptides gain access to the cytosol is an issue that still requires resolving.

### 1.3 Calreticulin

Calreticulin (CRT) is an abundant 46-kDa protein, resident in the lumen of the endoplasmic reticulum (ER). It is a highly conserved protein, found in a wide range of species and in all nucleated cell types. Calreticulin is a major intracellular calcium binding protein, displays lectin activity, and is known to participate in the folding and assembly of nascent glycoproteins [96-98]. Calreticulin has also been shown to serve an essential function in the regulation of peptide assembly onto nascent MHC class I molecules [99].

#### 1.3.1 The structure of CRT

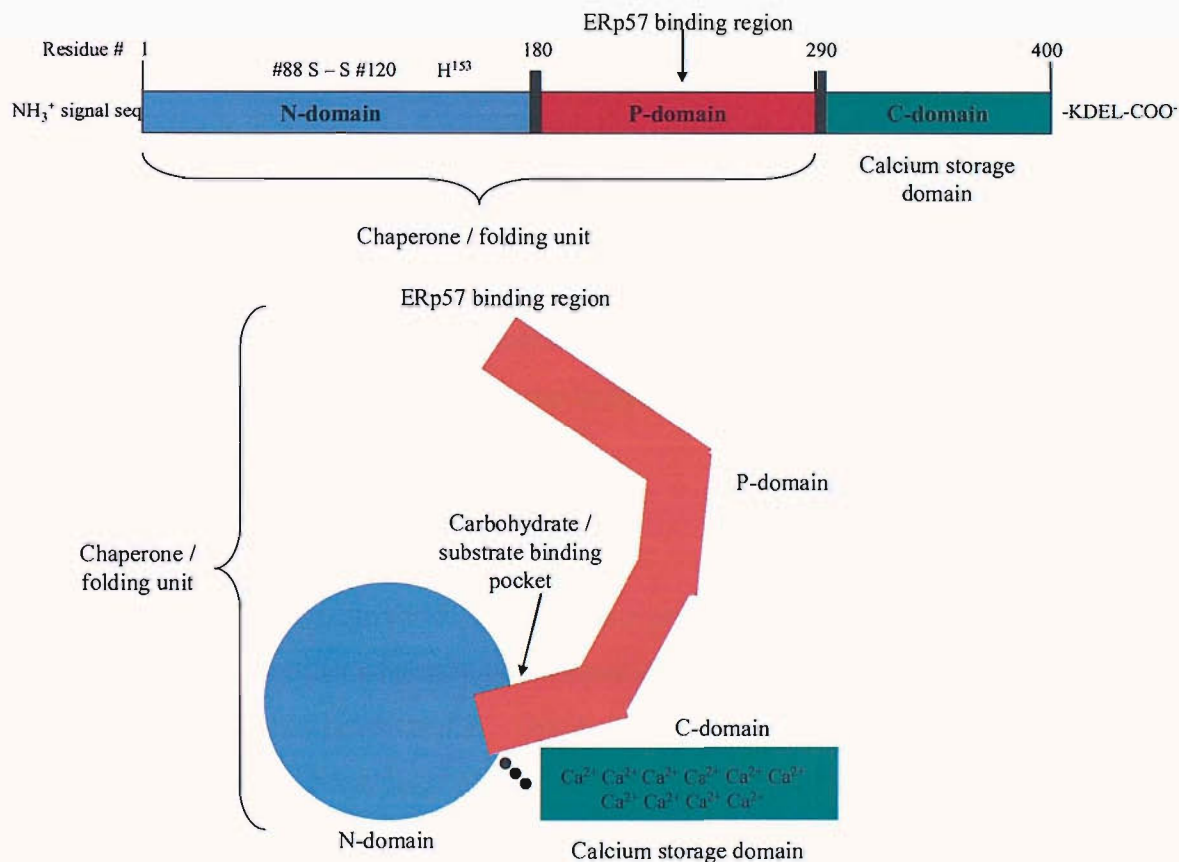


**Figure 1.11** Linear representation of CRT domains (A) and model of 3D structure (B). Adapted from [98].

Figure 1.11 (adapted from [98]), shows a linear representation of the 3 domains of CRT (A) and a model of the 3D structure (B). The N-domain (residues 1-180), believed to form a globular structure made up of 8 anti-parallel  $\beta$ -strands with a single disulfide bond, binds heavy metals and interacts *in vitro* with other ER chaperones, with the DNA-binding domain of nuclear receptors, and with nucleic acids. The N-domain and P-domain together are responsible for the chaperone function of CRT. The  $\text{His}^{153}$  residue shown in the diagrams has been shown to be

essential for chaperone function [100] and is found at the top of a loop in a  $\beta$ -strand at the interface between the N- and P-domains. It is thought that this loop may significantly influence the shape of the substrate-binding pocket.

The P-domain (residues 181-290) consists of 3 short helices, six short  $\beta$ -strands arranged as 3 anti-parallel  $\beta$ -sheets, and two sets of amino acid repeats. It contains a proline-rich region and forms an extended arm structure. This domain interacts with other chaperones in the ER lumen, as well as forming the substrate-binding pocket in concert with the N-domain.

The C-domain (residues 292-400) is highly acidic and binds  $\text{Ca}^{2+}$  with high capacity. This domain is involved in  $\text{Ca}^{2+}$  storage in the ER lumen. At present, no structural information is available for the C-domain.

CRT is proposed to have many functions, both intra- and extra-cellular. These functions are comprehensively reviewed in references [96-98, 101]. Selected functions of CRT of particular relevance to this project are described below.

### **1.3.2 Homeostatic functions of CRT**

#### *i) Molecular chaperone*

Calreticulin is involved in the folding of many proteins and glycoproteins (reviewed in [98, 102]). A number of newly synthesised proteins are targeted for N-linked glycosylation as they cross the ER – this involves addition of the nascent oligosaccharide  $\text{Glc}_3\text{Man}_9\text{GlcNAC}_2$  to the protein by a translocon-associated enzyme oligosaccharyl transferase (OST). CRT binds via its lectin site to the monoglucosylated high mannose oligosaccharide ( $\text{Glc}_1\text{Man}_9\text{GlcNAC}_2$ ) generated following cleavage of the terminal glucose by glucosidase I and the second glucose residue by glucosidase II. CRT and calnexin form complexes with Erp57 and together with glucosidase II and a UDP-glucose:glycoprotein transferase (UGGT) that can re-glucosylate glucose-trimmed chains, the chaperones form a cycle of de-glucosylation and re-glucosylation that ensures correct folding of the glycoprotein. When glucosidase II removes the third glucose in a time-dependent manner, the glycoprotein is released from the chaperones. UGGT can discriminate between folded and unfolded proteins, and only adds a new glucose residue to unfolded proteins, thus

enabling them to bind to CRT and calnexin again. This cycle is repeated until the glycoprotein is properly folded. It is thought that changes in the ER, such as changes in the concentration of  $\text{Ca}^{2+}$ ,  $\text{Zn}^{2+}$  or ATP, may affect the formation of chaperone complexes.

Repeated entries into this cycle are ended when excessive mannose removal from the glycan by mannosidases in the ER and *cis* Golgi prevents re-glucosylation. The glycoprotein is then recognised by EDEM and transported to the Sec61 pore, which translocates it into the cytosol, where it is degraded by proteasomes. This is termed ER-associated degradation (ERAD), and may play a role in the generation and selection of appropriate peptides for loading onto MHC class I molecules in the ER [14, 102].

*ii) MHC class I loading – role in the peptide loading complex*

As described in section 1.1.5, CRT plays an important role in the MHC class I peptide-loading complex [99, 103]. In the absence of calreticulin, MHC class I rapidly exits the ER, presents endogenous antigen poorly and has greatly reduced surface levels [104]. CRT binds to the MHC class I- $\beta_2\text{m}$  heterodimer *in vivo*, although *in vitro* interactions appear to be less dependent on the assembly status of class I [105]. The association of both CRT and MHC class I with the peptide-loading complex have been shown to be inhibited by castanospermine, indicating involvement of N-linked glycans in these associations. Cresswell's group have shown that almost all MHC class I heavy chains associated with the peptide-loading complex have monoglucosylated N-linked glycans and that interaction of CRT with class I heavy chain was dependent on the presence of these [14, 105]. This is the main evidence behind the theory that CRT binds the MHC class I- $\beta_2\text{m}$  heterodimer and that this complex subsequently associates with the TAP-ERp57-calnexin core of the peptide-loading complex, as described in section 1.1.5.

The CRT-calnexin-ERp57 folding cycle described in the previous section may also be involved in determining whether the MHC molecule contains a peptide and is correctly folded, although as yet there is no direct evidence for this.

### *iii) $\text{Ca}^{2+}$ homeostasis*

CRT plays an important role in  $\text{Ca}^{2+}$  homeostasis, as it is an important  $\text{Ca}^{2+}$  binding protein and buffers  $\text{Ca}^{2+}$  levels within the ER. Elevated levels of CRT increase cellular stores of  $\text{Ca}^{2+}$  and also alter store-operated  $\text{Ca}^{2+}$  influx. One of the major cellular functions affected by  $\text{Ca}^{2+}$  levels is apoptosis [102]. HeLa cells over-expressing CRT have an increased sensitivity to thapsigargin and staurosporine induced apoptosis, and over-expression of CRT in human embryonic kidney cells (HEK-293) results in increased ER  $\text{Ca}^{2+}$  levels, increased amounts of  $\text{Ca}^{2+}$  available for release, increased release of cytochrome c and increased susceptibility to apoptosis. Contrastingly, CRT-deficient cells showed decreased cytochrome c release and reduced sensitivity to apoptosis. These data correlate with evidence that over-expression of the Bcl-2 survival protein in prostate cancer epithelial cells leads to a reduction in levels of both CRT and SERCA, a transporter which transfers  $\text{Ca}^{2+}$  from the cytoplasm to the ER. CRT-deficient cells have a decreased capacity for  $\text{Ca}^{2+}$  storage in the ER and impaired agonist-mediated  $\text{Ca}^{2+}$  release. The CRT-knockout mouse is embryonically lethal at around 14.5 days gestation and this is due to impaired  $\text{Ca}^{2+}$ -dependent signalling pathways, demonstrating the importance of this function of CRT.

### **1.3.3 Extracellular functions of CRT**

As well as these intracellular homeostatic functions, CRT has also been reported to have a number of extracellular effects on a variety of cell types.

#### *i) Cell adhesion*

It has been demonstrated that CRT can bind the KxGFFKR motif within the C-terminal tail  $\alpha$ -subunits of integrins and thus regulate integrin-mediated adhesion [106]. Interaction between integrins and CRT can be induced by integrin activation [107]. Murine CRT-null ES cells show severely impaired integrin-mediated adhesion to extracellular matrix proteins fibronectin and laminin, and integrin-mediated calcium influx from extracellular sources [108]. CRT also appears to affect cell-substratum adhesion that is dependent on formation of focal adhesions [109].

The mechanism(s) by which CRT modulates integrin function are not yet clear, and there is some debate as to whether the effects are mediated by direct interaction of

CRT with the cytoplasmic tails of integrins, or through indirect effects mediated by CRT signalling from within the ER. Evidence for the latter comes from reports that CRT can increase expression of vinculin, a molecule associated with adhesion, in the cytosol indirectly from the ER, thus altering the formation of focal adhesions [110]. However vinculin levels are not altered in CRT-null ES cells [97], a fact that raises questions about the relevance of these findings. CRT has also been shown to affect the total cellular levels of phosphotyrosine from within the ER [109], and there is a well established correlation between this level and cell adhesiveness. It has also been suggested that CRT may bind directly to integrins, thus helping to stabilise integrins conformationally as part of an “early adhesion complex”. It is proposed that this transient interaction could allow for  $\text{Ca}^{2+}$  influx and promote downstream signalling events that permit establishment of focal plaques [97]. This direct interaction of CRT with integrins has been shown to occur at the cell surface [101]. Although CRT is normally an ER-localised protein, its presence at the cell surface has been demonstrated in a variety of cell types [101]. How CRT may escape the ER is discussed in section 1.3.5.

As well as binding integrins, cell surface CRT can bind the extracellular matrix proteins Bb fibrinogen and laminin. Anti-CRT Abs have been shown to prevent spreading of B16 cells and block neurite formation in differentiating NG-108-15 cells [101]. Further evidence for an important role for cell surface CRT in adhesion comes from findings that thrombospondin-induced disassembly of focal adhesion in endothelial cells is mediated by cell surface CRT [111]. The same authors demonstrated that this effect was mediated by the N-terminal domain of CRT [112]. Interestingly, it was subsequently demonstrated that this is mediated by CD91 [113]. It is thought that cell surface CRT may signal through CD91 as part of a co-receptor complex. These authors also demonstrated that signalling through this complex stimulates both random and directional cell migration, to be expected if cell adhesion is reduced [114]. CRT-thrombospondin 1 interaction also appears to play an important role in induction of T cell motility [115], an effect apparently mediated by signalling through CD47.

Related to these findings, CRT and its N-terminal fragment have been reported to inhibit angiogenesis and suppress tumour growth [116, 117]. This was achieved by

specific inhibition of the proliferation of endothelial cells by CRT [118]. Since tumour growth and formation of metastasis depend on generation of new blood vessels in order to maintain an adequate blood supply, disruption of this process may be of great importance for development of anti-cancer therapy, and CRT is under investigation for this purpose [117, 119-121]. In evidence of the highly conserved nature of CRT, it has been demonstrated that CRT from the parasite *Trypanosoma cruzi* also has an anti-angiogenic effect in an *in vivo* assay measuring inhibition of angiogenesis in the chorioallantoic membrane (CAM) of chick embryos [122].

## ii) Phagocytosis

Several reports support a role for CRT in phagocytosis. CRT expressed at the cell surface is a receptor for the complement component C1q [123-125]. Ogden and colleagues demonstrated that C1q and mannose binding lectin (MBL) opsonise apoptotic cells and subsequently interact with CRT on phagocytic cells. As in the cell adhesion studies, CRT was found to form a complex with CD91, and stimulation of this CRT/CD91 complex by C1q/MBL induced ingestion of the apoptotic cells [126]. Interestingly, the same group have recently shown that CRT on the surface of apoptotic cells can directly bind CD91 on phagocytic cells and stimulate engulfment of the apoptotic cells [127]. The authors found that CRT was upregulated and redistributed in apoptotic cells. As CRT can be found on the surface of many cell types, why does it not constantly stimulate phagocytosis of these cells? The authors propose that on non-apoptotic cells, activation of SIRP- $\alpha$  by CD47 blocks apoptosis, but in apoptotic cells, CD47 appears to be down-regulated and also to be redistributed into patches away from the pro-apoptotic CRT and phosphatidylserine. This involvement of CD47 is interesting, considering its role in CRT-thrombospondin-induced T cell motility mentioned earlier [115].

A recent study by Chen et al. [128] demonstrated that apoptosis of rabbit kidney cells induced by the bacterial cell wall component muramyl dipeptide (MDP) was mediated by cell surface CRT in a  $\text{Ca}^{2+}$ -dependent manner. The authors further suggested that the signal induced by CRT-MDP binding was transduced through TNF-receptor 1 (TNFR1) and TNFR-associated death domain protein (TRADD), which were both found in complex with CRT on the membrane of the apoptotic cells.



These findings indicate that CRT can not only induce phagocytosis of apoptotic cells, but may also be involved in the actual induction of apoptosis.

Cell surface CRT has also been shown to affect phagocytosis of yeast cells by insect hemocytes [129]. In the phagocytic microorganism *Dictyostelium*, intracellular CRT affects the efficiency of uptake of yeast particles [130], possibly by its effects on intracellular  $\text{Ca}^{2+}$  levels, which are important for the cytoskeleton remodelling required for pseudopodia formation during phagocytosis. Muller-Taubenberger et al. [131] have demonstrated that elimination of CRT and calnexin in *Dictyostelium* does not significantly impair adhesion of yeast particles to the phagocyte surface, but that uptake of these particles was significantly impaired. A direct link was shown between the ER and the phagocytic cup, and it was again proposed that impaired  $\text{Ca}^{2+}$  storage in the absence of CRT and calnexin was likely to be responsible for impaired phagocytosis.

#### **1.3.4 Cellular localisation of CRT**

It is well known that CRT is concentrated within the ER lumen and plays a number of important roles within this organelle, as described in section 1.3.3. However, as described in the previous section, CRT is also involved in a number of functions that require it to function at the cell surface (as C1q receptor, in phagocytosis) and possibly in the cytosol (interaction with integrin tails). The sequence on the cytoplasmic tails of integrins that interacts with CRT is also found in the DNA binding domain of nuclear receptors, such as those for glucocorticoids, androgen, retinoic acid and vitamin D. CRT has been demonstrated to antagonise nuclear receptor transcription activity and to block nuclear receptor binding to DNA response elements, suggesting that nuclear CRT may limit interactions of nuclear receptors with promoter elements. CRT has also been shown to stimulate nuclear export of glucocorticoid receptor *in vitro*, and export of this receptor is deficient in CRT-deficient cells (cited in [132]).

All of this data indicates that distribution of CRT is not restricted to the ER. The question is how does CRT move from the ER to the cell surface, or to other areas within the cell, such as the cytoplasm or nucleus? There is evidence that cell-surface CRT traffics through the secretory pathway (reviewed in [101]), although it is unclear

how CRT escapes the influence of its ER-retention sequence, KDEL. Theories on this mechanism are discussed and evidence cited in [101] and include cleavage of the KDEL sequence, transporting of CRT to the cell surface in complex with KDEL receptor, saturation of the ER-retention machinery and glycosylation of CRT under stress conditions. The mechanisms by which CRT accesses the cytosol or nucleus are even less clear, and pose more of a problem. Subcellular fractionation has been used to demonstrate the existence of a cytosolic pool of CRT (cited in [132]). In a recent study [132], Afshar and colleagues set out to determine whether this cytosolic pool of CRT resulted from synthesis of CRT outside the ER or on relocalisation of CRT from the ER to the cytosol. They found that during synthesis of CRT, it was fully inserted into the ER, and was subsequently retrotranslocated to the cytoplasm. The C-terminal  $\text{Ca}^{2+}$ -binding domain appeared to be important for retrotranslocation and the process was ubiquitin- and proteasome-independent, indicating that retrotranslocation was not merely a result of ERAD. Interestingly, cytosolic CRT was resistant to trypsin digestion in the absence of  $\text{Ca}^{2+}$ , whereas ER-resident CRT is normally trypsin-sensitive under these conditions and becomes trypsin resistant in the presence of  $\text{Ca}^{2+}$ , presumably as a result of a  $\text{Ca}^{2+}$ -induced conformational change [133]. Cytosolic CRT thus appears to undergo some form of  $\text{Ca}^{2+}$ -independent conformational change, although the nature and cause of this are as yet unknown.

Despite these studies, our knowledge of the intracellular trafficking pathways of CRT is still very limited, and much more research is required in these areas in order to answer all of the questions raised.

## 1.4 Calreticulin as an immunostimulatory HSP

Numerous studies have provided evidence that HSPs play an important role in many aspects of the immune system. These highly conserved, ubiquitous proteins are released from cells undergoing death by necrosis and the observations that they bind peptides and can interact with APCs to influence immune responses have important therapeutic implications. HSPs are the first identified adjuvants of mammalian origin and, being self-antigens, do not elicit immune responses against themselves. The immunogenicity of HSP-peptide complexes in many systems has significant implications for vaccination against infection and also for treatment of pre-existing disease. Further research into the mechanisms by which HSP-chaperoned peptides are processed and presented by APCs should give a greater insight into how they influence immune responses and enhance the potential for practical therapeutic use.

Compared to hsp70 and gp96, the role of CRT in inducing immune responses has been studied relatively poorly, particularly its adjuvant properties. Interest was raised in the role of CRT as a chaperone by observations that TAP-transported peptides associated with CRT in the ER lumen [103]. Subsequent studies identified CRT as a peptide binding protein and indicated that CRT-bound peptides can be re-presented on dendritic cell MHC class I molecules, inducing specific CTL responses [134]. As with the other HSPs, it was shown that CRT preparations from tumours elicit specific immunity to the source tumour but not to antigenically distinct tumours and that the immunogenicity is due to the peptides associated with the CRT molecules rather than the CRT molecules themselves [38]. These findings led to the assumption that, as was believed for hsp70 and gp96, CRT has direct stimulatory effects on APCs as well as delivering bound peptides for presentation as no exogenous adjuvant was used in these studies. However, no such function of CRT has directly been demonstrated. As described in section 1.2.5, there is evidence from Nicchitta's group that low endotoxin CRT induced an increase in ERK phosphorylation in macrophages, but did not induce production of iNOS or NO, nor activate NF- $\kappa$ B signalling [93]. Also, as described in section 1.2.4, while CRT has been shown to bind to SR-A and SREC-1 and possibly CD91, these are all uptake rather than signalling receptors, and no data on CRT binding to receptors such as TLRs that are likely to induce APC activation have been published to date. Thus there is a large gap in the data relating to the

immunostimulatory effects of CRT that result in the observed *in vivo* immune responses.

Our interest in CRT was further enhanced by previous work in the laboratory. Golgher et al [135] generated CD4<sup>+</sup> T cells against the murine CT26 colon cancer and found that three independent CT26-specific CD4<sup>+</sup> hybridomas recognized the env gene product gp90. The CD4<sup>+</sup> response was completely tumour-specific in that the same glycoprotein expressed by different tumours was not recognised by the CT26-specific hybridomas. Recognition of the CT26 gp90 was dependent on glycosylation, not on primary sequence alterations. Inhibition of N-glycosylation by tunicamycin treatment of CT26 or enzymatic deglycosylation of gp90 completely abrogated recognition. Deglycosylation prevented a fraction of misfolded gp90 in the endoplasmic reticulum from binding to CRT. It was found that this was the primary reason for loss of antigenicity, and that immunoprecipitates of CRT from CT26 (which co-precipitates gp90) were far more potent antigens compared to immunoprecipitates of gp90 (which co-immunoprecipitates very little CRT). This was the first demonstration of CRT acting as an immunogen for CD4<sup>+</sup> T cells by binding to immunogenic peptides and has paved the way for further investigations into the mechanisms behind this phenomenon.

These data suggest a potentially important immunostimulatory role for CRT and, combined with data relating to its role in phagocytosis and anti-angiogenesis, mark CRT as a promising target for cancer immunotherapies. The aim of my project was to further study and dissect the adjuvant and antigen-chaperoning functions of murine CRT in a mouse model system, in order to expand our knowledge of these functions of CRT and of HSPs in general, and also to provide a valuable insight into the effects of autologous HSPs on the immune response, an area that has been relatively under investigated in the published literature, which often focuses on the effects of bacterial HSPs in mammalian systems.

## 2. Materials and Methods

### 2.1 Mice

C57Bl/6 mice were bred and housed in local animal facilities. DBA/2 mice were obtained from Harlan laboratories UK and housed in local animal facilities. OT-II mice on the C57Bl/6 background express a transgenic TcR that recognizes OVA<sub>323-339</sub> peptide in the context of MHC II (I-A<sup>b</sup>), and were a gift from David Gray, Edinburgh. OT-I mice on the C57Bl/6 background express a transgenic TcR that recognizes OVA<sub>257-264</sub> (SIINFEKL) in the context of MHC I (H-2K<sup>b</sup>). All transgenic mice were bred and housed in local animal facilities. All mice were used at 6-12 weeks of age. All animal procedures followed University of Southampton and UK Home Office regulations.

### 2.2 Reagents

Lipopolysaccharide (LPS) from *S.typhosa*, ovalbumin (OVA) protein, BSA and Polymyxin B-Agarose were purchased from Sigma. SIINFEKL peptide was synthesised by GL Biochem (Shanghai) Ltd. CpG-containing phosphorothioate-modified oligonucleotides ODN1668 5'-TCCATGACGTTTCCTGATGCT-3' and control ODN1720 5'-TCCATGAGCTTCCTGATGCT-3' were synthesised by MWG Biotech (Germany). Recombinant murine GM-CSF and TNF- $\alpha$  were purchased from Peprotech Inc. Low endotoxin recombinant murine Hsp70-A2 was purchased from Stressgen Biotechnologies. Monoclonal antibody to human LRP/ $\alpha_2$ macroglobulin receptor ( $\alpha$ -CD91) was purchased from Progen. Human  $\alpha_2$ macroglobulin was purchased from BioCentrum (Krakow, Poland). Maleylated BSA was a kind gift from N. Platt (University of Southampton). Calregulin (C-17) antibody was purchased from Santa Cruz Biotechnology Inc. Rabbit  $\alpha$ -CRT (PA3-900) was purchased from Affinity BioReagents. Rabbit  $\alpha$ -OVA was a kind gift from Alison Tutt (Tenovus Research Institute, Southampton, UK).  $\alpha$ -rabbit-HRP and  $\alpha$ -goat-HRP were purchased from Sigma.  $\alpha$ -rabbit-texas red was purchased from Jackson Labs. Alexa-Fluor 488 was from Molecular Probes. Collagenase D was from Roche.

## **2.3 Tissue culture and cell biology**

### *2.3.1 Cell lines and tissue culture*

Murine CRT was purified from the murine mastocytoma cell line P815. These cells were cultured in pre-warmed and aerated complete RPMI (RPMI-1640 medium (Gibco) supplemented with 10% foetal calf serum (Gibco), 1% each of penicillin/streptomycin/glutamine, sodium pyruvate and non-essential amino acids (Gibco) and 50 $\mu$ M 2-mercaptoethanol (Sigma)) in roller bottles at 37°C. Cells were harvested and pellets frozen at -80°C twice a week.

The semi adherent murine DC-like cell line, DC2.4 was cultured in 0.22 $\mu$ m filtered R10 medium (RPMI 1640 medium supplemented with 10% Heat Inactivated Foetal Calf Serum (HI-FCS) (Gibco) and 1% penicillin/streptomycin/glutamine) at 37°C, 5% CO<sub>2</sub> for up to 25 passages. The murine macrophage cell line J774 and the CRT-null fibroblast cell line K42 were also maintained in R10. The SIINFEKL-specific T cell hybridoma cell line, B3Z, was cultured in B3Z medium (RPMI 1640 medium – L-glutamine supplemented with 10% HI-FCS, 1% penicillin/streptomycin/glutamine, 1% sodium pyruvate and 50 $\mu$ M 2-mercaptoethanol), at 37°C, 5% CO<sub>2</sub> for up to 25 passages.

### *2.3.2 Purification and Culture of Bone-marrow Derived Dendritic Cells*

Bone marrow cells were prepared from the femurs of 4-12 week old C57Bl/6 mice and cultured according to the method of Lutz et al. [136]. Briefly, femurs were removed and as much muscle tissue as possible cleaned from the bones, which were then disinfected in 70% EtOH for 2-5min and washed in PBS. From now on worked in tissue culture hood. Both ends of bones were cut and marrow flushed out with PBS using 10ml syringe and 19.5 gauge needle. Clumps of marrow were passed through needle several times to disintegrate. Cells were resuspended and passed through cell strainer into 50ml Falcon tube. Rinsed petri dish with 2ml PBS and passed this through cell strainer into same tube. Spun 1200rpm for 5min at room temp. Aspirated supernatant and resuspended cells in 10ml DC media (RPMI-1640 supplemented with 10% heat-inactivated and filtered FBS (autogen bioclear), 1% Pen/Strep/Glu, 1xNEAA, 1xSodium pyruvate and 50 $\mu$ M 2-mercaptoethanol). Counted cells, resuspended at 2x10<sup>5</sup> cells/ml in DC media, supplemented with 20ng/ml GM-CSF,

plated in bacteriological petri dishes at 10ml/dish and incubated at 37°C, 5%CO<sub>2</sub>. On day 3, added 10ml DC media supplemented with 20ng/ml GM-CSF to each plate, returned to incubator. On day 6 and day 8, half the supernatant was removed from each plate, spun at 1300rpm for 5 minutes, aspirated supernatant and resuspended pellets in 10ml DC media plus 20ng/ml GM-CSF per plate and returned 10ml to each plate. Plates returned to incubator. Cells were used for assays on day 8 (in which case day 8 feed was not carried out), day 9 or day 10.

### *2.3.3 Isolation of splenic dendritic cells*

For assays using freshly isolated splenic DCs, spleens were taken from 6-12 week old C57Bl/6 mice and CD11c<sup>+</sup> cells isolated by magnetic cell separation (Miltenyi Biotec, Germany) according to the manufacturers instructions. Each spleen was placed in a 6cm petri-dish in 5ml 1mg/ml solution of Collagenase D in HBSS, and injected with a further 500µl of this solution using a 1ml syringe and 25-gauge needle. Spleen was cut into 5-6 pieces with scissors and incubated in the Collagenase D solution at 37°C for 45 minutes then the solution and spleen pieces were passed through a 70µm cell strainer, using a syringe plunger to mash the large pieces through, to obtain a single cell suspension. White blood cells were isolated by spinning over a 1:1 volume of Ficoll, washed in buffer (PBS, 0.5% BSA, 2mM EDTA), counted, suspended in 1:5 mAb conjugated microbeads (CD11c (N418)) in buffer and incubated at 4°C for 15 minutes. Cells were washed with buffer to remove unbound mAb and then passed through an LS column on a magnetic field. Unlabelled cells were washed through with buffer, then the column was removed from the magnetic field and labelled cells eluted with buffer. Positive cells were counted and resuspended at appropriate concentration in DC media.

### *2.3.4 T Cell Purification*

Lymphocytes were purified from the spleens of OT-I or OT-II mice. DC media was used as culture medium. Single cell suspensions were obtained by passing through a 70µm cell strainer then white blood cells were isolated by spinning over 1:1 volume of Ficoll. Where indicated, CD8 or CD4 cells were purified by magnetic cell separation (Miltenyi Biotec, Germany) according to the manufacturers instructions. Briefly, lymphocytes were suspended in MACS buffer (0.5% BSA in PBS) and

incubated at 4°C for 15 minutes with 1:10 mAb conjugated microbeads (CD4 (L3T4) or CD8 (Ly-2)). Cells were washed with MACS buffer to remove unbound mAb and passed through an LS column on a magnetic field. Unlabelled cells were washed through with MACS buffer then the column was removed from the magnetic field and labelled cells eluted with MACS buffer. Positive cells were counted and resuspended at appropriate concentration in DC media.

## **2.4 Dendritic Cell Activation and Antigen Presentation Assays**

### *2.4.1 DC assay setup*

To assess the activation state of DCs and their ability to prime naïve T cells in response to various stimuli, BMDCs on indicated day of culture were resuspended and counted then washed and resuspended in DC media supplemented with 20ng/ml GM-CSF. Alternatively, freshly isolated splenic DCs were used. DCs were plated out for FACS analysis of surface markers at  $10^5$  cells/well in U-bottom 96-well plates, for analysis of DC cytokine production cells were plated out at  $2 \times 10^5$  cells/well in flat-bottom 96-well plates, and for antigen presentation assays DCs were plated out at  $10^4$  cells/well in flat-bottom 96-well plates. In all cases, indicated concentrations of activating stimulus, such as LPS, or CRT or hsp70 were added. Indicated concentrations of OVA were added either immediately or following a six-hour incubation at 37°C in 5%CO<sub>2</sub> to the antigen presentation assay plates. Cells were then incubated overnight at 37°C in 5%CO<sub>2</sub>. The following day activation state of DCs was assessed by flow cytometric analysis of surface marker expression and by ELISA analysis of cytokine production as described later in this section. For antigen presentation assays, lymphocytes were purified from spleens of transgenic mice as described earlier in this chapter and  $0.25\text{--}0.5 \times 10^5$  cells added per well. Cells were incubated overnight at 37°C in 5%CO<sub>2</sub>. The following day, IL-2 production by the T cells was assayed by IL-2 ELISA as described later in this section.

### *2.4.2 Flow cytometry and antibodies*

DCs were washed in ice-cold FACS wash (2% FCS, 0.1% azide in PBS) then incubated on ice for 20 minutes with the following fluorescein isothiocyanate (FITC)- or phycoerythrin (PE)-labelled antibodies, diluted 1:100 in FACS wash: CD11c-PE (Armenian Hamster IgG1, HL3), CD86-FITC (Rat (Louvain) IgG2a, GL1), CD80-



FITC (Armenian Hamster IgG2, 16-10A1), MHC Class II I-A<sup>b</sup>-FITC (Mouse (C3H) IgG2a, 25-9-17). All antibodies were purchased from BD Pharmingen (San Diego, CA, USA). Cells were stained with each Ab alone, or with CD11c-PE in combination with one of the FITC-labelled Abs. Excess unbound Ab was removed by washing twice with ice-cold FACS wash, then cells were fixed in 1% formaldehyde in PBS. Samples were run through FACSCalibur flow cytometer (BD Biosciences) and data were collected and analysed using cell Quest software (BD Biosciences). 10<sup>4</sup> events were collected for each sample.

#### 2.4.3 Cytokine ELISAs

Production of cytokines by DCs and T cells was assessed by ELISA. Assays were set up as described earlier and supernatants harvested and tested for cytokine content after overnight incubation. DC culture supernatants were tested for IL-2, IL-12, IL-10 and IFN- $\gamma$ , and antigen presentation supernatants where transgenic T cells had been added were tested for IL-2 production. IL-2 production was assessed using IL-2 mouse minikit purchased from Endogen, Perbio as manufacturers instructions. All incubations were carried out at room temperature. Briefly, flat-bottom 96-well maxisorp plates (Nunc) were coated overnight with capture antibody diluted in PBS. Capture antibody was discarded and plate blocked with assay buffer (2% BSA in PBS) at room temperature for 1 hour. Wells were washed 3x with wash buffer (50mM Tris, 0.2% Tween pH7-7.5) then 50 $\mu$ l assay buffer and 50 $\mu$ l standard or sample was added to each well and incubated for 2 hours. After 3 washes, biotinylated detecting antibody diluted in assay buffer was plated out (100 $\mu$ l/well) and incubated for 1 hour. Wells were washed 3 times and 100 $\mu$ l/well avidin alkaline-phosphatase (Sigma) (1:1000 in assay buffer) added to each well and incubated for 40 minutes. After 3 washes, added 100 $\mu$ l Sigmafast pNPP substrate (Sigma) per well and watched for colour development. Absorbance read at 405nm.

For IL-12, IL-10 and IFN- $\gamma$  ELISAs, antibodies and standards were purchased from BD Pharmingen. Briefly, flat-bottom 96-well maxisorp plates were coated overnight at 4°C with 50 $\mu$ l/well appropriate concentration of capture Ab diluted in coating buffer (0.1M Na<sub>2</sub>HPO<sub>4</sub>, pH 9.0). Capture Abs were as follows: purified anti-mouse IL-12 (p70), rat IgG2b, 9A5, used at 2 $\mu$ g/ml; purified anti-mouse IL-10, rat IgG1,  $\kappa$ ,

JES5-2A5, used at 4µg/ml; purified anti-mouse IFN-γ, rat IgG1, R4-6A2, used at 4µg/ml. All subsequent incubations carried out at room temperature. Coating Ab was removed and wells blocked for 1 hour with 200µl/well blocking buffer (1% BSA in PBS). Plates washed 3 times with PBS/Tween (PBS + 0.05% Tween-20) then 50µl blocking buffer/tween (blocking buffer + 0.05% Tween) and 50µl appropriate cytokine standard or sample added to each well and incubated for 2-4 hours. After 3 washes, biotinylated detecting Abs were added at 1µg/ml in blocking buffer/tween and incubated for 1 hour. Detecting antibodies were as follows: biotin anti-mouse IL-12 (p40/p70), rat IgG2a, C17.8; biotin anti-mouse IL-10, rat IgM, SXC-1; biotin anti-mouse IFN-γ, rat IgG1, XMG1.2. After 3 washes, avidin alkaline-phosphatase was added (1:1000 in blocking buffer/tween) at 100µl/well and incubated for 40 minutes. Plates were washed 3 times and 100µl/well SigmaFast pNPP substrate added. Watched for colour development and read A405. All plates were read on Biorad model 550 plate reader using Microplate manager software. Results analysed and graphs plotted using Prism 4 program.

## **2.5 Purification of CRT**

### *2.5.1 Purification of CRT from P815*

To purify CRT, P815 cell pellets were thawed and pooled, then lysed at 4°C for 2 hours in lysis buffer (25mM CaCl<sub>2</sub>, 25mM MgCl<sub>2</sub>, 25mM MnCl<sub>2</sub>, 100mM Tris pH7.4, 100mM NaCl and 5% Triton X-100) supplemented with protease inhibitor cocktail (complete mini tablets, Roche). Cell lysates were spun at 19000rpm, 45min, 4°C and supernatants dialysed overnight at 4°C against 3litres buffer A (50mM Tris-HCl, 20mM NaCl, 10mM EDTA, pH8) and then for 8hours against 3l fresh buffer A. Dialysed lysate was filtered through 0.45µm syringe filters and loaded in several batches onto a Hi Prep 16/10 DEAE FF column (Amersham) connected to an AKTA Prime system (Amersham), equilibrated with buffer A. Proteins were eluted on a salt gradient, achieved by increasing the proportion of buffer B (50mM Tris-HCl, 1M NaCl, 10mM EDTA, pH8) to buffer A running through the column. The NaCl concentration is increased initially from 20mM to 220mM over 20 minutes, then the main separation occurs during the increase to 500mM over 50 minutes. To elute any remaining protein, the salt concentration is increased to 1M over 7 minutes and maintained for 6 minutes before the column is re-equilibrated in the start buffer.

Fractions containing CRT (identified by SDS-PAGE and western blot, see later) were pooled and concentrated using Amicon Ultra-15 centrifugal filters (Millipore) through a series of spins at 2000xg for 20 minutes at 4°C. This concentrate was loaded onto a Resource-Q column (Amersham) connected to an AKTA Prime system and equilibrated with buffer A and proteins eluted on a slightly different salt gradient to that used for the DEAE column. The concentration of NaCl is initially increased from 20mM to 220mM over 1 minute, followed by main separation over an increase to 700mM over 40 minutes. To remove unbound proteins the concentration of NaCl is increased to 1M over 0.5 minutes and maintained for 5 minutes before the column is re-equilibrated in the start buffer. Fractions containing CRT were identified by SDS-PAGE and western blot and dialysed twice against 2 litres PBS at 4°C. Following dialysis, fractions were tested for protein content using Micro BCA analysis and for levels of endotoxin contamination by Limulus Amebocyte Lysate assay (both described later in methods).

To further purify the CRT obtained from the ion exchange chromatography columns, the CRT-containing fractions from several Resource Q column runs (dialysed into PBS) were pooled, and concentrated using Amicon Ultra-15 centrifugal filters (Millipore) through a series of spins at 2000xg for 20 minutes at 4°C. This concentrate was then loaded onto a HiLoad 26/60 Superdex 200 prep grade gel filtration column (Amersham) connected to an AKTA Prime system and equilibrated with PBS and proteins eluted by size fractionation with PBS. The sample was eluted over 4 and a half hours with PBS at a rate of 2ml/min. 3ml fractions were collected from 25 minutes to 155 minutes. Fractions were analysed for CRT content by SDS-PAGE and western blot.

### *2.5.2 SDS-PAGE and Western Blot*

10µl samples from ion exchange chromatography fractions were added to 5µl loading buffer containing 600mM 2-mercaptoethanol and heated to 95°C for 5 minutes. Samples were then loaded onto 10% acrylamide gels and run at 180V for 1 hour. For Coomassie blue staining, gels were washed 3x5min in dH<sub>2</sub>O, stained for 1 hour in Bio-safe Coomassie blue stain (Bio-Rad) then destained for 30 minutes then overnight in dH<sub>2</sub>O. Gels were imaged using a Kodak digital science camera and KDS

ID2.0 software. For Western Blot, gels were transferred to Hybond-C nitrocellulose membranes (Amersham) overnight at 12V, 4°C in transfer buffer (Towbin – 192mM glycine, 25mM tris, 20% methanol). All subsequent incubations were carried out at room temperature. After transfer, membranes were blocked for at least 1 hour in blocking buffer (PBS, 0.05%Tween-20, 5% Marvel), then incubated for 1 hour with 1 µg/ml polyclonal goat anti-human Calreticulin (Calregulin (C-17), Santa Cruz Biotechnology Inc) in blocking buffer. The membranes were washed 4x10 minutes in wash buffer (PBS, 0.05%Tween-20), then incubated 40 minutes with HRP-conjugated anti-goat IgG diluted 1:4000 in wash buffer. Membranes were washed 3x10 minutes in wash buffer, then incubated for 5 minutes with SuperSignal West Pico chemiluminescent substrate (Pierce, Perbio, IL, USA) and developed using a Biorad Fluor-S Max Imager and Quantity One software. OVA western blots were carried out using the same protocol, with 5 µg/ml polyclonal rabbit anti-mouse OVA as primary antibody and HRP-conjugated anti-rabbit IgG diluted 1:20000 as secondary.

### 2.5.3 Protein Quantification

Protein content of CRT fractions was quantified using Micro BCA Assay (Pierce). This method utilises bicinchoninic acid (BCA) as the detection reagent for  $\text{Cu}^{1+}$  ions, which are formed when  $\text{Cu}^{2+}$  is reduced by protein in an alkaline environment. The chelation of two BCA molecules with one  $\text{Cu}^{1+}$  ion forms a purple-coloured reaction product. BCA and  $\text{Cu}^{2+}$  are provided in a set of reagents, which are mixed to form the working reagent, which is then added to protein samples. Assays were carried out using the 96-well plate method as detailed in kit instructions, with some modification, briefly 50 µl standard or sample dilutions were incubated with 50 µl working reagent at 37°C for 2 hours. Absorbance of samples at 570nm was read on a Biorad model 550 plate reader using microplate manager software. Prism 4 software was used to plot the standard curve and calculate the protein concentrations of the fractions.

### 2.5.4 Endotoxin Testing

Protein solutions were tested for levels of endotoxin contamination by Limulus Amebocyte Lysate (LAL) assay. LAL assays are based on the addition of LAL, which is prepared from the circulating amebocytes of the horseshoe crab *Limulus*

*polyphemus*, to samples and standards. Interaction of bacterial endotoxin with LAL initiates activation of a proenzyme that cleaves a peptide from a coagulogen to produce opacity. In the chromogenic system, a clear substrate is added, which is catalysed by the enzyme generated by proenzyme cleavage to produce a yellow colour, the absorbance of the samples can be read at 405nm and values compared to a standard curve to calculate the endotoxin units/ml (EU/ml). Endosafe chromogenic endpoint kits (Charles River Laboratories, France) were used as per kit instructions. Absorbances of samples at 405nm were read on a Biorad model 550 plate reader using microplate manager software. Prism 4 software was used to plot the standard curve and calculate the endotoxin levels in the samples in EU/ml.

#### 2.5.5 Endotoxin Removal from OVA and CRT

In order to remove contaminating endotoxin from OVA and CRT preps, we utilised Polymyxin B, a cyclic antibiotic isolated from *Bacillus polymyxa*, which binds to endotoxins with high affinity. Polymyxin B-agarose columns were used to remove contaminating endotoxin from OVA and CRT preparations. For OVA, a 5ml Polymyxin B-agarose column was reconstituted with 5 column volumes 1% deoxycholic acid, washed with 5 column volumes dH<sub>2</sub>O and equilibrated with 5 column volumes PBS. 1ml 100mg/ml OVA in PBS was loaded onto the column and 1ml flowthrough collected in an eppendorf tube. The column was then capped, 2ml PBS added and incubated at room temperature for 1 hour. OVA was eluted with PBS, and a further 29x1ml fractions collected. The column was reconstituted with 5 column volumes 1% deoxycholic acid, washed with 5 column volumes dH<sub>2</sub>O and stored in 25%EtOH+0.02%azide at 4°C. The A280 of the fractions was read on a Biorad Smartspec. Fractions with A280>0.3 were tested for protein and endotoxin content as previously described. Any fractions with endotoxin content of <1EU/ml were pooled, concentrated and retested. If fractions still had endotoxin content >1EU/ml, these were pooled, concentrated and treated again.

The procedure for CRT was similar, with a few exceptions: a 2ml Polymyxin B-agarose column was used and the CRT to be treated (consisting of a number of pooled and concentrated resource Q fractions) and PBS used for equilibration and elution were supplemented with 5mM EDTA and 40mM *N*-octyl β-D-

glucopyranoside (Sigma). After loading, CRT was eluted immediately from the column, omitting the 1 hour incubation used with OVA. After reading A280, fractions were dialysed vs several changes of PBS to remove any traces of *N*-octyl  $\beta$ -D-glucopyranoside prior to BCA and LAL testing.

OVA and CRT with endotoxin levels of less than 1EU/mg are referred to as “low endotoxin”, this being the level below which no biological effects were observed.

## **2.6 Phagocytosis Assays**

### *2.6.1 Phagocytosis assay setup*

DC2.4 cells were plated out in twelve well plates at  $4 \times 10^5$  cells per well in 2ml R10 medium and incubated at 37°C, 5% CO<sub>2</sub> over a 24 hour period. 1  $\mu$ g/ml LPS (~40000 EU/ml) or 5  $\mu$ g/ml CRT was added at 24, 12, 4, 2 or 0 hours prior to removal of R10 and incubation with latex beads (LB) (Fluoresbrite™ plain yellow-green 2.0 micron microspheres) suspension. Additional lengths of pre-exposure to CRT of 0.5 hours and 1.5 hours, for FCS opsonised LB only were included.

LB were opsonised overnight at 4°C, with either HI-FCS or 1mg/ml low endotoxin ovalbumin (OVA) in 25mM sodium citrate (Sigma), pH 4.3, both in 0.1% sodium azide (Sigma). Cells were washed once with PBS and opsonised for a further 1 hour at 37°C, in HI-FCS, then centrifuged at 13,000 rpm for 3 minutes and resuspended at  $1.42 \times 10^7$  LB/ml in R10. DC2.4 were incubated with 2ml of this LB suspension, or R10, for 1 hour at either 4°C or 37°C and maintained on ice while they were processed. Each sample was washed 3 times in its well with ice cold PBS, incubated with Trypsin for 5 minutes at 37°C, and an excess of R10 added. Cells were evenly resuspended by pipetting and the samples were divided into 3 equal fractions; the first fraction was processed for immediate FACS analysis, the second was incubated for 6 hours at 37°C, 5% CO<sub>2</sub> in R10, before FACS analysis, while the third was incubated for 6 hours at 37°C, 5% CO<sub>2</sub> in R10, and then used for an antigen presentation assay.

### *2.6.2 FACS Analysis of phagocytosis assays*

Following a wash in FACS Wash, samples exposed to LB were incubated with FACS Wash for 20 minutes on ice, while samples that had been incubated with R10 medium only were stained with 1:100 PE anti-mouse CD86, PE anti-mouse CD80, or PE

anti-mouse I-A<sup>b</sup> (all BD Pharmingen) for 20 minutes on ice. The samples were then washed three times with FACS Wash, and fixed 1:1 in FACS Wash, or Trypan Blue, and 2% formaldehyde. Each sample was subsequently analysed by FACS.

### 2.6.3 *Antigen Presentation Assays*

Samples were washed once with PBS, fixed with 1% paraformaldehyde, then treated with 0.25% Ammonium chloride (BDH Anala R). After one wash with PBS,  $8.5 \times 10^4$  B3Z T cells were added per sample. B3Z T cells are activated by recognition of SINFEKL, the antigenic epitope presented to them following DC processing of the model antigen OVA. Following such activation, B3Z T cells upregulate  $\beta$ -galactosidase, which produces a red product from the yellow CPRG substrate. These samples were incubated overnight at 37°C, 5% CO<sub>2</sub>, then washed once with PBS and incubated with 0.15mM chlorophenol red  $\beta$ -galactoside (CPRG) (Roche) in PBS/0.5% Nonidet P-40 (Sigma) for 2 hours. T cell activation was determined by assessing the absorbance of each sample at 570nm on Model 550 plate reader using microplate manager software. Graphs were plotted using Prism Graph Pad 4 software. This experiment was performed in triplicate at 37°C and once at 4°C.

## **2.7 Assessment of CRT binding to cells**

### *2.7.1 Alexa-488 labelling of CRT*

In order to investigate binding of CRT to APCs, CRT was labelled with Alexa-Fluor 488 (Molecular Probes) according to manufacturers instructions. This is an amine reactive dye, which forms very strong amide bonds by interacting with lysine residues in the protein. 3mg CRT was incubated, stirring, at room temperature for 1 hour with 0.15mg or 0.3mg Alexa-488. The reaction was stopped by adding 100 $\mu$ l 1.5M hydroxylamine, pH8.5, and stirring at room temperature for a further 1 hour. Free dye was removed by running the protein over a Nap-5 column. Labelled CRT (Alexa-CRT) was stored at 4°C.

### *2.7.2 Assessment of CRT binding to APCs - FACS*

BMDC, J774, DC2.4 and K42 cells were plated out in U-bottom 96 well-plates at  $2 \times 10^5$  cells/well, and incubated with Alexa-CRT in the presence or absence of inhibitors maleylated BSA (mBSA),  $\alpha_2$ m, BSA or unlabelled CRT on ice for 1 hour. Cells were washed 3 times with ice-cold FACS wash, fixed in 1% formaldehyde in PBS and analysed using a FACSCalibur flow cytometer (BD Biosciences) and Cell Quest software (BD Biosciences).  $10^4$  events were collected for each sample.

### *2.7.3 Assessment of CRT binding and internalisation to BMDCs – confocal microscopy*

Day 10 BMDCs were resuspended, spun and the pellet resuspended in DC media. The DCs were spun onto coverslips coated with polymers (a kind gift from Dr Juanjo Diaz Mochon, University of Edinburgh) in 6-well plates at 200xg for 2-3minutes then incubated at 37°C for 1 hour, to allow them to adhere to the coverslips. Plates were then cooled on ice before adding 50 $\mu$ g/ml Alexa-CRT in the presence or absence of 200 $\mu$ g/ml mBSA. The coverslips were then incubated on ice for 15 minutes (timepoint 0), or at 37°C for 15 minutes or 2 hours. All subsequent incubations are at room temperatures, and washes are in PBS. Following incubation, media was removed and cells were fixed in 1ml 4% paraformaldehyde (PFA) for 7 minutes, washed, and incubated with 1ml 0.25% ammonium chloride for 10 minutes to quench the PFA. Cells were washed then permeabilised in 1ml 0.1% Triton X-100 for 10 minutes, washed, blocked in 3% BSA for 1 hour, stained with rabbit anti-CRT (PA3-900) diluted 1:100 in PBS for 1 hour, washed, incubated with anti-rabbit-Texas Red



diluted 1:100 in PBS for 1 hour, washed and incubated for 5 minutes in the dark with 1:1000 TOPRO-3 nuclear stain (Molecular Probes). Cells were washed once more then the coverslips mounted on slides using PVA-DABCO (Fluka) and left to dry in the dark at 4°C before sealing the coverslips with nail varnish and analysing on the confocal microscope.

## **2.8     Complexing CRT to SIINFEKL**

CRT was incubated with SIINFEKL at 1:10 molar ratio in binding buffer (20mM Hepes pH7.2, 20mM NaCl, 2mM MgCl<sub>2</sub>) at 55°C for 10 minutes, then at room temperature for 30 minutes. As controls, CRT and SIINFEKL were simply mixed, and the procedure was carried out using BSA instead of CRT. Free SIINFEKL was removed from complexes by several rounds of dialysis vs. 31 PBS at 4°C.

## **2.9     *In vivo* proliferation of CFSE-labelled T cells**

On day 0, CD4<sup>+</sup> splenocytes from OT-II mice and CD8<sup>+</sup> splenocytes from OT-I mice were prepared as described in section 2.3.4. Cells were resuspended at 1x10<sup>7</sup>/ml in PBS 0.1% BSA and incubated with 2μM CFSE for 30 minutes at 37°C. Cells were washed once in ice-cold PBS 0.1% BSA, once in PBS, then resuspended at 0.5-1x10<sup>7</sup>/ml in PBS. C57Bl/6 mice were adoptively transferred with 200μl labelled OT-I or OT-II T cells IV. On day 1, mice were immunised with indicated concentrations of OVA and/or CRT in PBS, 200μl IV/mouse. On day 3, mice were culled and spleens harvested. Single cell suspensions were prepared by macerating through a 70μm cell strainer with a syringe plunger in R10. White blood cells were isolated by spinning over 1:1 volume of Ficoll, washed in R10 then washed in FACS wash, incubated for 20 minutes on ice with 1:100 PE anti-CD4 (Rat (Lewis) IgG2b, κ, GK1.5, for OT-II adoptive transfers) or PE anti-CD8 (Rat (LOU/Ws1/M) IgG2a, κ, 53-6.7, OT-I adoptive transfers) in FACS wash. Both antibodies were purchased from BD Pharmingen. Cells were washed twice in FACS wash then analysed on FACSCalibur flow cytometer using Cell Quest software. 1.5x10<sup>5</sup> events were collected for each sample.

### **2.10 *In vivo* tumour protection**

Female DBA/2 mice were inoculated twice at weekly intervals with 10 $\mu$ g CRT or PBS alone as control in 100 $\mu$ l volume subcutaneously. 7 days after the second immunisation, mice were challenged subcutaneously with 2.5x10<sup>4</sup> P815 cells, which had been cultured as described earlier in this chapter, washed 3 times in PBS, counted and resuspended in PBS (100 $\mu$ l/mouse). Mice were culled when tumour size was 1cm diameter.

### **3. Preparation of calreticulin and ovalbumin**

#### **3.1 Introduction**

An early observation that gave rise to my interest in extracellular CRT was that loss of binding of gp90 to CRT in CT26 tumour cells resulted in loss of antigenicity of the tumour, with respect to recognition by CD4<sup>+</sup> T cell hybridomas [135]. This suggested an intriguing potential immunostimulatory role for extracellular CRT, which could be related to reports that CRT isolated from tumours could induce specific immunity to the tumour of origin, a property apparently shared by many HSPs [33-39]. I set out initially to test the hypothesis that – as was emerging for other HSPs like gp96 and hsp70 – this anti-tumour activity resided in 2 separate functions of CRT, namely antigen delivery and an adjuvant function.

Much of the literature relating to the immunostimulatory properties of HSPs has utilised HSPs purified from bacteria or from the organs of larger animals such as pigs, in order to obtain a high yield. As I was working in a murine model system, I felt that it was important to use murine CRT to gain the most accurate impression of the likely *in vivo* effects of autologous HSPs on immune responses, an area that has been relatively under-investigated in the literature. As murine CRT is not commercially available, it was necessary to purify the CRT in house. The murine mastocytoma cell line P815 was chosen as the source of CRT as this cell line grows rapidly in suspension in culture, making it easy to grow and harvest large quantities of cells from which to extract the protein. The method for purifying CRT was adapted from that used by Paul Eggleton to isolate human CRT from HC60 and Jurkat cells.

As described in section 1.2.5, in the last few years a number of groups have reported that immunostimulatory effects attributed to HSPs have, in fact, been caused by contaminating bacterial products in the HSP preparations [91-93]. This is a highly contentious issue in the HSP field, with some authors demonstrating that removal of bacterial endotoxin from HSP preps abrogates their immunostimulatory activity and others reporting that it does not. In order to avoid artefactual results caused by contamination of proteins with bacterial endotoxin, every effort was made to use only reagents with minimal endotoxin contamination. To this end, both CRT and commercial OVA were tested for endotoxin contamination using limulus amebocyte

lysate assays, and contamination was removed using Polymyxin B, a cyclic antibiotic that binds to endotoxin.

## 3.2 Results

### 3.2.1 Purification of murine CRT from the mastocytoma cell line P815

P815 cells were cultured in roller bottles and cells harvested as described in materials and methods. Following Triton X-100 lysis and removal of cell debris by centrifugation, cell lysates were dialysed against two changes of buffer A, the starting (low salt) buffer for ion exchange chromatography. CRT has a highly acidic C-terminal domain, which can be exploited for purification using anion exchange chromatography. Separation was carried out in 2 stages, utilising 2 different anion exchange columns. The first of these, the DEAE column, is based on a weak anion exchanger, whereas the second, Resource Q, is based on a strong anion exchanger. The difference between strong and weak anion exchangers refers to the extent of variation of ionisation with pH, strong ion exchangers are completely ionised over a wide pH range, whereas the degree of dissociation and thus exchange capacity varies more markedly with pH. The first column, DEAE, was thus used to perform a crude separation before the finer separation on the Resource Q column, which removed most of the remaining proteins that co-eluted with CRT from the DEAE column. Had the lysate been run directly on the Resource-Q column, there would have been too much material in the lysate to achieve such a good separation of CRT.

The dialysed lysate was filtered and loaded onto a HiPrep 16/10 DEAE FF ion exchange column in 5ml batches. Figure 3.1 shows a representative chromatogram from DEAE purification. Fractions collected during the elution were tested for the presence of CRT by SDS-PAGE and Western Blot analysis as described in materials and methods. Figure 3.2 shows Coomassie blue staining and Calreticulin-specific western blot of fractions from DEAE columns. These data are representative of the patterns seen in all DEAE runs. CRT elutes at approximately 265-370mM NaCl. Although the molecular weight of CRT is 46kDa, it migrates to approximately 60kDa on SDS-PAGE due to the extended structure of the P domain. The coomassie blue staining shows that there are still several major contaminants of the CRT-containing fractions, so further purification is needed. The identity of these contaminants is unknown, the major contaminant is approximately 90kD, with others of 75kD, 40kD, 24kD and 22kD. The CRT-containing fractions from all DEAE runs of the initial dialysed lysate were pooled and concentrated to <10ml using amicon ultra centrifugal

filters. This concentrate was then loaded onto a Resource Q column. A representative chromatogram is shown in figure 3.3. This, relatively slower, gradient of already semi-purified lysate over the high resolution column results in a series of sharper peaks than are seen on DEAE fractionation, and usually produces 2 or 3 fractions with high CRT content and minimal contamination with other proteins as can be seen in the SDS-PAGE and Western Blot analysis of the fractions (Fig 3.4). The remaining major contaminants have molecular weights of ~90kD and 22kD. CRT elutes at approximately 490-560mM NaCl. This is higher than the concentration at which CRT elutes from the DEAE column due to the fact that Resource Q is a strong ion exchanger and at pH8 a higher salt concentration is therefore required to elute the CRT from this column than from the DEAE column. Those fractions containing CRT were dialysed against 2 changes of PBS to remove all traces of EDTA and salt, and were then tested for protein content by micro BCA analysis. Typically, from a starting number of around  $10^{10}$  P815 cells, a yield of approximately 1-3mg of CRT would be obtained, equating to 30pg/cell. The reasons for the variability in yield are unclear, but may be due to differences in cell health or numbers obtained on different days of harvesting, which may also affect the effectiveness of the lysis procedure.

In order to increase the purity of the CRT obtained from these two ion exchange chromatography steps, the CRT-containing fractions from several Resource Q runs were pooled, concentrated and run on a HiLoad 26/60 Superdex 200 prep grade gel filtration column. Figure 3.5 shows the chromatogram from a gel filtration of pooled, concentrated Resource Q fractions. As shown in figure 3.6, this additional step generates 7 CRT fractions with very little contamination as demonstrated by Coomassie blue staining and western blot.

Most experiments described in this thesis have been carried out using Resource Q-purified CRT, as the gel filtration step vastly reduced the yield of CRT and also subsequent protein clean-up results in increased purity compared to Resource Q fractionation, probably due to binding of other contaminating proteins to the Polymyxin-B column (see section 3.1.3, Fig 3.9).

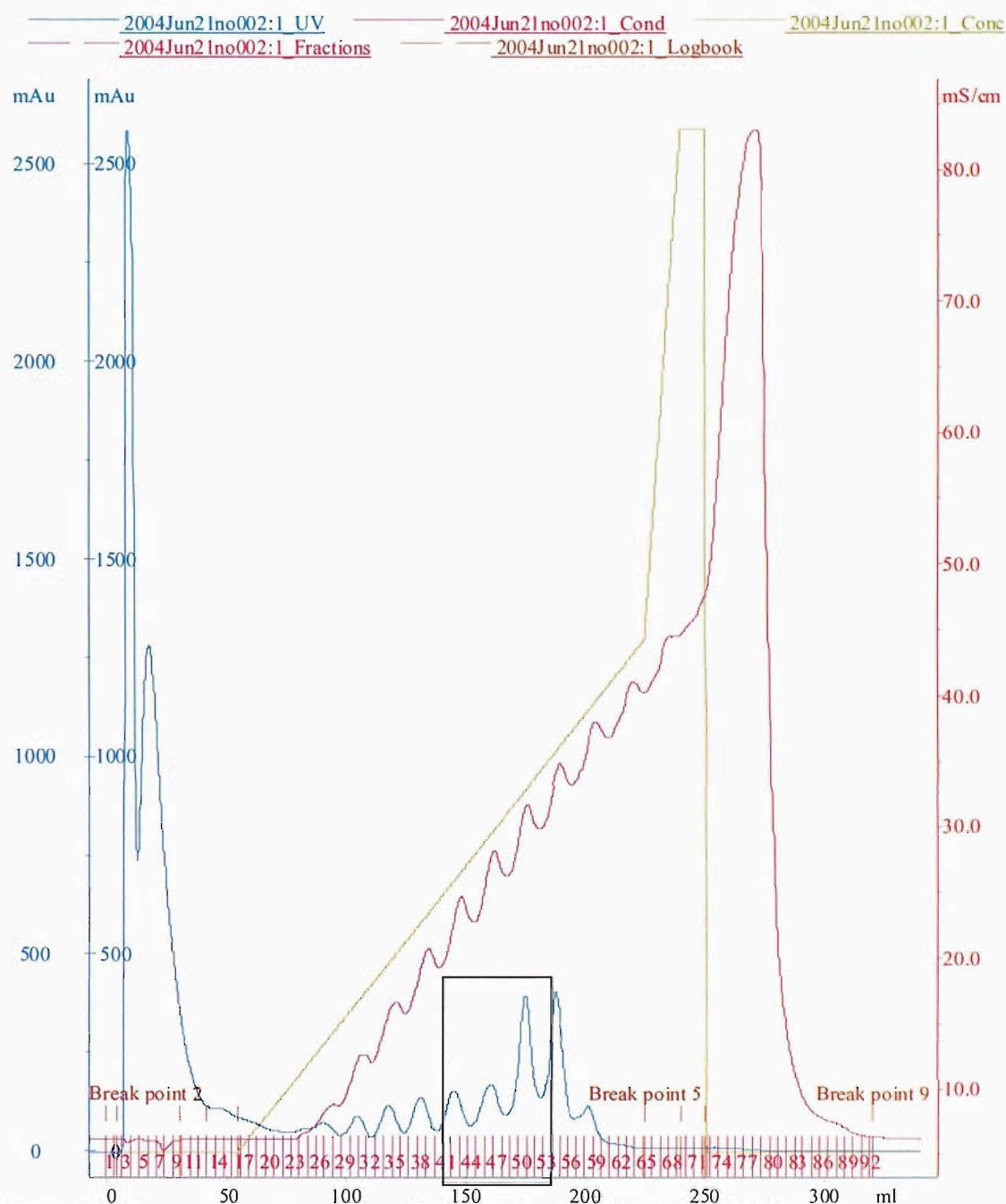


**Figure 3.1** Representative chromatogram from running 5ml filtered, dialysed P815 lysate on DEAE column controlled by AKTA Prime system. Data collected using Prime View software. Blue line represents absorbance, red represents conductivity and green represents % buffer B being run through column. Fractions are indicated on x-axis (red lines). Black box indicates approximate location of CRT containing fractions.



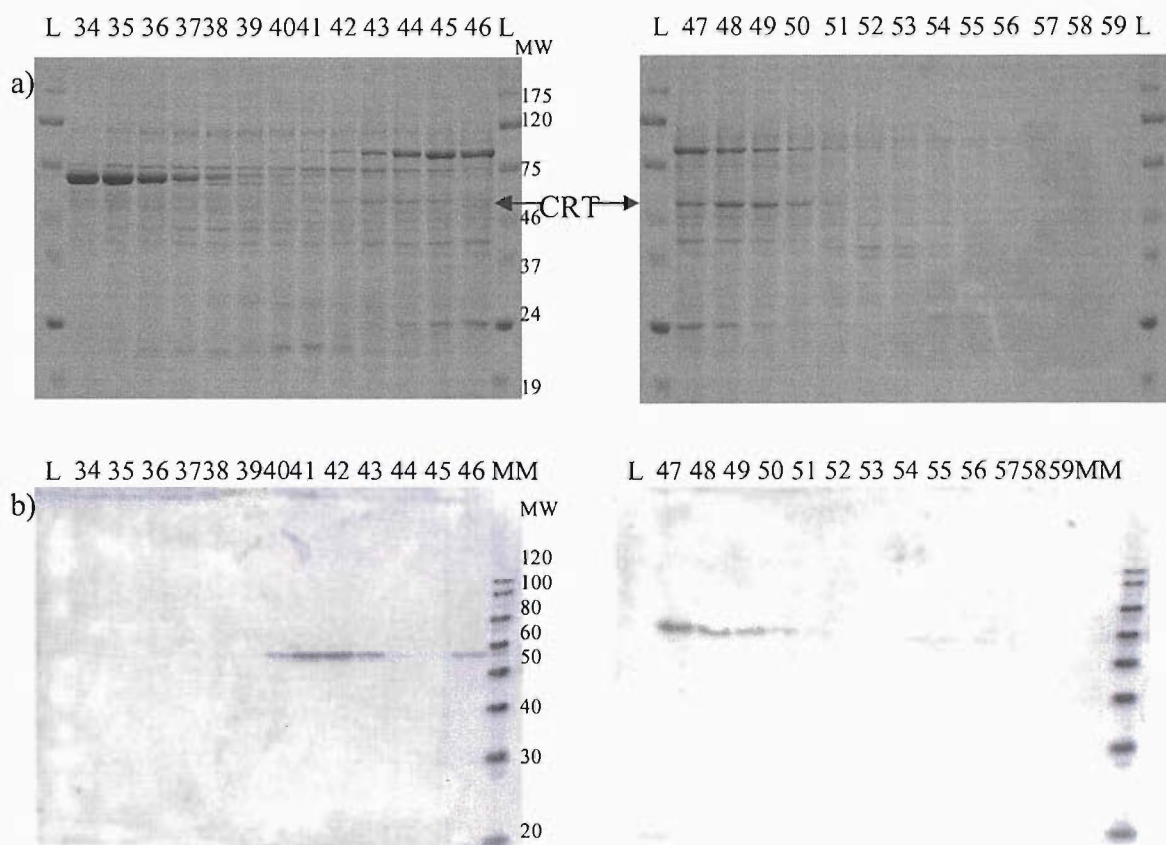


**Figure 3.2** Coomassie blue staining and calregulin western blot of fractions from DEAE columns. Samples mixed with loading buffer and boiled at 95°C for 5 min, then loaded onto 10% SDS gels and run at 180V for 1 hour. Gels were then either a) rinsed 3 times in dH<sub>2</sub>O, then stained in Coomassie Blue for 1 hour and destained in dH<sub>2</sub>O before imaging on KDSID2.0 digital camera and software, or b) were transferred to nitrocellulose membranes overnight at 12V, 4°C then probed with calregulin primary antibody and anti-goat-HRP secondary, developed with SuperSignal and imaged on Fluor S-Max imager and Quantity One Software. L= prosieve ladder, MM = magic mark. Sizes of markers (kD) are indicated.

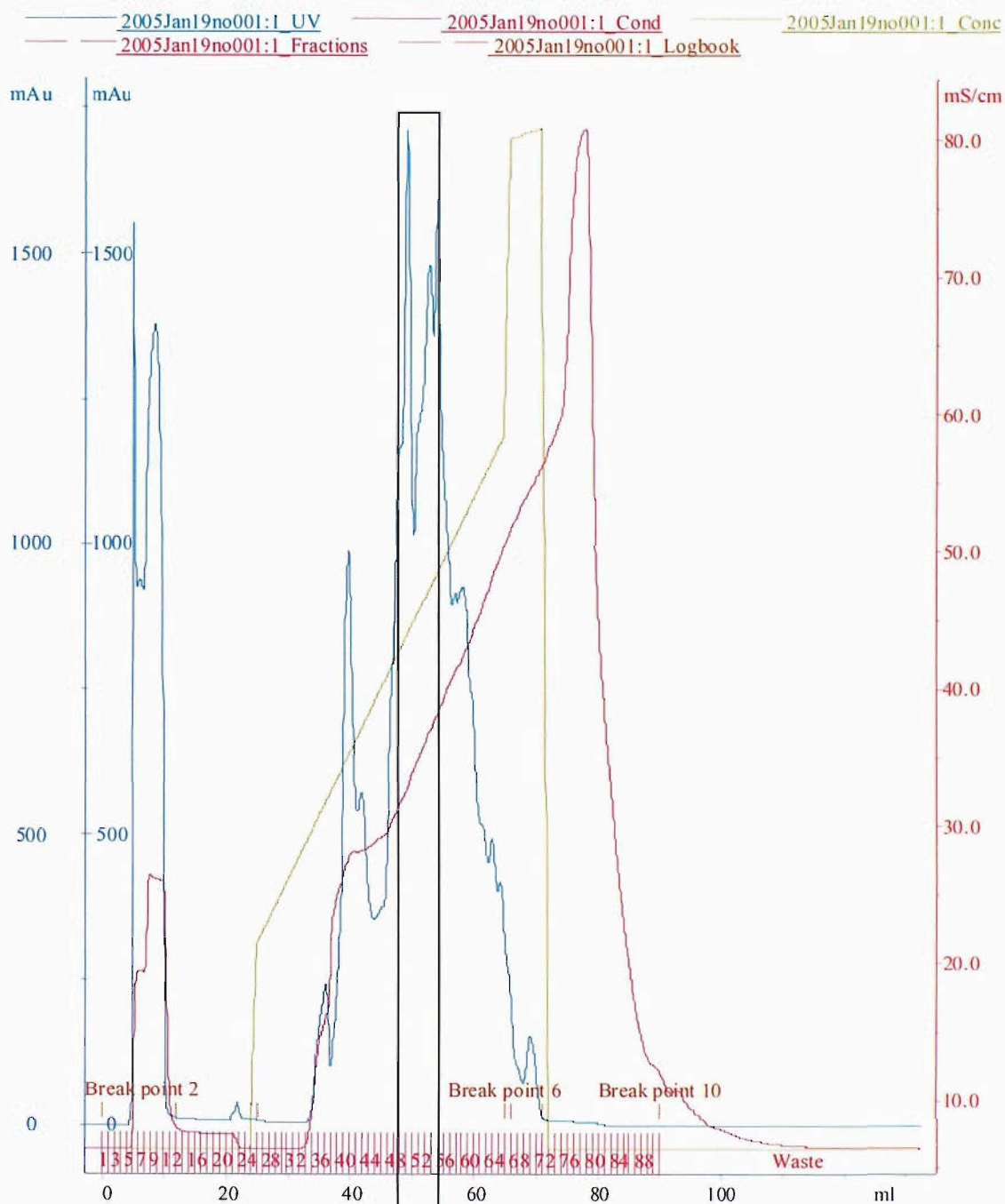


**Figure 3.3** Representative chromatogram from running 10ml pooled, concentrated DEAE fractions on Resource Q column controlled by AKTA Prime system. Data collected using Prime View software. Lines as previous chromatogram. Black box indicates CRT containing fractions, as assessed by SDS-PAGE and western blot – see fig. 3.4.

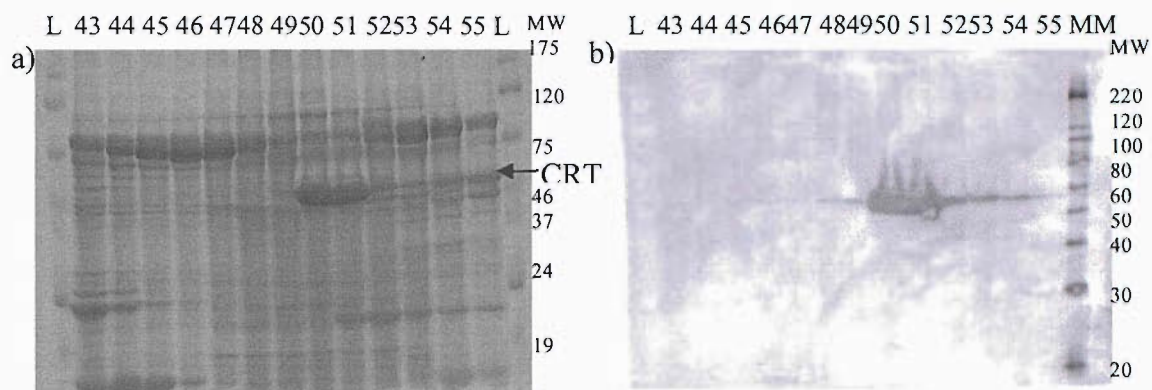


**Figure 3.4** Coomassie blue staining and calregulin western blot of fractions from Resource Q column. Samples mixed with loading buffer and boiled at 95°C for 5 min, then loaded onto 10% SDS gels and run at 180V for 1 hour. Gels were then either a) rinsed 3 times in dH<sub>2</sub>O, then stained in Coomassie Blue for 1 hour and destained in dH<sub>2</sub>O before imaging on KDSID2.0 digital camera and software, or b) were transferred to nitrocellulose membranes overnight at 12V, 4°C then probed with calregulin primary antibody and anti-goat-HRP secondary, developed with SuperSignal and imaged on Fluor S-Max imager and Quantity One Software. L= prosieve ladder, MM =magic mark. Sizes of markers (kD) are indicated.

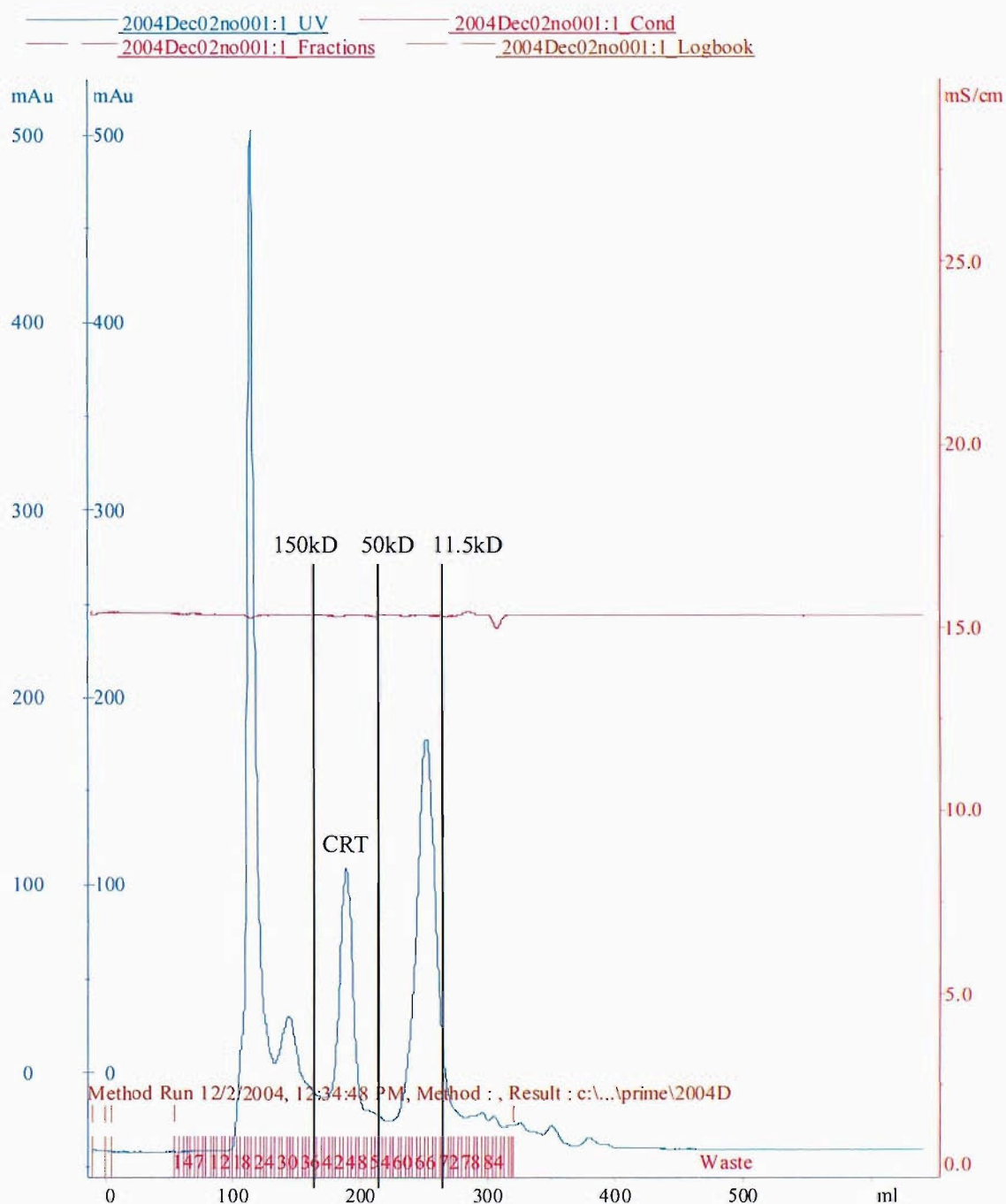


**Figure 3.5** Representative chromatogram from running pooled, concentrated CRT-containing Resource Q fractions on HiLoad 26/60 Superdex 200 prep grade column controlled by AKTA Prime system. Data collected using Prime View software. Blue line represents absorbance, red horizontal line indicates conductivity, vertical red lines indicate fractions. Vertical black lines indicate where proteins of indicated masses eluted on calibration runs on same column using same method. CRT peak indicated, as established by SDS-PAGE and Western Blot – see fig. 3.6.

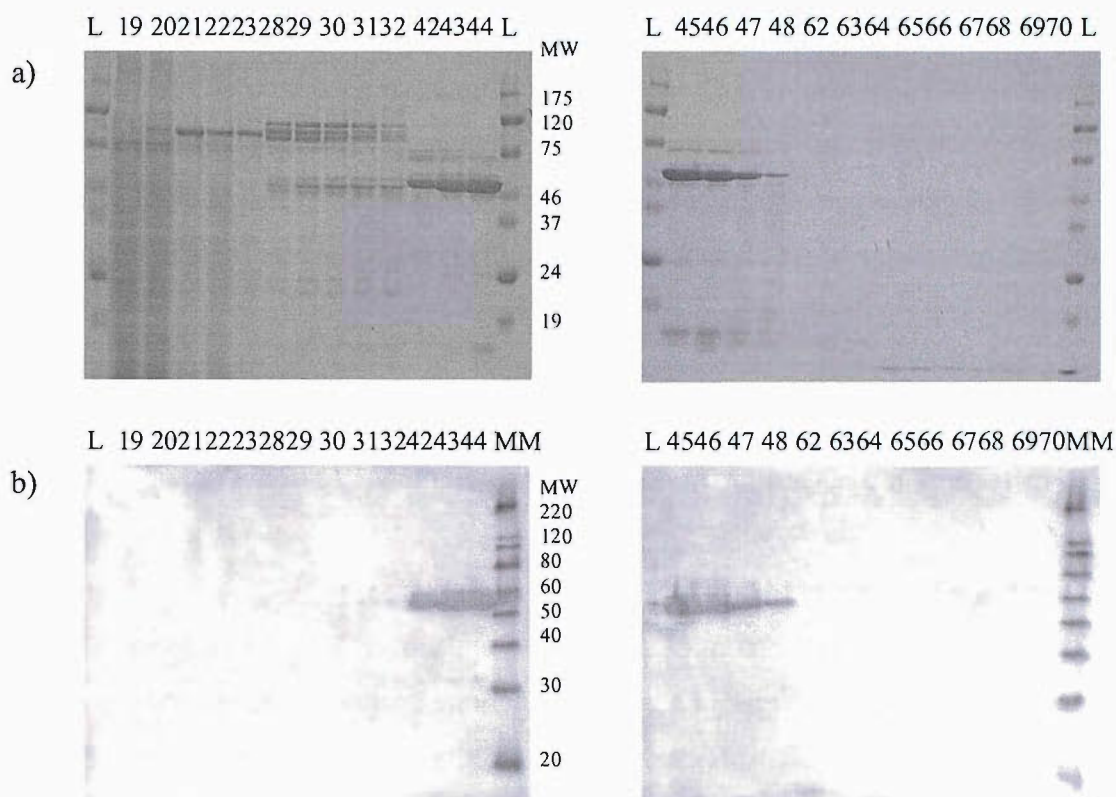


**Figure 3.6** Coomassie blue staining and calregulin western blot of fractions from gel filtration column. Samples mixed with loading buffer and boiled at 95°C for 5 min, then loaded onto 10% SDS gels and run at 180V for 1 hour. Gels were then either a) rinsed 3 times in dH<sub>2</sub>O, then stained in Coomassie Blue for 1 hour and destained in dH<sub>2</sub>O before imaging on KDSID2.0 digital camera and software, or b) were transferred to nitrocellulose membranes overnight at 12V, 4°C then probed with calregulin primary antibody and anti-goat-HRP secondary, developed with SuperSignal and imaged on Fluor S-Max imager and Quantity One Software. L= prosieve ladder, MM =magic mark. Sizes of markers are indicated (kD).

### **3.2.2 Endotoxin contamination leads to significant experimental artefact**

Initial experiments to establish the optimum concentrations of OVA and LPS to use in CRT assays by preparing standard curves of these factors indicated that transgenic T cells responded well to OVA-pulsed DCs in the absence of any stimulatory factor such as LPS, and that OVA alone appeared capable of stimulating upregulation of activation markers on DCs (data not shown). These results led to suspicions that our OVA may be contaminated with LPS. This finding coincided with several published reports suggesting that some of the immunostimulatory properties of HSPs were in fact due to contamination with bacterial endotoxin, thus we thought it was important to determine the extent of endotoxin contamination in our reagents and establish an endotoxin-free system.

All components of our DC media and OVA and CRT preparations were tested for endotoxin contamination using Limulus Amebocyte Lysate (LAL) assays. We found that, while the components of the DC media and our GM-CSF were endotoxin-free, both OVA and CRT contained significant levels of endotoxin, >40EU/mg and >90EU/mg respectively in typical preparations. While there is no “golden rule” as to a biologically insignificant level of endotoxin contamination, <1EU/mg seems to be a benchmark. The levels measured in our proteins were comparable to concentrations of LPS that have been observed to induce maturation of DCs. This could explain why T cells responded to OVA-pulsed DCs in the absence of LPS, as the endotoxin present in the OVA could activate the DCs directly. It was therefore crucial to remove the contamination from these proteins to eliminate artefact.

### **3.2.3 Removal of endotoxin contamination from ovalbumin and calreticulin**

Polymyxin B was purchased conjugated to agarose beads and was poured into disposable plastic columns. These columns can be reconstituted and used for detoxification up to 10 times. Endotoxin removal from OVA was relatively simple to carry out: 1ml of 100mg/ml solution of OVA in PBS could be loaded directly onto a 5ml Polymyxin B-agarose column, incubated at room temperature for 1 hour and then eluted from the column with PBS. During elution, 30x1 ml fractions were collected and their absorbances measured at 280nm. Fractions containing a reasonable amount

of protein were tested accurately for protein concentration by micro BCA assay and for endotoxin content by LAL assay.

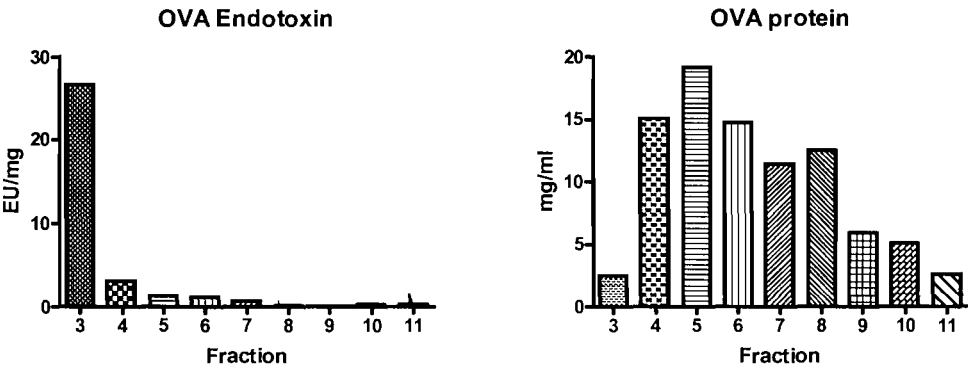


**Figure 3.7** Protein concentration (mg/ml, right hand graph) and endotoxin contamination levels (EU/mg, left hand graph) of fractions obtained by loading 1ml 100mg/ml OVA in PBS onto a 5ml Polymyxin B-agarose column, incubating for 1 hour and then eluting 1ml fractions with PBS. Endotoxin levels were tested by LAL assay and protein levels by Micro BCA.

**Fraction Protein (mg/ml) EU/mg**

3	2.5	26.6	<b>Table 3.1</b> Values used to prepare graphs in fig. 3.7. Protein concentrations as determined by micro BCA assay are averages of duplicate readings. EU/mg values were obtained by measuring endotoxin contamination in EU/ml by LAL assay and dividing this value by the protein concentration in mg/ml to obtain the EU/mg value.
4	15.1	3.05	
5	19.2	1.36	
6	14.7	1.13	
7	11.4	0.68	
8	12.5	0.15	
9	5.85	0.17	
10	5.05	0.19	
11	2.55	0.25	

According to the criteria of <1EU/mg being a relatively “safe” level of endotoxin, fractions 7-10 were pooled and stored, aliquoted, at -20°C for use in experiments. This OVA had a final concentration of 7mg/ml, with 0.5EU/mg. Thus, from the initial 100mg OVA, approximately 28mg useable protein was obtained after only 1 run over Polymyxin B-agarose. Pooling the other fractions and treating them again could further enhance this yield. In total, the fractions tested contained 89mg of protein – this represents a very good recovery from Polymyxin B-agarose, where yield is often <50%.

The issue of high percentage protein loss during the cleaning process was more evident with treatment of CRT. Polymyxin B is strongly cationic, and thus binds with high affinity to negatively charged, anionic, proteins. Unfortunately for this process,



CRT is a strongly anionic protein; so loading CRT in PBS directly onto Polymyxin B resulted in >80% protein loss, as the negatively charged CRT bound strongly to the positively charged Polymyxin B. This problem was partially overcome by supplementing the buffer used for purification with 5mM EDTA and 40mM *N*-octyl  $\beta$ -D-glucopyranoside. This was based on a method published by Reed et al. [93]. Table 3.2 and figure 3.8 show the data for fractions collected from one run of approximately 4mg CRT over a 2ml Polymyxin B-agarose column. As well as the supplements used in the CRT and PBS, the method for detoxifying CRT utilises a 2ml instead of a 5ml Polymyxin column and the 1-hour incubation is omitted to minimise protein loss.

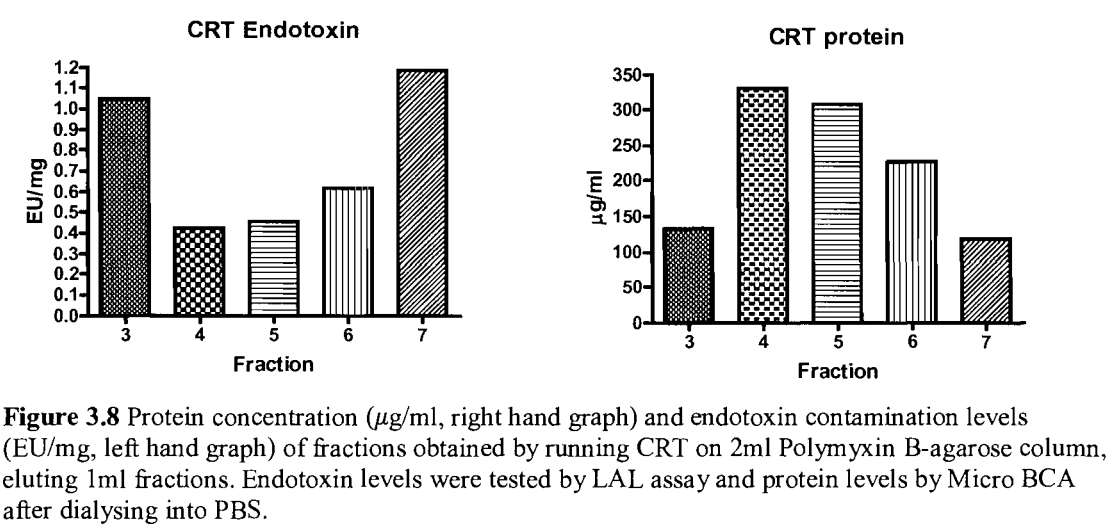


**Figure 3.8** Protein concentration ( $\mu\text{g/ml}$ , right hand graph) and endotoxin contamination levels (EU/mg, left hand graph) of fractions obtained by running CRT on 2ml Polymyxin B-agarose column, eluting 1ml fractions. Endotoxin levels were tested by LAL assay and protein levels by Micro BCA after dialysing into PBS.

Fraction	Protein (mg/ml)	EU/mg
3	0.133	1.05
4	0.331	0.423
5	0.307	0.456
6	0.227	0.617
7	0.118	1.186

**Table 3.2** Values used to prepare graphs in fig. 3.8. Protein concentrations as determined by micro BCA assay are averages of duplicate readings. EU/mg values were obtained by measuring endotoxin contamination in EU/ml by LAL assay and dividing this value by the protein concentration in mg/ml to obtain the EU/mg value.

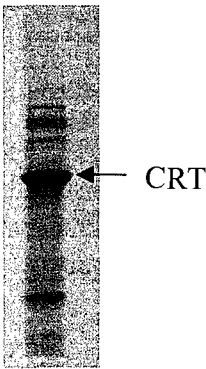


**Fig. 3.9** Coomassie blue staining of pooled, concentrated fractions from Polymyxin B treatment of CRT.

It should also be noted that before testing by LAL and micro BCA, the fractions were dialysed against 2 changes of PBS to remove any traces of 40mM *N*-octyl  $\beta$ -D-glucopyranoside and EDTA. These fractions and fractions from another Polymyxin B treatment were pooled and concentrated to give 2ml of a 1.2mg/ml solution with <0.2EU/mg contamination. Figure 3.9 demonstrates that this detoxification step also increases the purity of the CRT compared to the CRT obtained from Resource Q fractionation. As with OVA, the CRT was aliquoted and stored at -20°C for use in future assays. Unless otherwise stated, all CRT and OVA used in subsequent experiments are low-endotoxin (<1EU/mg). Removal of contamination from OVA led to no stimulation of DCs (fig. 3.10) or priming of T cells (fig. 3.11) in the absence of other stimuli.

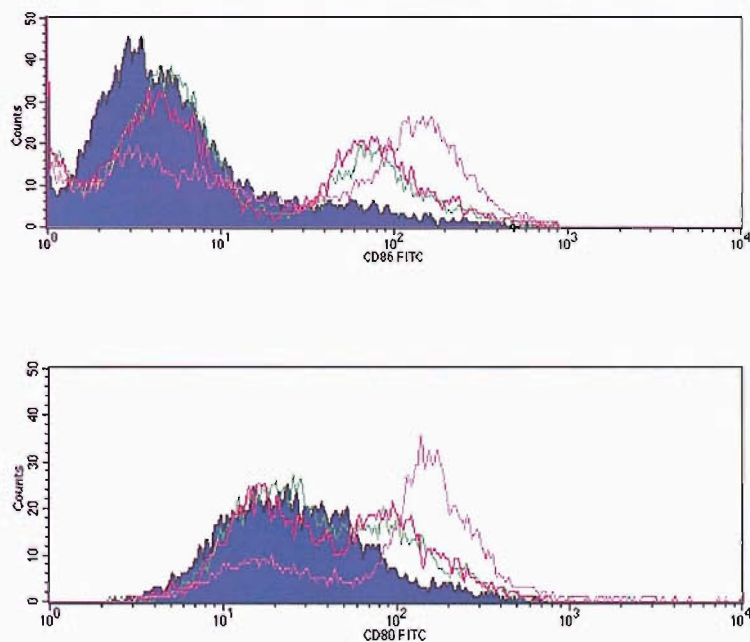


**Figure 3.10** Low-endotoxin OVA does not activate DCs in the absence of external stimulation. Day 10 DCs, prepared as in materials and methods, were incubated overnight in DC media alone (green line), or in the presence of 2.5µg/ml OVA (pink line) or 2.5µg/ml OVA plus 0.5ng/ml LPS (purple line). Cells were stained with CD11c-PE and either CD86-FITC or CD80-FITC. Blue solid area represents cells stained on day 10 prior to incubations. Histograms represent cells expressing CD86 (top) or CD80 (bottom), gated on live cells and further on CD11c-positive cells.

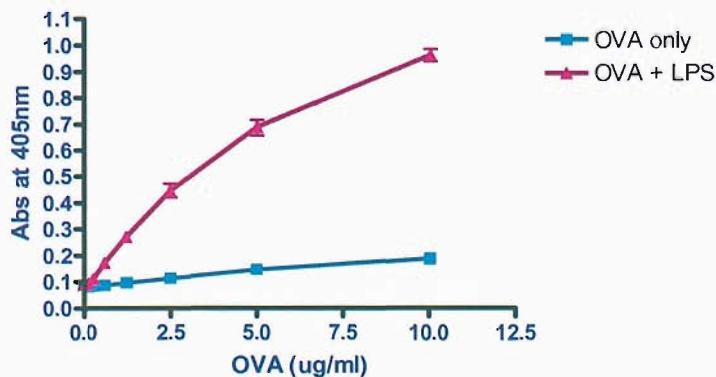


**Figure 3.11** DCs pulsed with low endotoxin OVA do not prime naïve OTII T cells in the absence of external stimulation. Day 10 DCs were incubated overnight with indicated concentrations of OVA alone or in the presence of 0.5ng/ml LPS then CD4<sup>+</sup> T cells from OTII mice were added and supernatants tested for IL-2 content by ELISA after overnight incubation.

### 3.2.4 Is the calreticulin functional?

A key area to be addressed is whether the calreticulin I have produced is functional. As the CRT is purified from cells, rather than being expressed as a recombinant protein, the likelihood of any loss of function is minimal. Also, the method our purification was based on is known not to alter the protein conformation and does not include any steps that are denaturing, and CRT is a very stable protein, resistant to temperatures in excess of 60°C, as well as enzymatic digestion under certain conditions (see discussion). As established earlier in the chapter, CRT migrates as a soluble monomer on a gel filtration column and also migrates to the expected weight (60kD) on SDS gels, indicating that there is no major misfolding. We thought that the ultimate test of functionality would be to use CRT for tumour immunotherapy. As I had purified CRT from a tumour cell line, P815, I attempted to protect DBA/2 mice against P815 challenge by vaccinating them twice at weekly intervals with 10µg/mouse CRT or PBS as a control. Mice were challenged with P815 7 days after the second immunisation. As can be seen in figure 3.12, mice immunised with CRT survived longer than those immunised with PBS. Of the first 3 mice of each group, those immunised with CRT survived on average 10 days longer than those immunised with PBS. All PBS-immunised mice had died 3 days before the CRT-immunised mice began to die. As this experiment contained only 4 mice per group, these data are not statistically significant ( $p=0.094$ ), but are promising preliminary results indicating that CRT is functional and does protect against tumour challenge, as previously reported. A better way to assess the protective effect of CRT would have been to measure tumour growth, and this is a key part of my future work.

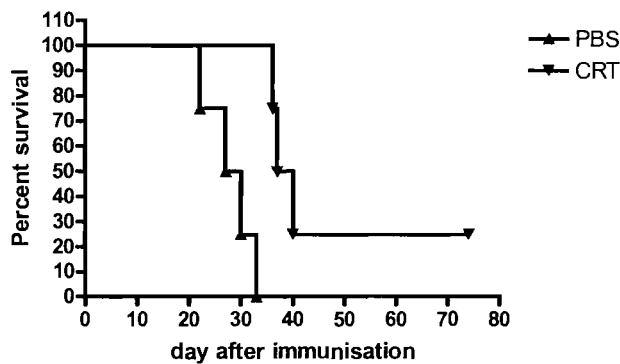


**Figure 3.12** Protective effect of CRT. 4 female DBA/2 mice were immunised subcutaneously at d-14 and d-7 with either 10µg CRT or PBS, and challenged with  $2.5 \times 10^4$  P815 cells on d0. Mice were culled when tumours reached 1cm in diameter.

Other potential methods of assessing the functionality of CRT are few, and this is considered in more detail in the discussion.

### **3.3 Discussion**

In this project, I felt it was important to focus on autologous CRT, i.e. murine CRT in a murine system, as much of the HSP work previously published has used non-autologous HSPs from bacteria or pigs in murine or human systems.

#### **3.3.1 Experimental artefact due to endotoxin contamination**

Initial experiments designed to establish optimal concentrations of OVA and LPS for the model system produced some surprising results. When DCs were pulsed with OVA in the absence of LPS and then incubated with OVA-specific T cells, a strong T cell response was generated, as measured by IL-2 production. This result contradicted the expected outcome, whereby a T cell response would only be generated in the presence of both Ag (OVA) and a DC activating stimulus (LPS), as both would be necessary to generate both signal 1 and signal 2 required for T cell priming by DCs. FACS analysis of co-stimulatory molecules on DCs demonstrated that OVA alone did induce some upregulation of the co-stimulatory molecule CD86, although to a lesser extent than LPS. These discrepancies were found to be due to contaminating bacterial endotoxin in the commercial OVA preparations, and once this was removed no T cell response to OVA-pulsed DCs was seen unless LPS was added.

In light of reports suggesting that some of the immunostimulatory effects attributed to HSPs are in fact due to contaminating endotoxin [91-93], along with our initial observations that endotoxin contamination of OVA led to artefactual responses, great care was taken to remove all traces of contaminating endotoxin from both OVA and CRT preparations for use in further experiments. All OVA and CRT preparations were tested for endotoxin contamination and treated with Polymyxin B until they contained <1EU/mg endotoxin, a level which does not induce any background activation. This means that all data on the effects of CRT reported in this thesis can be interpreted without concern about possible artefact caused by contamination.

### 3.3.2 Structure and functionality of CRT

As mentioned in section 3.2.4, as CRT was purified from cells and not expressed as a recombinant protein, there seems little reason that it should not be properly folded and functional. CRT is extremely thermally stable, so there should be no problems caused by periods at room temperature during chromatography steps. Gel filtration, SDS-PAGE and western blot analysis all indicated that CRT migrated as a soluble monomer to the appropriate molecular weight point, indicating no major structural problems. Independent measures of the native structure and function of CRT are limited, and are based on the cellular functions of CRT. One method of assessing that CRT is properly folded takes advantage of the protein's  $\text{Ca}^{2+}$ -binding function. Binding of  $\text{Ca}^{2+}$  to CRT appears to induce a conformational change in CRT, generating a 27kD N-terminal fragment that is resistant to trypsin digestion, whereas CRT that has not bound  $\text{Ca}^{2+}$  is completely digested by trypsin. Binding of CRT to other metal ions also affects its conformation, resulting in generation of protease-resistant fragments [133].

The ability of recombinant CRT to bind ERp57 and the oligosaccharide  $\text{Glc}_1\text{Man}_9\text{GlcNAc}_2$  can also be assessed, by radiolabelling ERp57 or the oligosaccharide and then mixing them with CRT immobilised on glutathione-agarose beads and measuring the radioactivity when the substrate is eluted from the beads. This, however, relies on the CRT being produced as a recombinant protein in bacteria with a GST-tag to enable binding to glutathione beads, and so is not feasible for use with the native CRT purified here.

Another method that could be used in this case is determination of the lectin and polypeptide-binding functions of CRT by its ability to suppress the aggregation of the glycoprotein  $\alpha$ -mannosidase or the non-glycosylated proteins citrate synthase and malate dehydrogenase respectively. The ability of CRT to refold heat-inactivated citrate synthase has also been used to demonstrate its chaperone function, and could be used to confirm the function of the native CRT. These methods could be used alone or in combination to confirm that the CRT I have purified has not lost any of its functions during the purification process. All methods are described in [137].

My preliminary vaccination data indicate that purified CRT does have a protective effect *in vivo*, and while these data require consolidation and further investigation, they confirm previous reports of the immunotherapeutic effects of CRT and suggest that it has not been inactivated during the purification process. As described in chapter 1, CRT has been reported to have anti-angiogenic effects both *in vitro* and *in vivo* [123-131], and this function of purified CRT is currently being investigated by Lesley Maskell in Paul Eggleton's laboratory, where the effects of CRT and CRT-fragments on growth of HUVEC cells *in vitro* are regularly studied. These data should provide further information on the functionality of the CRT used in this thesis, but experiments were still ongoing at the time of writing.

In summary, the available data show no indications that there should be any structural or functional abnormalities of the CRT purified from the P815 cell line.

## 4. Calreticulin does not have an adjuvant effect on antigen presenting cells

### 4.1 Introduction

Having prepared low-endotoxin CRT and demonstrated that this had a protective anti-tumour effect *in vivo*, I next investigated how this protection might be mediated. Studies on other HSPs, mainly hsp70 and gp96, have indicated that HSPs can induce a number of peptide-independent effects on cells of the immune system (described in section 1.2.3), including cytokine and chemokine secretion and upregulation of costimulatory molecules by DCs [52-60]. These effects are proposed to be critical for the immunogenicity of HSP-peptide complexes, as delivery of Ag by HSPs in the absence of APC activation would result in tolerance rather than immunity.

This function of CRT has not been well studied, indeed the only published study on the direct effects of CRT on APC activation, by Reed and co-workers, demonstrated that low endotoxin CRT induced an increase in ERK phosphorylation, but did not activate NF- $\kappa$ B signalling, or production of nitric oxide (NO) or inducible nitric oxide synthase (iNOS) production by macrophages [93]. My preliminary *in vivo* protection data described in chapter 3 along with previously published *in vivo* studies imply an immunostimulatory role for CRT in that an immune response can be generated against CRT-chaperoned peptides in the absence of any additional adjuvant, and CRT can be used to induce protective anti-tumour responses, again in the absence of exogenous adjuvant. Direct evidence of this function is, however, lacking, as are details on the mechanisms and of the effects induced.

In this chapter, I set out to investigate the effects of low-endotoxin autologous CRT on DC maturation by assessing the expression of costimulatory markers and production of pro-inflammatory cytokines by bone marrow-derived DCs in response to CRT compared to known activation stimuli LPS, CpG DNA and TNF $\alpha$ . I also wanted to study the ability of these DC to prime naïve T cells when pulsed with the model antigen OVA in the presence of the aforementioned stimuli, thus building up a comprehensive picture of the peptide-independent effects of CRT on APCs.

## 4.2 Results

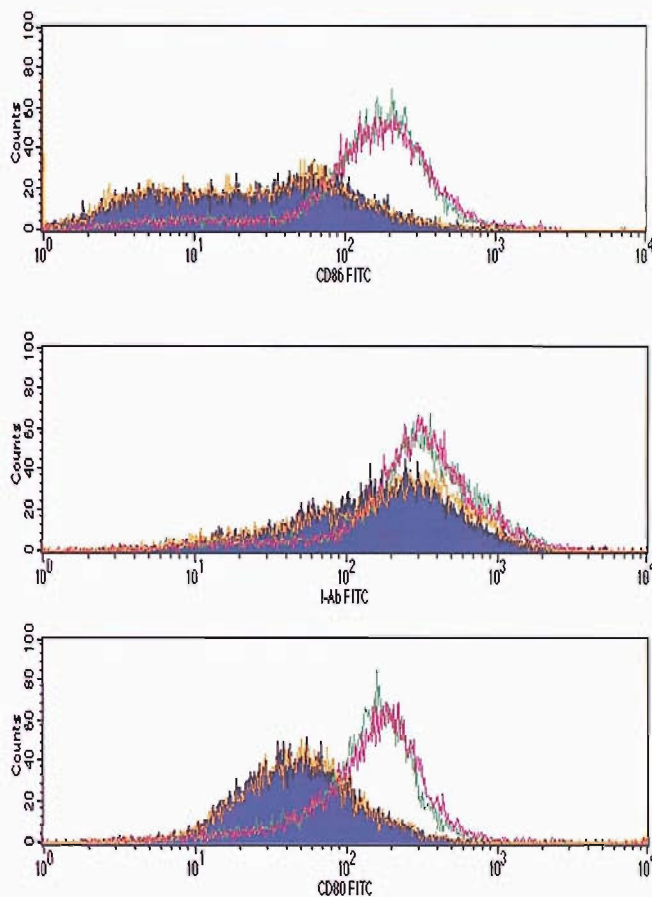
### 4.2.1 BMDCs upregulate cell surface markers in response to various activation stimuli, but not in response to calreticulin

All *in vitro* experiments were carried out on bone marrow-derived DCs generated from C57Bl/6 mice according to the method published in 1999 by Lutz et al. [136] and described in materials and methods. This method was highly successful, with typically >80% of cells obtained on day 8 or day 10 of culture being CD11c<sup>+</sup>. Cells generated by this method also undergo very little spontaneous maturation.

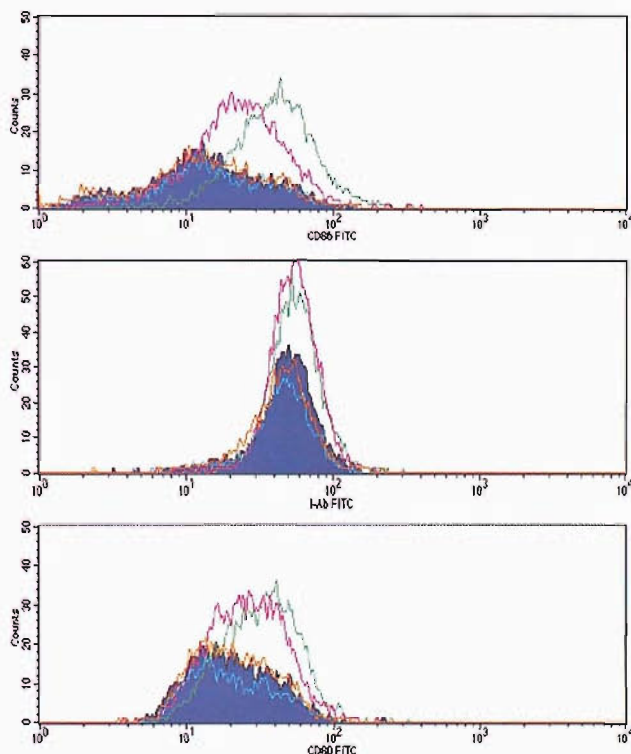
In order to assess the effects of CRT on DCs, it was first important to establish positive controls for DC activation. One method utilised to assess DC activation was measurement by FACS of expression of cell surface MHC class II and the costimulatory molecules CD80 and CD86. To ensure that DCs responded to a range of ligands, LPS, TNF $\alpha$  and CpG DNA were all tested for their ability to induce increases in marker expression by DCs.

Figure 4.1 demonstrates that DCs upregulated cell surface levels of MHC II and costimulatory molecules CD80 and CD86 in response to LPS and the CpG oligonucleotide 1668, but not in response to media alone or the control oligonucleotide 1720. This also confirms the lack of spontaneous DC maturation in the system. No upregulation of any marker was seen with OVA alone (see section 3.2.3).





**Figure 4.1** LPS and CpG DNA enhance DC expression of cell surface activation markers. Day 10 DCs were incubated overnight with 1ng/ml LPS (green), 5μg/ml immunostimulatory CpG oligo 1668 (pink), control oligo 1720 (orange) or DC media control (blue). Cells were then stained for FACS as described in materials and methods. Cells were stained with combination of CD11c-PE and CD86-, CD80- or MHC II-FITC and analysed on FACSCalibur. Live cells were gated from the total population and this population was further gated on CD11c<sup>+</sup> cells. Histograms represent expression of CD86 (top), MHC II (middle) and CD80 (bottom) by CD11c<sup>+</sup> cells.



**Figure 4.2** LPS and TNF $\alpha$  enhance DC expression of cell surface activation markers, whereas CRT does not. Day 10 DCs were incubated overnight with 0.5ng/ml LPS (green), 1μg/ml TNF $\alpha$  (pink), 10μg/ml CRT (orange) or boiled CRT (blue line), or DC media control (blue solid area). Cells were then stained for FACS as described in materials and methods. Cells were stained with combination of CD11c-PE and CD86-, CD80- or MHC II-FITC and analysed on FACSCalibur. Live cells were gated from the total population and this population was further gated on CD11c<sup>+</sup> cells. Histograms represent expression of CD86 (top), MHC II (middle) and CD80 (bottom) by CD11c<sup>+</sup> cells.

Figure 4.2 shows that, while DCs upregulated cell surface MHC II, CD80 and CD86 in response to LPS and TNF $\alpha$ , levels of these molecules on DCs incubated with CRT were not increased from the background level observed with DC media alone. This suggests that CRT does not activate DCs. Boiled CRT was used as a control for any remaining endotoxin contamination. A similar lack of activation was seen with low endotoxin murine hsp70 (Figure 4.3). These initial experiments were carried out using 10 $\mu$ g/ml CRT, a concentration chosen based on published literature for other HSPs. However some studies have used concentrations of HSPs up to 100 $\mu$ g/ml in order to see an effect, so these experiments were repeated and CRT was titrated up to 200 $\mu$ g/ml. As can be seen in figure 4.4, none of the concentrations tested had any effect on expression of DC surface markers, whereas LPS induced marked increases in expression of all markers.

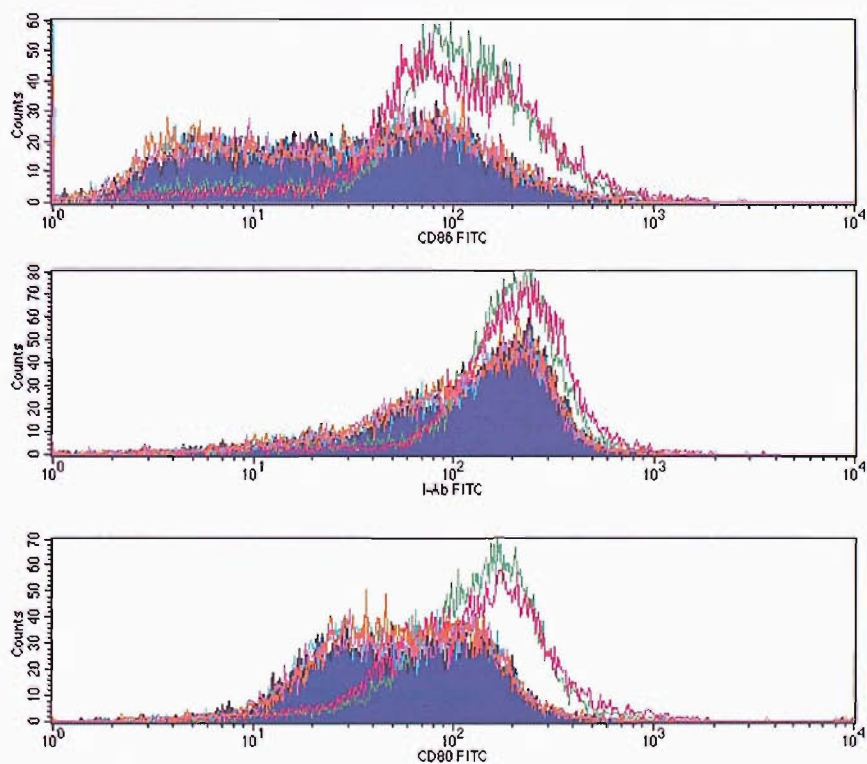


**Figure 4.3** LPS and CpG DNA enhance DC expression of cell surface activation markers, whereas CRT and hsp70 do not. Day 10 DCs were incubated overnight with 0.5ng/ml LPS (green), 1 $\mu$ g/ml stimulatory CpG (pink), 1 $\mu$ g/ml control CpG (blue line), 10 $\mu$ g/ml hsp70 (orange), 10 $\mu$ g/ml CRT (purple line), or DC media control (blue solid area). Cells were then stained for FACS as described in materials and methods. Cells were stained with combination of CD11c-PE and CD86-, CD80- or MHC II-FITC and analysed on FACSCalibur. Histograms represent expression of CD86 (top), MHC II (middle) and CD80 (bottom) by CD11c<sup>+</sup> cells.

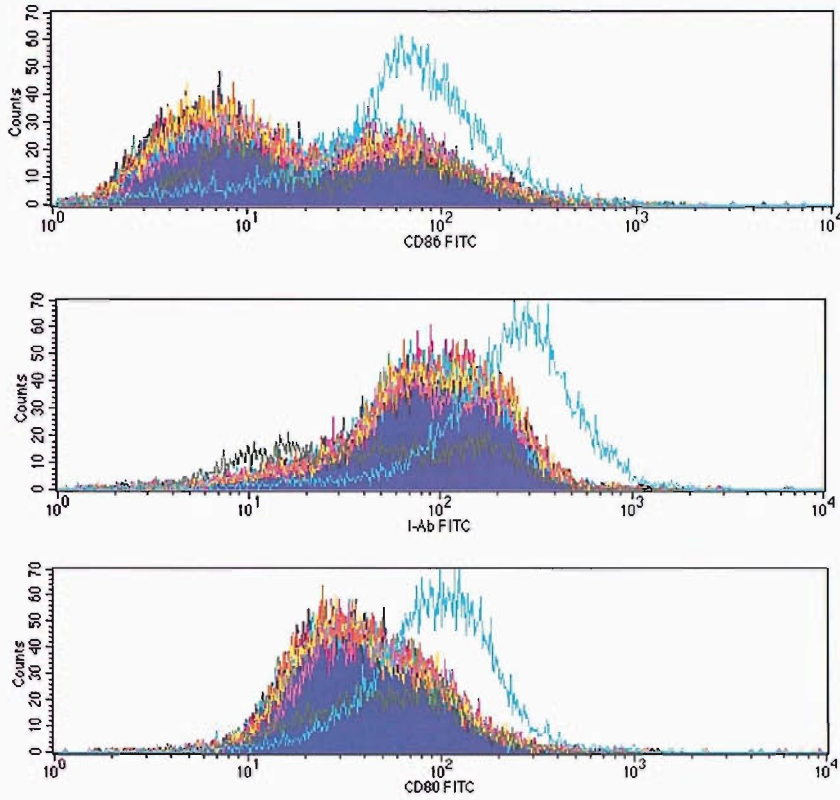


**Figure 4.4** CRT at concentrations up to 200 $\mu$ g/ml fails to induce any upregulation of DC surface activation markers. Day 10 DCs were incubated overnight with 1ng/ml LPS (light blue), concentrations of CRT from 3 to 200 $\mu$ g/ml (other lines), or DC media control (blue solid area). Cells were then stained for FACS as described in materials and methods. Cells were stained with combination of CD11c-PE and CD86-, CD80- or MHC II-FITC and analysed on FACSCalibur. Live cells were gated from the total population and this population was further gated on CD11c<sup>+</sup> cells. Histograms represent expression of CD86 (top), MHC II (middle) and CD80 (bottom) by CD11c<sup>+</sup> cells.



4.2.2 Freshly isolated splenic DCs upregulate cell surface markers in response to LPS, but not in response to calreticulin

The ability of stress proteins to initiate immune responses *in vivo* in the absence of adjuvant has previously been explained by the fact that HSPs themselves have adjuvant properties via their direct effect on DCs. My data presented above do not support this model, using BMDC as representative APCs. Other DCs might be affected and to this end I investigated the effect of CRT on expression of cell surface activation markers by splenic DCs. CD11c<sup>+</sup> cells were isolated from the spleens of C57Bl/6 mice as described in materials and methods and incubated overnight with LPS (0.1ng/ml-1μg/ml) or CRT (0.19-200μg/ml).

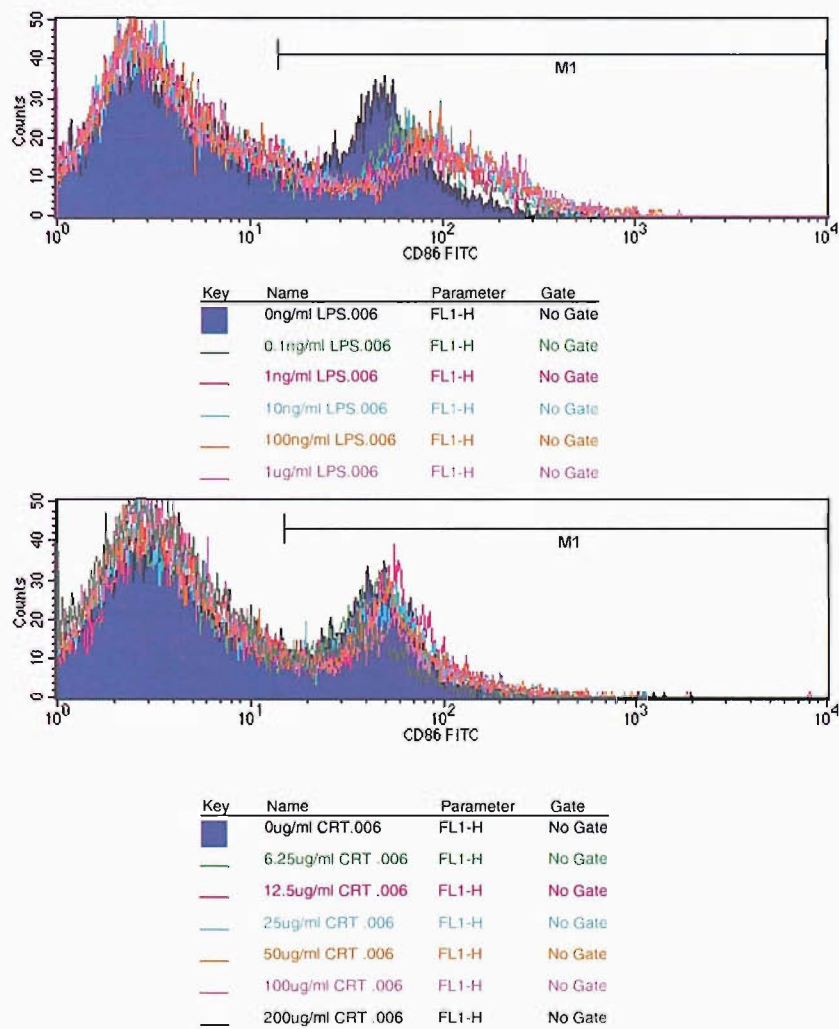


**Figure 4.5** LPS induces upregulation of CD86 by splenic DCs, whereas CRT does not. CD11c<sup>+</sup> cells isolated from spleens of C57Bl/6 mice were incubated overnight with indicated concentrations of LPS or CRT then stained with FITC-anti-CD86 as described in materials and methods. Events shown in histogram have been gated on live cells and further on CD11c<sup>+</sup> cells. Region M1 indicates cells expressing CD86.

Figure 4.5 shows representative histograms of CD86 expression by freshly isolated DCs incubated with varying concentrations of CRT or LPS overnight. Incubation with DC media was used as a control for spontaneous activation. Whereas cells incubated with LPS show a clear upregulation of CD86 as indicated by the region marked M1, there is no obvious increase in expression by cells incubated with CRT.

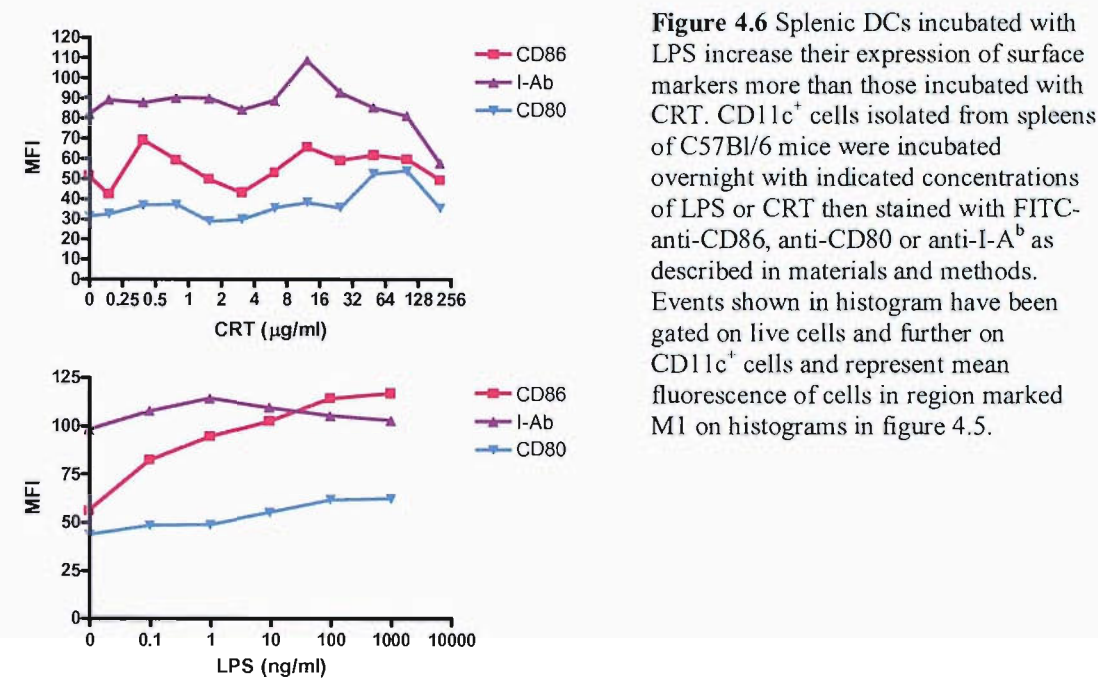
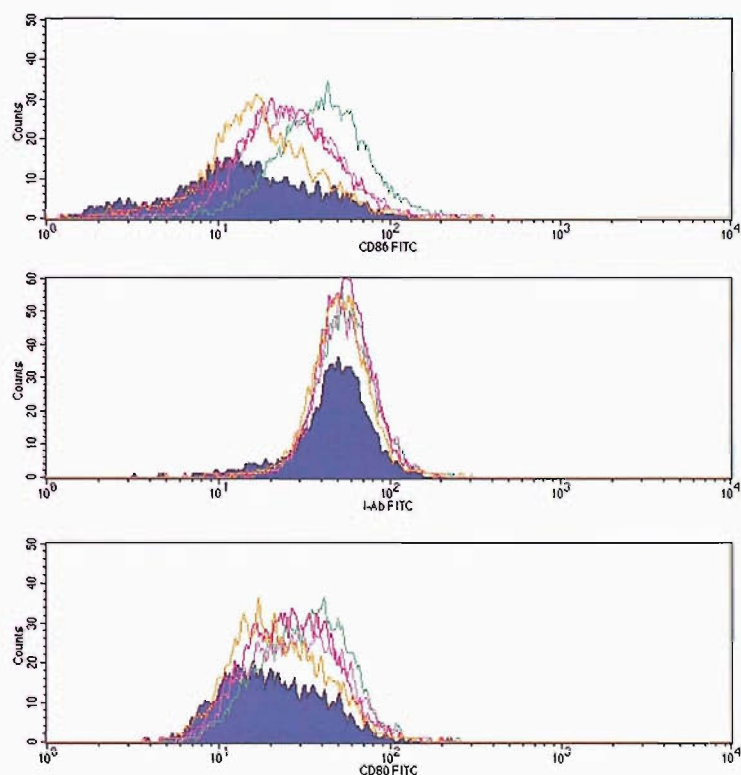


Figure 4.6 shows expression of CD86, CD80 and MHC class II by splenic DCs incubated overnight with CRT or LPS. The most marked difference in expression is in CD86, as also indicated in figure 4.4. All cells express high levels of MHC class II, even in the absence of stimulation. CD80 expression is much lower than that of the other two markers. In the case of CD86, there is also a clear dose-dependent effect of LPS, whereas there is no such clear effect with CRT. In fact, high concentrations of CRT appear to cause a decrease in expression, particularly of MHC Class II. This is consistent with previous reports of high doses of gp96 inducing immunosuppression [138-139].

Related to these findings, I have observed that, as shown in figure 4.7, CRT inhibits LPS- and TNF $\alpha$ -induced CD80 and CD86 expression on the DC surface. Together, these results point towards CRT having an immuosuppressive function, at least under certain circumstances. The concentration of CRT tested here is 10 $\mu$ g/ml, lower than the concentrations observed to decrease co-stimulatory marker expression on splenic DCs, and this concentration of CRT alone appears to have no effect on bone marrow-

derived DCs, so further investigation is required to fully elucidate the mechanisms by which CRT may be mediating suppression, an issue which is considered more fully in the discussion at the end of this chapter.



**Figure 4.7** Effect of CRT on DC surface marker expression induced by LPS. Day 10 DCs were incubated overnight with 0.5ng/ml LPS (green) or 1µg/ml TNFα (pink), alone or in the presence of 10µg/ml CRT. LPS + CRT = purple line, TNF + CRT = orange line. DC media alone used as control (blue solid area). Cells were then stained for FACS as described in materials and methods. Cells were stained with combination of CD11c-PE and CD86-, CD80- or MHC II-FITC and analysed on FACSCalibur. Live cells were gated from the total population and this population was further gated on CD11c<sup>+</sup> cells. Histograms represent expression of CD86 (top), MHC II (middle) and CD80 (bottom) by CD11c<sup>+</sup> cells.

### 4.2.3 DCs produce IL-12 and IL-2 in response to LPS and CpG DNA, but not in response to calreticulin or hsp70

The FACS data demonstrated that CRT and hsp70 did not enhance expression of costimulatory molecules or MHC II by DCs, so I next investigated whether these factors affected production of cytokines by DCs. Day 10 DCs were cultured overnight with LPS, CpG DNA, CRT or hsp70 and supernatants tested for cytokines by ELISA as described in materials and methods. Figure 4.8 shows that DCs produce IL-2 and IL-12 in response to both LPS and CpG oligonucleotide 1668 in a concentration-dependent manner, whereas media and control oligo 1720 do not induce production of either of these cytokines. No IFNγ or IL-10 production could be detected.



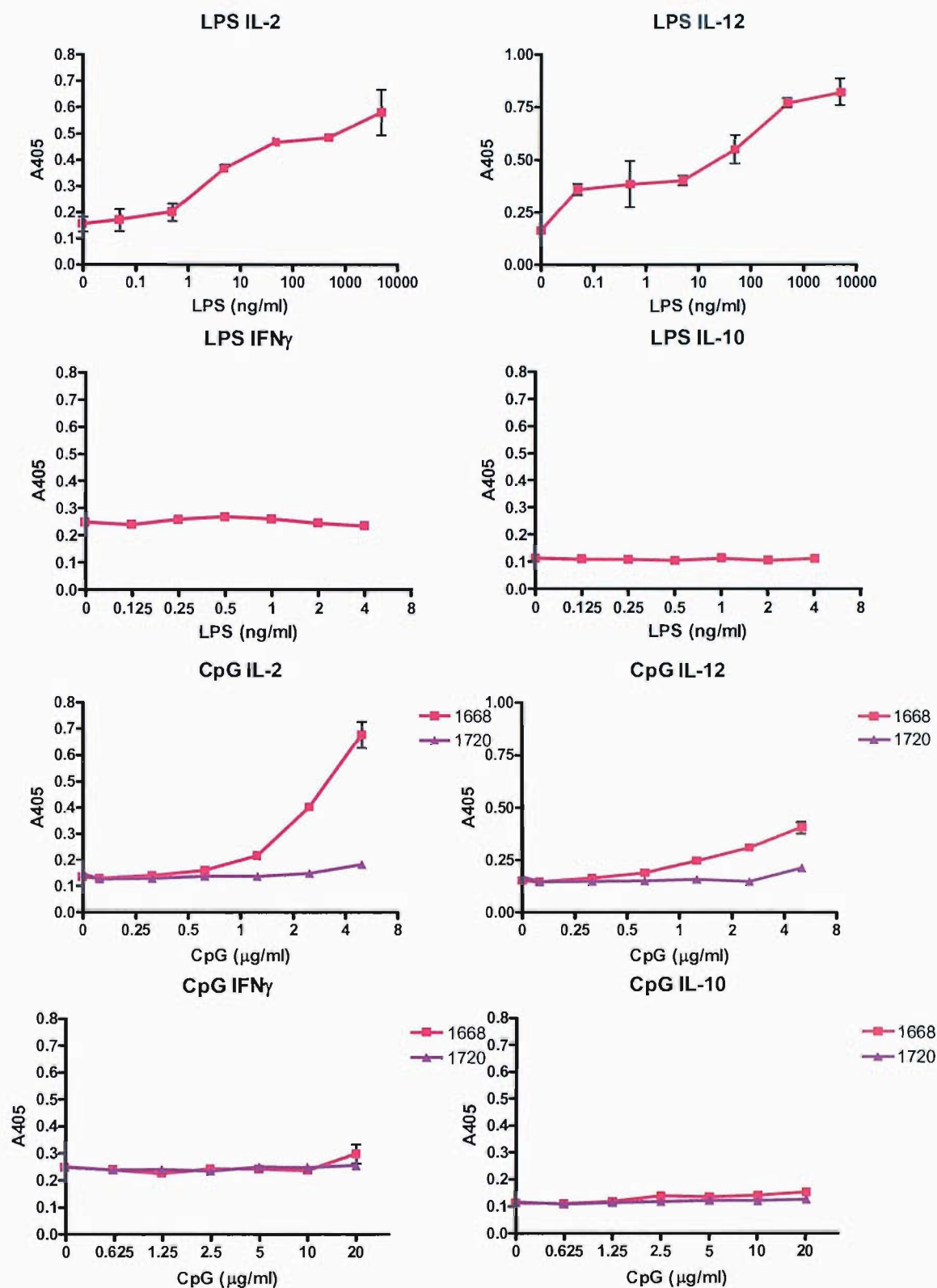


**Figure 4.8** LPS and CpG DNA induce production of IL-2 and IL-12, but not IL-10 or IFN $\gamma$ , from DCs in a concentration-dependent manner. Day 10 DCs were incubated with indicated concentrations of LPS, CpG oligo 1668 or CpG oligo 1720 overnight and then supernatants were tested for cytokine production by ELISA as described in materials and methods section. Points plotted represent means of 2 replicates, with error bars representing standard deviation.

Figure 4.9 shows that neither CRT nor hsp70 induce cytokine production by DCs. It should be noted that, in these figures, cytokine production in response to CpG DNA was lower than in the previous experiments, however there was a clear concentration-dependent increase in cytokine levels that was not evident with CRT or hsp70. As with the FACS data, there was a concern that the concentrations of CRT tested may have been too low to elicit a response, so the cytokine production by DCs in response to concentrations of CRT up to 200 $\mu$ g/ml was tested. As with the expression of surface markers, none of the tested concentrations induced significant IL-2 or IL-12 production by BMDC (Fig 4.10).

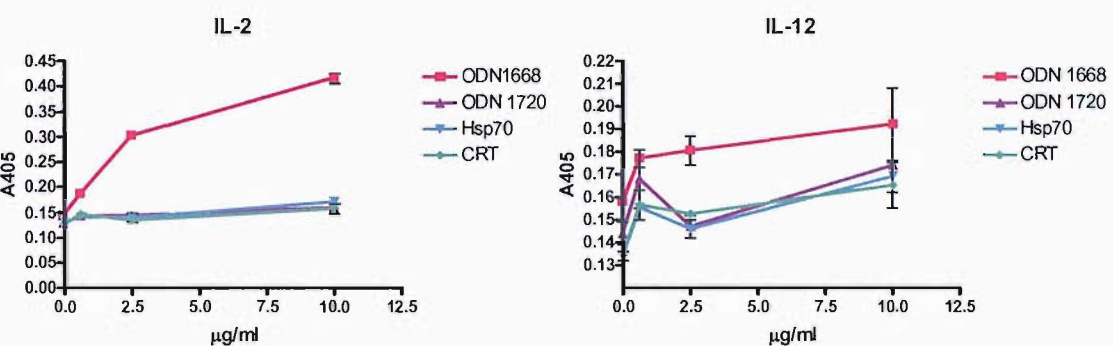


**Figure 4.9** Neither CRT nor hsp70 induce production of IL-2 or IL-12 by DCs. Day 10 DCs were incubated with indicated concentrations of CpG oligos 1668 or 1720, or CRT or hsp70 overnight then culture supernatants assessed for IL-2 and IL-12 content by ELISA as described in materials and methods. Points represent mean of 2 replicates, with error bars representing standard deviation.

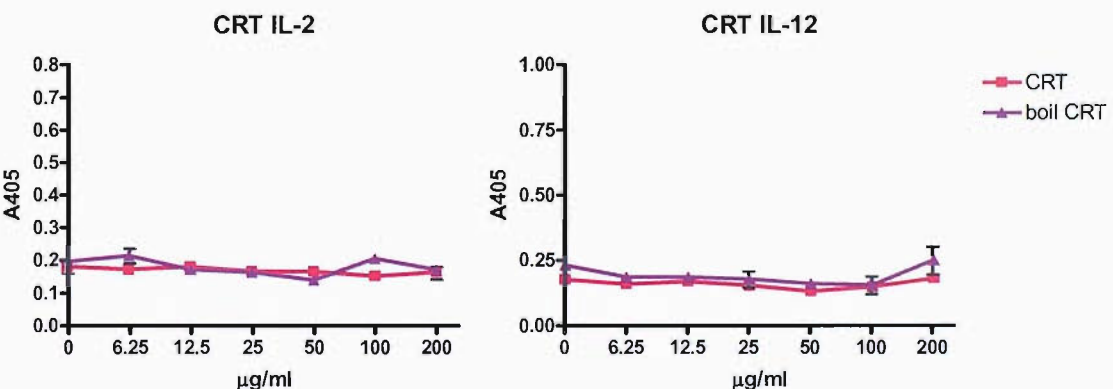


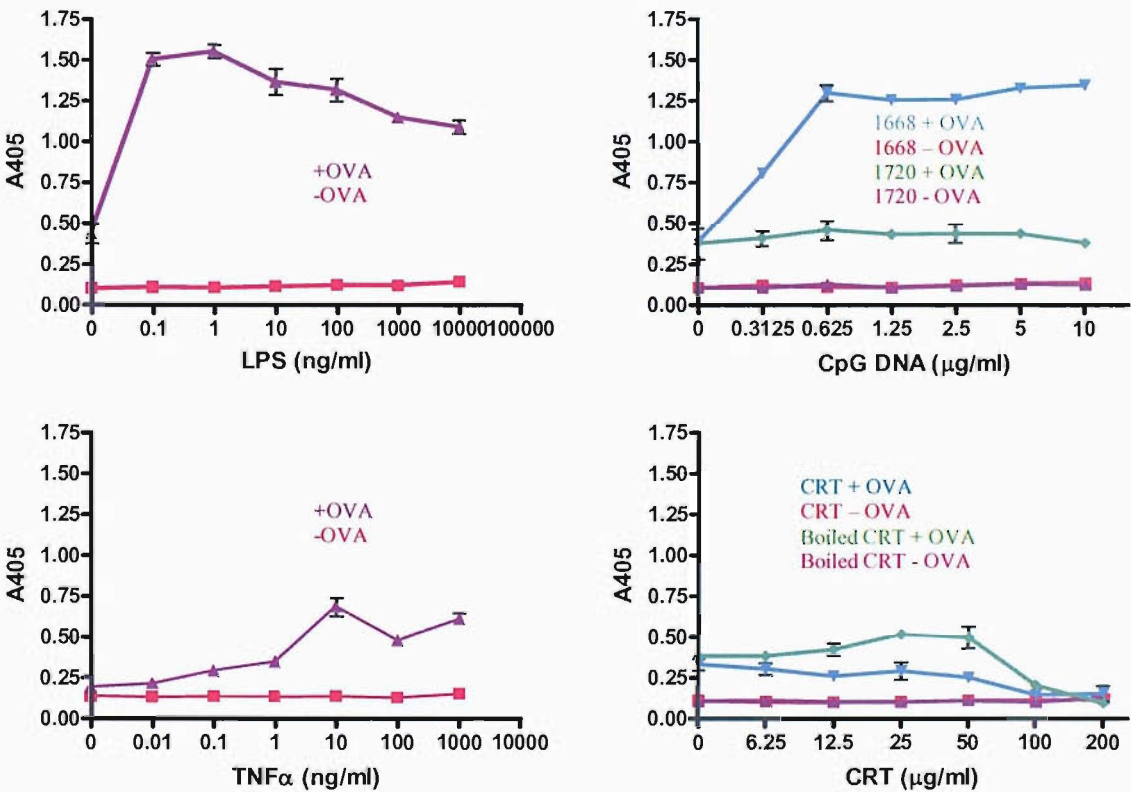
**Figure 4.10** Concentrations of CRT up to 200 $\mu$ g/ml do not induce IL-2 or IL-12 production by DCs. Day 10 DCs were incubated with indicated concentrations of CRT overnight then culture supernatants assessed for IL-2 and IL-12 content by ELISA as described in materials and methods. Points represent means of 3 replicates, error bars represent standard deviation.

These data combined with the FACS data provide strong evidence that neither CRT nor hsp70 activate immature bone marrow derived DCs or ex vivo splenic DCs.



**4.2.4 Stimulation with LPS, TNF $\alpha$  or CpG-DNA enables OVA-pulsed DCs to prime naïve CD4<sup>+</sup> transgenic T cells, whereas CRT and hsp70 do not**

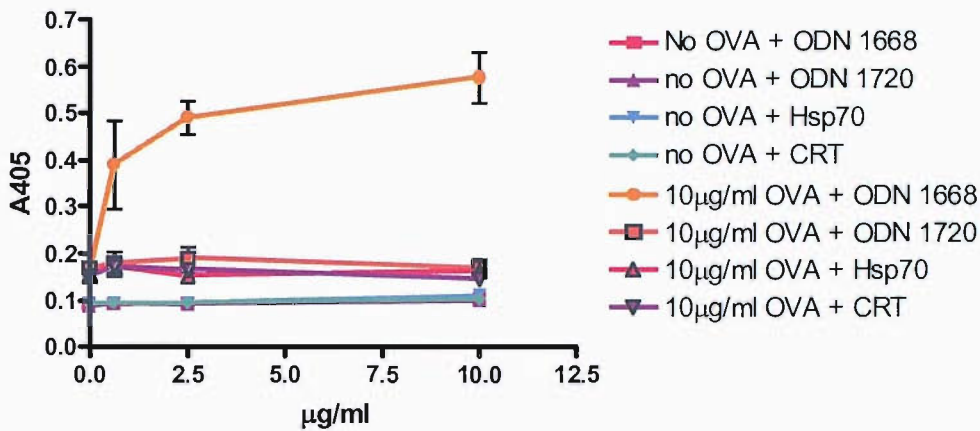
Following results indicating that CRT and hsp70 do not upregulate key activation markers nor induce secretion of key inflammatory cytokines by bone marrow derived DCs, I investigated whether CRT or hsp70 had any effect on the ability of OVA-pulsed DCs to prime naïve T cells from transgenic mice. Figure 4.11 demonstrates that day 10 DCs incubated with 20 $\mu$ g/ml OVA in the presence of increasing concentrations of LPS, TNF $\alpha$  or CpG DNA are capable of inducing IL-2 production by naïve CD4<sup>+</sup>T cells from OT-II mice. However, if CRT is added instead of LPS, TNF $\alpha$  or CpG DNA, no IL-2 production is observed. As with FACS experiments, boiled CRT is used as a control for any residual endotoxin contamination.



**Figure 4.11** LPS, TNF $\alpha$  and CpG DNA enable OVA pulsed DCs to induce IL-2 production from naïve T cells, whereas CRT does not. Day 10 DCs were incubated overnight with indicated concentrations of LPS, TNF $\alpha$ , CpG DNA (stimulatory 1668 or non-stimulatory control 1720) or CRT in the presence or absence of 20 $\mu$ g/ml OVA. CD4<sup>+</sup> T cells from OTII mice were added and overnight supernatants tested for IL-2 by ELISA. Bars represent means of triplicates, with error bars representing standard deviation.

This result confirms the FACS and DC cytokine data, indicating that CRT does not have any positive effect on activation of primary bone marrow-derived DCs.

Since these findings seemed to contradict previously published reports that other HSPs, such as hsp70 and gp96, enhance immune responses, and previous reports as well as my own experiments indicating that CRT is immunologically active, these T cell assays were repeated, over a smaller titration range) including hsp70 in order to see how hsp70 behaves in our model system. FACS and DC cytokine data seemed to indicate that hsp70, like CRT, does not activate DCs.



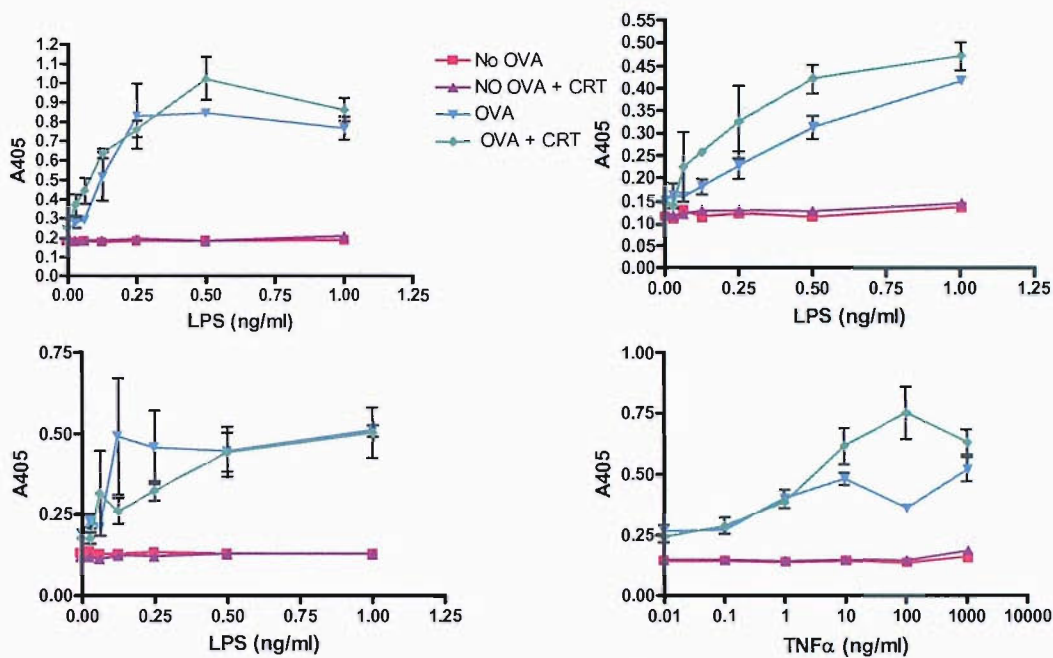
**Figure 4.12** CpG DNA, but not CRT or hsp70, enables OVA-pulsed DCs to induce IL-2 production from naïve CD4<sup>+</sup>T cells. Day 10 DCs were incubated overnight with indicated concentrations (x-axis) of stimulatory CpG oligo 1668, control oligo 1720, hsp70 or CRT. CD4<sup>+</sup>T cells from OTII mice were added and supernatants from overnight incubation tested for IL-2 content by ELISA. Means of duplicate values are plotted +/- standard deviation.

Figure 4.12 shows that hsp70, like CRT, does not enable OVA-pulsed DCs to induce IL-2 production from OVA-specific T cells. These findings apparently contradict the published findings relating to the immunostimulatory functions of hsp70, although this study differs from previous work in that I have examined the effect of low-endotoxin, autologous hsp70 rather than using bacterial hsp: a difference that will be discussed in greater depth at the end of this chapter.

#### 4.2.5 Calreticulin does not affect IL-2 production by transgenic CD4<sup>+</sup> T cells in response to LPS- or TNF $\alpha$ -activated OVA-pulsed DCs

The results described thus far indicated that DCs respond to various stimuli by upregulating cell surface activation markers and producing pro-inflammatory cytokines. This activation of DCs enables them to prime naïve T cells in the presence of antigen. CRT and hsp70 do not induce any of these features of DCs. In the absence of any positive effects of CRT, and in light of my observations, described in section

4.2.2, that CRT can have suppressive effects on expression of DC activation markers, I investigated whether CRT modulated the T cell response to OVA-pulsed DC activated by LPS or TNF $\alpha$ . HSPs have been reported to utilise many of the same receptors as LPS in particular, so it is possible that CRT may compete with LPS for receptor binding, antagonising its effects. This idea was supported by FACS data described in section 4.2.2, which showed that CRT inhibits LPS- and TNF $\alpha$ -induced CD80 and CD86 expression by BMDCs.



**Figure 4.13** CRT has no effect on response of OTII T cells to LPS- or TNF $\alpha$ -activated, OVA-pulsed DCs. Day 10 DCs were incubated for 6 hours with indicated concentrations of LPS or TNF $\alpha$  in the presence or absence of 10 $\mu$ g/ml CRT prior to overnight incubation with 20 $\mu$ g/ml OVA. CD4 $^{+}$  T cells from OTII mice were added and overnight culture supernatants tested for IL-2 content by ELISA. Points plotted are means of triplicate values with standard deviation represented by error bars. 3 repeats of LPS assay are shown.

As can be seen in figure 4.13, CRT did not significantly affect the production of IL-2 by transgenic T cells in response to OVA-pulsed DCs activated with either LPS or TNF $\alpha$ . Thus, while this apparently contradicts the FACS data described earlier, the data may nevertheless be compatible and it may be that the reduced DC activation levels are still sufficient to induce the same levels of T cell priming.

#### 4.2.6 Effect of CRT on priming CD8 $^{+}$ T cells *in vitro*

The effect of exogenous CRT on priming of naïve transgenic CD8 $^{+}$  T cells was also investigated. Experiments were carried out as described for CD4 $^{+}$  responses, but instead of using CD4 $^{+}$  T cells from OTII mice, CD8 $^{+}$  T cells were purified from OTI



mice. OTI mice have CD8<sup>+</sup> T cells which express a TcR specific for OVA<sub>257-264</sub> (SIINFEKL) in the context of the MHC class I molecule H-2K<sup>b</sup>.

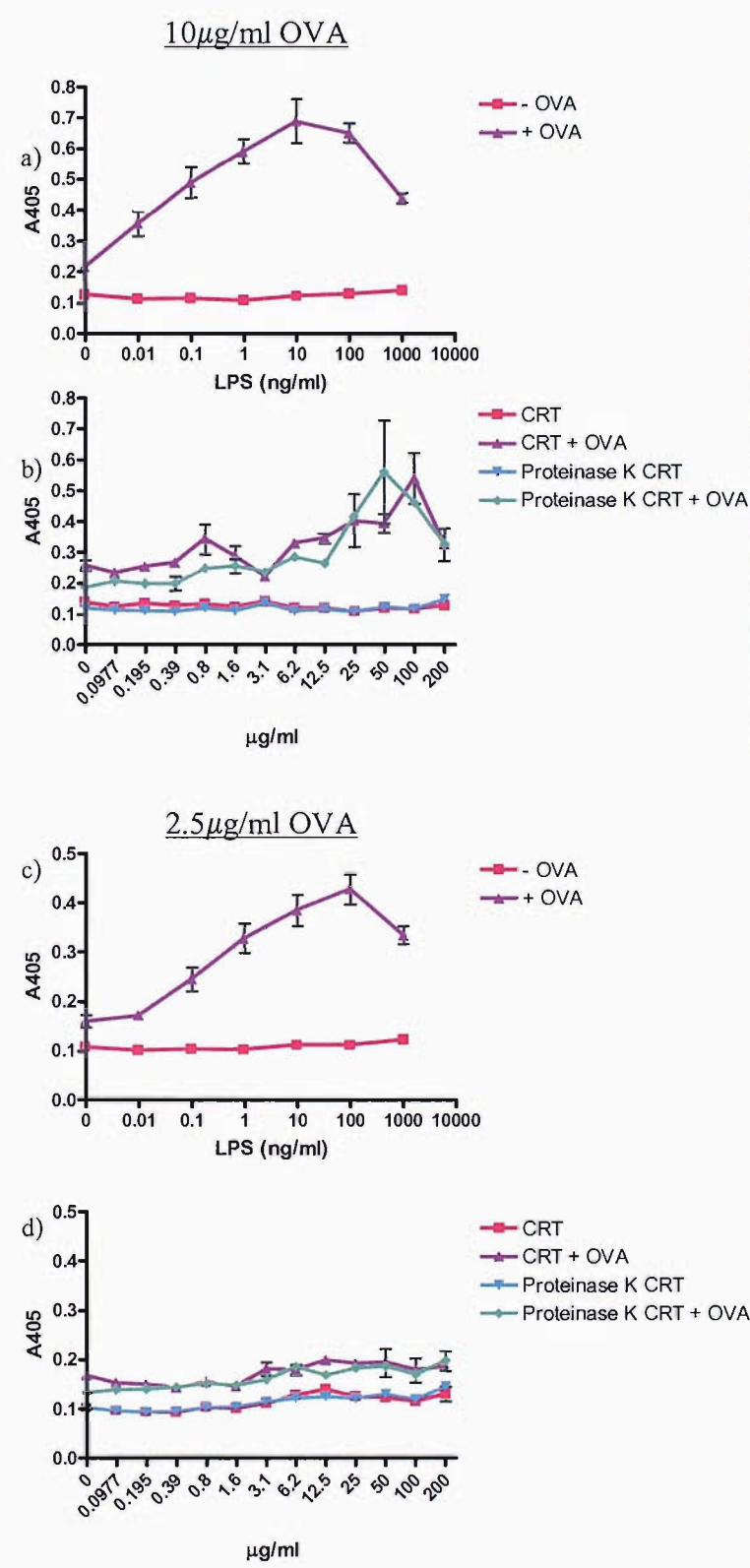


**Figure 4.14** Effects of CRT and LPS on priming of naïve OVA-specific CD8<sup>+</sup> T cells. Day 10 DCs were incubated overnight with 10µg/ml (a,b) or 2.5µg/ml (c,d) OVA in the presence of indicated concentrations of LPS (a,c) or CRT (b,d). CRT that had been incubated with 50µg/ml proteinase K for 1 hour at 37°C was used as a control for endotoxin contamination. CD8<sup>+</sup> T cells from OTI mice were then added and cultures incubated overnight. IL-2 produced was measured by ELISA on supernatants. Points represent mean of 2 replicates, with error bars representing standard deviation.

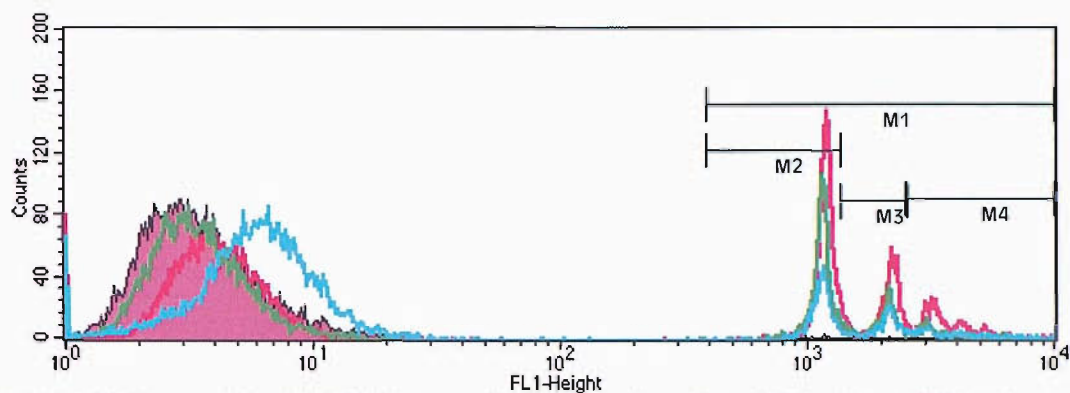
Figure 4.14 illustrates the effects of CRT and LPS on the ability of OVA-pulsed DCs to prime naïve OVA-specific CD8<sup>+</sup> T cells. 4.14a and c show that LPS induces

priming in a concentration-dependent manner, and that priming is also dependent on concentration of Ag, as more IL-2 as produced in response to DCs pulsed with 10 $\mu$ g/ml OVA than those pulsed with 2.5 $\mu$ g/ml. It should also be noted that the highest concentrations of LPS led to a decrease in response – an example of the LPS overdose effect. 4.14b and d illustrate the effects of CRT on priming. In fig. 4.14b, there appears to be some ability of CRT to induce priming at concentrations over 6.25 $\mu$ g/ml. Concentrations over 100 $\mu$ g/ml induce a decrease in response, further supporting my findings relating to downregulation of splenic DC markers at these concentrations. However, at the lower concentration of OVA (fig. 4.14b), CRT appears to have no effect on priming, whereas LPS is still capable of inducing priming (fig. 4.14d). It must also be noted that the same effects are induced by Proteinase K-treated CRT as by native CRT. Proteinase K treatment was included as a control for endotoxin contamination, as treatment with Proteinase K should denature CRT, but not any contaminants. Thus, a response to treated CRT may indicate an effect of endotoxin contamination. However, the CRT has been extensively tested for contamination and treated with Polymyxin B until there were no detectable levels of contamination, and this combined with the lack of effect of CRT at the lower concentration of OVA suggest that contamination may not be the explanation. CRT has been demonstrated to be susceptible to digestion by Proteinase K [140], although the efficacy of digestion in this experiment has not been tested. Analysis of the extent of Proteinase K digestion would allow me to determine whether the increase in OTI priming observed at high concentrations of CRT was significant.

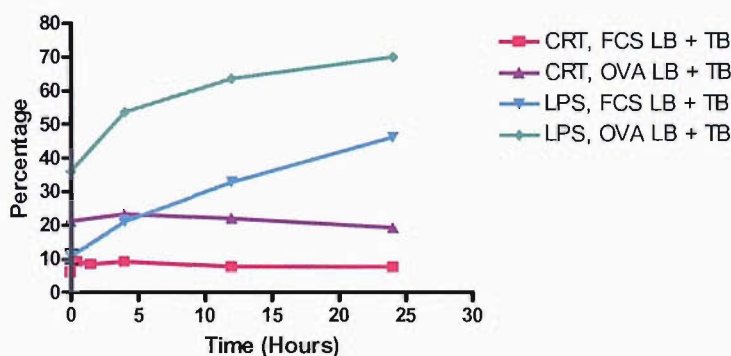
#### **4.2.7 Calreticulin does not enhance phagocytosis of latex beads by DC2.4 cells, whereas LPS does**

Another aspect of the biological effect of CRT that this project aims to explore is its effect on phagocytosis. My interest in this arose from previous reports of the role of CRT in phagocytosis as described in chapter 1, and also from a study demonstrating that activation of DCs with LPS led to a transient increase in phagocytosis [141]. This contrasts with the traditional view that phagocytosis is down-regulated immediately upon activation, but makes sense as a transient burst of phagocytic activity to coincide with DC activation should ensure that Ags are captured from the source of the activating stimulus. For this investigation, the DC-like cell line DC2.4 was used in preference to bone marrow-derived DCs as these cells are adherent and thus easier to use in this assay system.

Phagocytosis assays were carried out as described in materials and methods. Figure 4.15 is a representative histogram obtained from running DC2.4 cells pre-incubated with LPS and then with FCS-coated latex beads through the FACS machine. The population of cells forming the peaks on the left represent those cells that are not associated with LB. Each peak on the right represents cells that are associated with beads - therefore, the percentage of cells contained within the first marker region (M1) represents the total percentage of cells in this sample that were associated with LB. The cells in the M2 marker region represent the percentage of cells that were associated with 1 LB, the cells represented in the M3 marker region show the percentage of cells that were associated with 2 LB and the cells in the M4 marker region are those that were associated with 3 or more LB. Figure 4.16 is a graph of the total percentage of the DC2.4 cells that had taken up latex beads after a 24-hour timecourse of pre-exposure to LPS or CRT. With either OVA- or FCS-opsonised beads, uptake was enhanced as the length of pre-exposure to LPS was increased. However, with CRT, no such increase was observed. TB indicates samples to which trypan blue was added prior to running through the FACS machine, to quench any beads that were merely stuck to the cell surface, rather than internalised.

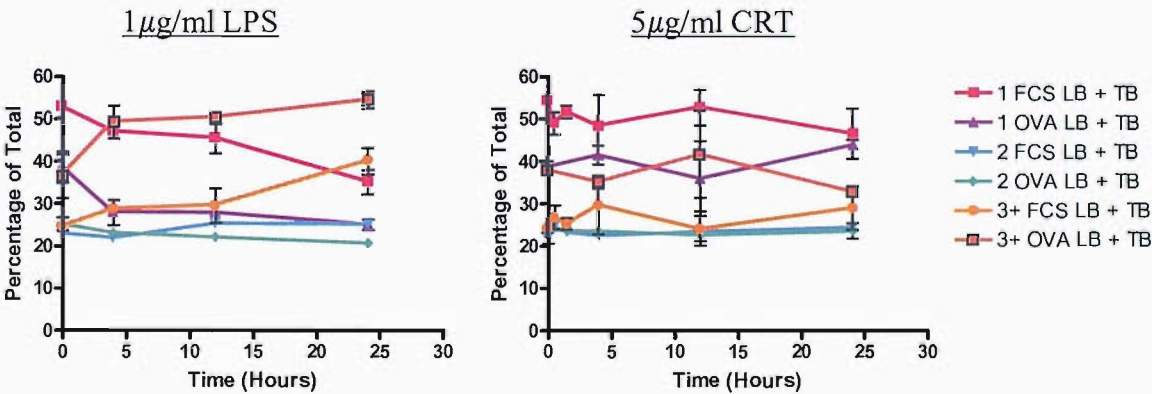


**Figure 4.15** Representative FACS histogram plot showing the peaks of LB uptake at 37°C with no LPS pre-exposure (green), 4 hours LPS pre-exposure (pink) and 48 hours LPS pre-exposure (blue) by cells that were not quenched by TB. The peaks on the left represent cells not associated with LB. Each peak on the right represents cells associated with beads - the percentage of cells contained within region M1 represents the total percentage of cells associated with LB. The cells in region M2 represent cells associated with 1 LB, the cells represented in the M3 marker region show the percentage of cells associated with 2 LB and the cells in region M4 represent those associated with 3 or more LB. These percentages are shown in the graphs which follow, plotted using Prism 4 software.



**Figure 4.16** Total LB uptake increases with pre-exposure to LPS, but not CRT. FACS analysis was performed immediately after incubation with FCS or OVA opsonised LB, which itself followed pre-exposure to 5µg/ml CRT or 1µg/ml LPS for 0, 0.5, 1.5, 4, 12 or 24 hours. (0.5 and 1.5 hours in samples for CRT pre-exposure and subsequent HI-FCS opsonised LB pulse only). Mean and Standard deviations of triplicates are shown.

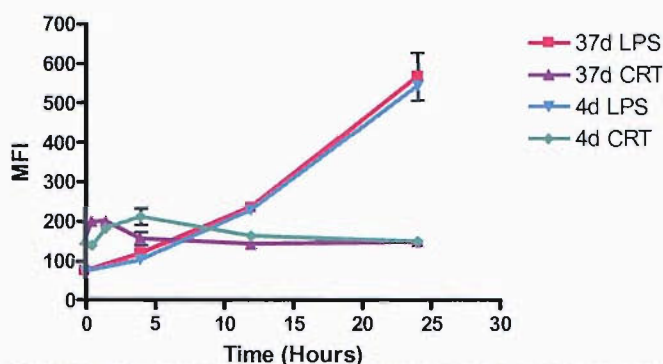
Fig 4.17 shows how the number of LB captured by DC2.4 cells shifts with length of pre-exposure to LPS. Data is derived from calculating the percentage of the cells that took up one or two or three and above LB as a percentage of the total percentage of cells in the population that did take up LB (i.e., M2 as a percentage of M1, M3 as a percentage of M1 and M4 as a percentage of M1). It shows that with increasing length of pre-exposure to LPS over a 24-hour time course, the total percentage of TB quenched cells associated with 1 LB, opsonised with either FCS or OVA, falls – most dramatically when LPS exposure is for the 4 hours immediately before the pulse with LB. The percentage of cells associated with two LB remains reasonably constant, while the percentage of cells associated with three or more LB increases in a manner approximately proportionate to the reduction seen in uptake of one LB. No such pattern was observed following pre-incubation with CRT – the number of cells taking up each number of beads remains reasonably constant throughout. These experiments demonstrate that pre-incubation with LPS leads to an increase both in the total number of cells taking up LB and in the number of beads taken up by individual cells, whereas CRT does not.



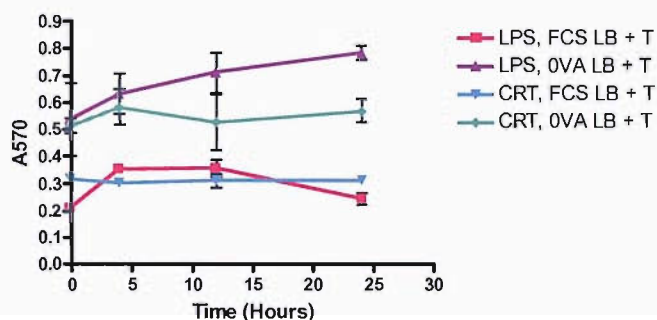
**Figure 4.17** Pre-exposure to LPS, but not CRT, leads to increase in the number of beads internalised per cell. DC2.4 cells were incubated with medium containing 1 µg/ml LPS (left hand graph) or 5 µg/ml CRT (right hand graph), for 0, 0.5, 1.5, 4, 16 or 24 hours after which times the media was removed and cells pulsed for 1 hour with HI-FCS or OVA opsonised LB at 37°C. Mean and standard deviation of triplicates are shown.

Figure 4.18 shows that expression of CD80 on the cell surface was also enhanced by pre-exposure at 37°C to LPS, but not by pre-exposure at 37°C to CRT. Similar results were obtained for CD86 and MHC class II (not shown). Experiments were also carried out at 4°C as a control, as cells should be inactive at this temperature, and indeed no increase in marker expression was seen at this temperature. Phagocytosis and antigen presentation were also inhibited at 4°C (data not shown).





**Figure 4.18** Pre-exposure to LPS, but not CRT, leads to enhanced CD80 expression by DC2.4 cells. DC2.4 were incubated for 0, 0.5, 1.5, 4, 12 or 24 hours with medium containing  $1\mu\text{g/ml}$  LPS or  $5\mu\text{g/ml}$  CRT then incubated for 1 hour at either  $37^\circ\text{C}$  or  $4^\circ$  with R10 medium only, stained with PE anti-mouse CD80 and analysed by FACS. Mean and standard deviation of duplicates (CRT and LPS both at  $37^\circ\text{C}$  and CRT at  $4^\circ\text{C}$ )/single values (LPS at  $4^\circ\text{C}$ ) are shown. 37d =  $37^\circ\text{C}$ , 4d =  $4^\circ\text{C}$ .



**Figure 4.19** Change in Antigen Presentation by DC2.4 to B3Z T cells, following pre-exposure of DC2.4 to LPS or CRT, at points over a 24 hour time course. DC2.4 were incubated with  $1\mu\text{g/ml}$  LPS or  $5\mu\text{g/ml}$  CRT for 0, 4, 12 or 24 hours. Supernatant was removed and cells pulsed for 1 hour with HI-FCS or OVA opsonised LB at  $1.42 \times 10^6 \text{ LB/ml}$  in R10. Cells were then incubated for a 6 hour chase with R10 at  $37^\circ\text{C}$  to allow time for processing of OVA antigen that opsonised LB. This was followed by an overnight incubation with B3Z T cells, before addition of CPRG substrate and a further one hour incubation to allow colour to develop at  $37^\circ\text{C}$  before absorbance was read at 570nm. Mean and standard deviation of triplicates are shown.

Figure 4.19 demonstrates that presentation of OVA to B3Z T cells by DC2.4 cells that have been incubated with OVA-opsonised latex beads was also enhanced by pre-exposure to LPS, but not by pre-exposure to CRT. The B3Z response was Ag-specific, as some background response was seen in response to FCS-opsonised beads, but this was not of the same magnitude as the response to OVA-opsonised beads.

Taken together, these data suggest that extracellular CRT does not have any effect on phagocytosis of latex beads by DC2.4. Further experiments are planned to extend these findings to primary cells (i.e. bone marrow-derived DCs).

#### 4.2.8 CRT stimulates proliferation of CD8<sup>+</sup> but not CD4<sup>+</sup> T cells *in vivo*

The results described so far in this chapter provide a range of evidence that CRT has no immunostimulatory effects on bone marrow-derived DCs. However, as described in chapter 3, the same CRT has a protective anti-tumour effect *in vivo*. This points to CRT having some stimulatory effect other than those I have examined so far. In order to further elucidate the *in vivo* effects of CRT, I investigated whether co-administration of CRT with OVA enhanced proliferation of OVA-specific T cells *in vivo*.

As shown in figure 4.20a, some proliferation of OVA-specific CD8<sup>+</sup> T cells occurred when CRT was co-administered with OVA, whereas there was no proliferation when mice were immunised with OVA alone. The percentage of cells in the gated region marked “1”, i.e. non-proliferating cells, was 3.28% in the animal immunised with OVA alone, compared to 1.62% in the animal immunised with OVA+CRT. This 50% reduction was representative of results from all 3 animals in each group. The average percentage of non-proliferating cells was 2.26 for mice immunised with OVA alone, versus 1.37 for mice immunised with CRT+OVA. While these results are not statistically significant ( $p=0.219$ ), there is a clear difference between the 2 groups of mice. No proliferation of CD4<sup>+</sup> T cells was observed (fig. 4.20b), with the average percentage of non-proliferating cells in each group being 1.19%. Table 4.1 further illustrates the division of OTI but not OTII cells. The figures in this table represent the events in each gated region as a percentage of the total events in both regions. This eliminates the large background of non-labelled cells. A clear division of OTI cells can be seen when CRT was co-administered with OVA, but not when OVA was administered alone. No division of OTII T cells is seen under either condition. This was a preliminary experiment and further study of a broader range of CRT and OVA concentrations to optimise conditions using larger groups of mice should confirm these data, and increase the significance of the findings for the OTI mice. It should also be considered that an alternative explanation of these data is that CRT may be enhancing survival of CD8 T cells *in vitro* rather than inducing proliferation, a question which could be addressed in further studies. These results provide some evidence of the *in vivo* effects of CRT, which may be involved in the generation of the anti-tumour immunity observed in chapter 3. Possible explanations for these data are discussed below.

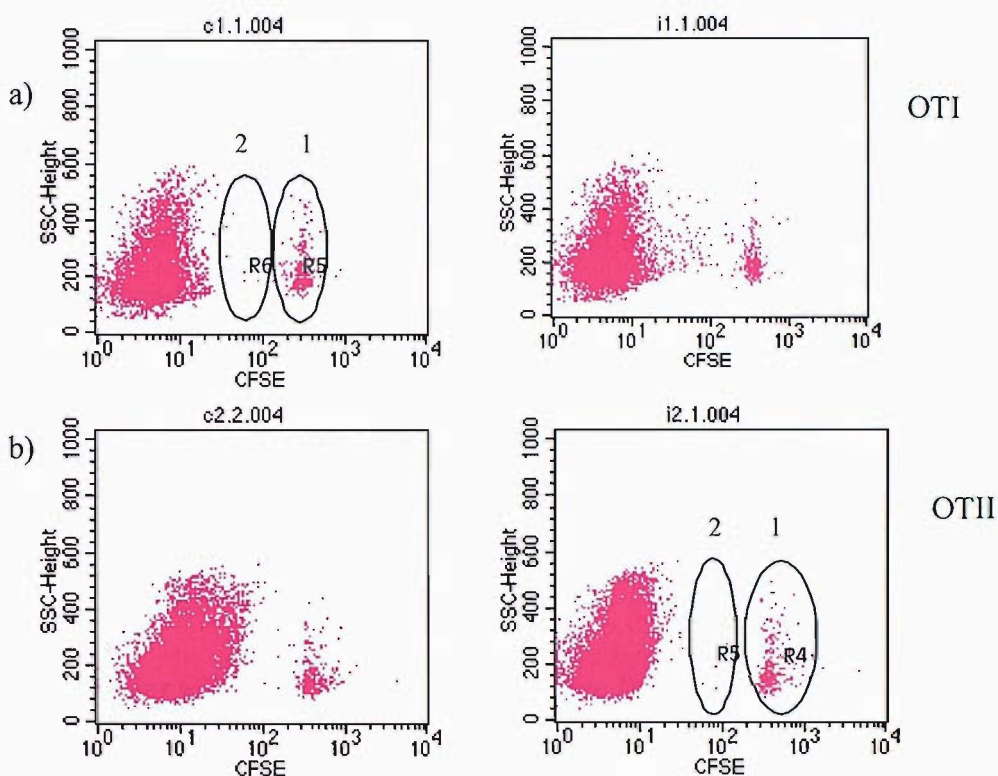


**Figure 4.20** Co-administration of CRT with OVA results in proliferation of CFSE-labelled CD8<sup>+</sup> T cells.  $10^6$  CFSE-labelled CD8<sup>+</sup> T cells from OTI mice (a) or  $2 \times 10^6$  CFSE-labelled CD4<sup>+</sup> T cells from OTII mice (b) were adoptively transferred into C57Bl/6 mice, which were subsequently immunised with 500ng OVA alone (left hand graph) or 500ng OVA plus 50 $\mu$ g CRT (right hand graph). 2 days after immunisation, spleens were harvested and CFSE-labelled cells assessed. Dot plots represent cells gated on CD8<sup>+</sup> (a) or CD4<sup>+</sup> (b) lymphocytes, marked region indicate cells that have not undergone proliferation. Each plot shows splenocytes from one mouse, and data are representative of those obtained from 3 mice per group.

	OVA		CRT + OVA	
	1	2	1	2
OTI	97	3	77	23
OTII	98	2	97	3

**Table 4.1** Proliferation of OTI T cells *in vivo*. Figures represent percentage of total events found in gate 1 + gate 2 in figure 4.20 that are in each gate.

## 4.3 Discussion

Previous work on HSPs, mainly gp96 and hsp70, suggests that these act both as chaperones of antigenic peptides to APCs and as direct activators of APCs through a number of potential pattern recognition receptors (described in section 1.2). Although CRT has been shown to have anti-tumour effects, and to chaperone antigens [38,134], no work has focused on the potential immunostimulatory effects of CRT. In this project, I particularly wanted to focus on autologous CRT, i.e. murine CRT in a murine system, as much of the HSP work previously published has used non-autologous HSPs from bacteria or pigs in murine or human systems. The work described in this chapter focused mainly on the effects of exogenously added CRT on the activation state of DCs.

### 4.3.1 Autologous CRT and hsp70 do not activate DCs

FACS analysis of expression of MHC class II and the co-stimulatory molecules CD80 and CD86 by DCs demonstrated that overnight incubation of DCs with concentrations of up to 200 $\mu$ g/ml CRT did not lead to upregulation of any of these markers. The same lack of effect was observed with up to 10 $\mu$ g/ml of low-endotoxin murine hsp70. In contrast, several known DC activators, LPS, TNF $\alpha$  and CpG DNA, all induced marked increases in expression of all three molecules after the same incubation. It was also observed that overnight incubation with LPS or CpG DNA induced production by DCs of pro-inflammatory cytokines IL-2 and IL-12. No induction of either of these cytokines was seen following incubation with CRT or hsp70. CRT was also observed not to enhance phagocytosis by DCs. Consistent with the apparent lack of DC activation induced in response to CRT or hsp70, it was observed that incubation with either of these did not enable OVA-pulsed DCs to prime naïve transgenic OVA-specific CD4<sup>+</sup> T cells whereas incubation with LPS, CpG DNA or TNF $\alpha$  did induce IL-2 production from these T cells, in a manner dependent on both Ag- and activator-concentration. These results contradict previous reports that some HSPs (e.g. hsp70, gp96) have stimulatory effects on DCs [52,53,57-59], although there have been no previous reports on the actions of CRT on DCs. The lack of effect of hsp70 was particularly surprising, as this was initially included in experiments to be a positive control for DC activation, based on its published effects.

Why do we see no stimulatory effect of CRT or hsp70 in this system? One possible explanation is that I have used low-endotoxin proteins. It has been suggested that the published data on APC activation by HSPs are artefactual, and are really caused by contamination with bacterial products, however many of these studies were carried out using cells induced to express HSPs, either by genetic engineering [57] or by induction of stress or necrosis [59,63], and others using exogenously purified gp96 showed that the effects were sensitive to boiling [58,59,83] or proteinase-K treatment [59], which should effectively abrogate the effects of HSPs but not of LPS.

Insensitivity of responses to Polymyxin B is also often used as a control. The boiling control has come under some scrutiny due to findings that boiling does, in fact, abrogate some of the activity of LPS [91], but in general there is a large body of convincing evidence that HSPs can induce activation of DCs as measured by pro-inflammatory cytokine production and surface marker upregulation. Therefore, it seems unlikely that the difference between my results and the published data are simply due to lack of contamination.

Another possible explanation arises from another fundamental difference between the studies carried out here and those published in the literature – the source of the HSPs. I have used only autologous CRT and hsp70, and while the HSPs are highly conserved between species, evidence is emerging that the source of the HSP may have an effect on its immunostimulatory capacity. Work from Paul Lehner's laboratory suggests that, although human hsp70 has a higher affinity for peptide than mycobacterial hsp70, it is less potent at generating an Ag-specific human CTL response (Babak Javid, PhD thesis, University of Cambridge). They have demonstrated that mycobacterial hsp70 induces a calcium signalling cascade, whereas human hsp70 does not. This difference in signalling suggests that the different hsp70s may utilise different receptors on APCs, or may bind to the same receptor with different affinities. There is some evidence to support this theory in the literature – in 2001, Wang identified CD40 as a receptor for mycobacterial but not human hsp70 [76], however a subsequent study by Becker [77] demonstrated that human hsp70 does bind CD40, but only in its ADP-bound conformational state. Further studies comparing the usage of receptors by HSPs from different species and the affinities of

these interactions would be highly useful in addressing the observed functional differences.

#### **4.3.2 Relevance of tested concentrations of CRT and hsp70**

10 $\mu$ g/ml was picked as a concentration of CRT and hsp70 to use in initial experiments based on concentrations used in previously published studies, for example 10 $\mu$ g/ml human hsp60 has been shown to induce TNF $\alpha$ , nitrite and IL-2 production from J774 cells and murine macrophages [90]. However, other reports in the literature use a wide range of HSP concentrations, up to around 100 $\mu$ g/ml, in order to see effects. For example, 30 $\mu$ g/ml gp96 has been reported to induce cytokine production and CD86 upregulation by murine BMDCs [58], chemokine production by monocytic cell lines is maximal at 20-50 $\mu$ g/ml hsp70 [76], 20 $\mu$ g/ml CRT saturates SR-A binding [79] and RME of Alexa-CRT by cells expressing SREC-1 is half maximal at approximately 20 $\mu$ g/ml, with increasing uptake seen even from 40-100 $\mu$ g/ml Alexa-CRT [80]. I thus titrated CRT from 0.39-200 $\mu$ g/ml, and still observed no DC activation or T cell priming at any of these concentrations. In order to confirm the physiological relevance of the tested concentrations, it may be of use in the future to attempt to measure the levels of HSPs, particularly CRT, found in normal serum, and in the medium of cells induced to die by necrosis or apoptosis.

#### **4.3.3 An immunosuppressive role for CRT?**

Interestingly, FACS analysis of CD80, CD86 and MHC class II indicates that co-incubation with CRT and LPS or TNF $\alpha$  results in decreased expression of these markers compared to incubation with LPS or TNF $\alpha$  alone. However, T cell responses are induced to a similar level. While these results appear not to correlate, it is likely that even the reduced levels of CD80, CD86 and class II are still sufficient to generate potent T cell responses, as these levels were still considerably higher than those on non-activated DCs. These results may indicate that CRT is indeed binding to a receptor or receptors utilised by LPS and TNF $\alpha$ , as has been proposed in the literature, and competing with the activating stimuli, thus antagonising their effects, although further studies are required to establish this. The effects of CRT on the response to CpG-DNA have not been investigated thus far, but would provide an interesting comparison, as the CpG DNA receptor, TLR-9, is not believed to be involved in binding CRT.

Another interesting explanation for these effects could be that CRT is actively suppressing the immune response. This theory is supported by the decrease in costimulatory marker expression by splenic DCs at high concentrations of CRT ( $>25\mu\text{g/ml}$  for CD86 and  $>100\mu\text{g/ml}$  for CD80 and MHC class II) and also by the decrease in CD8<sup>+</sup> T cell priming at high concentrations. This “high-dose” suppression by HSPs has been reported in the literature previously. Srivastava’s group have shown that the protective effect of immunising against tumours with gp96 resides within a fairly tight “window” of concentration [138]. The precise doses vary depending on the route of immunisation, but for subcutaneous delivery,  $<5\mu\text{g}$  tumour-derived gp96 is insufficient to immunise,  $10\mu\text{g}$  is the optimal immunising dose, and the anti-tumour activity is gradually diminished as concentrations increase, with mice immunised with  $50\mu\text{g}$  or more not protected. This was found to be due to active suppression of the immune response at high concentration of gp96, rather than a null effect, and suppression was found to reside in the CD4<sup>+</sup> T cell compartment. The same authors have subsequently demonstrated that high-dose gp96 can also downregulate autoimmune responses, protecting mice against development of experimental autoimmune encephalitis (EAE) and diabetes [139]. Further dissection of this response indicated that immunisation with high-dose gp96 could be adoptively transferred with CD4<sup>+</sup> T cells as previously shown, but did not partition with the CD25<sup>+</sup> phenotype, suggesting that suppression is not mediated by traditional regulatory T cells. The high-dose gp96 did not have to be purified from the tumour of origin, provided that the original immunising dose was tumour-derived, nor from organs affected by autoimmune disease, indicating that the suppressive activity resides either within gp96 itself or in a common peptide associated with gp96 regardless of its origin. Timing of delivery also appears to be important – suppression appears to be most active on activated T cells, but ineffective on memory responses. In light of these data, it would be of interest to further examine the *in vivo* effects of various doses of CRT, to see if a similar dose effect exists. Further studies of if and how CRT directly interacts with T cells would also help to elucidate the mechanisms behind this phenomenon.

#### 4.3.4 CRT and phagocytosis

Initial experiments have shown that exogenously added CRT does not enhance the phagocytic capacity of the DC-like cell line DC2.4. While pre-exposure of DC2.4 to LPS led to enhanced uptake of protein-opsonised latex beads, co-stimulatory molecule expression and presentation of Ag, pre-incubation with CRT induced none of these effects. It is well known that cell-surface CRT is involved in the phagocytosis of apoptotic cells, and it may be that this surface localisation is important for CRT to carry out its role, and that free extracellular CRT cannot act in a similar fashion. Interaction with other cellular molecules, such as CD91 and TNFR1, may prove crucial for this function. An interesting way to advance these studies would be to coat latex beads directly with CRT, mimicking CRT expression on apoptotic cells, to see if these beads were phagocytosed more efficiently than non-opsonised beads, or beads coated with other proteins. By co-administering OVA-coated beads, or by coating beads with CRT and OVA, the effect on processing and presentation of OVA could be examined. It should also be noted that our timecourse data contradict those published by West et al [141], which indicated that FITC-dextran uptake by bone marrow-derived and splenic DCs was enhanced for 30-45 minutes following LPS stimulation, after which time Ag capture decreased. We observed enhanced phagocytosis over the full 24 hour timecourse studied in our experiments. One possible explanation for this is the different cells used – West and co-workers used primary DCs, whereas we used the DC-like cell line DC2.4. We know that DC2.4 differ from primary DCs in their levels of co-stimulatory marker expression and there may be other functional differences between the cell line and primary DCs that are responsible for the discrepancies in the timecourses. Improvement of our assay method to allow use of primary DCs for these assays would allow us to compare the cells directly, and hopefully provide an answer to this question.

#### 4.3.5 Preferential activation of CD8<sup>+</sup> T cells

Despite the apparent lack of *in vitro* effects on DC activation, I have observed both protective anti-tumour effects (see chapter 3) and bystander induction of CD8<sup>+</sup> T cell proliferation *in vivo* (figure 4.20). These results correlate with the observed *in vitro* priming of OVA-specific CD8<sup>+</sup> T cells. Thus it appears that CRT preferentially



activates CD8<sup>+</sup>, rather than CD4<sup>+</sup> T cells. There are precedents for this in the literature, as described in chapter 1. Most of the work on HSPs has focused on induction of CTL responses, however one study comparing induction of CD4<sup>+</sup> and CD8<sup>+</sup> T cell responses demonstrated that while both CD4<sup>+</sup> and CD8<sup>+</sup> T cell proliferation were induced by gp96, only the CD8<sup>+</sup> T cells developed effector function [50]. Although I did not see any CD4<sup>+</sup> T cell proliferation, the general theme of preferential activation of CD8<sup>+</sup> T cells is the same. Why this occurs is, as yet, unclear, and the answer may be related to the nature of the activation signal delivered by CRT.

#### **4.3.6 Where does the activation signal come from?**

I have clearly demonstrated that CRT does not induce cytokine production or activation marker upregulation by DCs, yet it can induce *in vivo* and *in vitro* activation of CD8<sup>+</sup> T cells. T cell activation requires both Ag and activation signals, generally thought to be delivered by DCs, so where is the activation signal in this case? It may be that there are other effects on DCs that I have not observed, for example CD40 expression has not been monitored. It has also previously been reported that, although low endotoxin CRT and gp96 do not induce cytokine production and costimulatory marker upregulation, they do induce ERK phosphorylation [93]. Again, I have not yet investigated the activation of signalling molecules in DCs in response to CRT, and this may help to identify the effects induced. It is also possible that CRT interacts directly with T cells, bypassing the need for costimulation from DCs, although again, this requires further investigation. *In vivo*, other cell types may be involved that I have not studied here, for example interaction of DCs with NK or NKT cells may be required for the efficient generation of a response, and it may be that CRT interacts directly with these cells, rather than, or as well as, with DCs. This is not precluded by the observed *in vitro* CD8<sup>+</sup> T cell priming, as this response was weak, and while I have not ruled out that this was an artefactual result, it is also possible that this response would be strengthened *in vivo* in the presence of other cell types.

## **5. Receptor-mediated binding of calreticulin to antigen presenting cells and chaperoning function**

### **5.1 Introduction**

As discussed in the introduction, HSPs including CRT are proposed to induce immune responses via their dual function as molecular chaperones, delivering bound peptides to APCs, and as direct activators of APCs. In chapter 4 of this thesis, I have found no adjuvant effect of murine CRT on autologous DCs, so I next wanted to investigate the chaperoning function of CRT. In light of this apparent lack of immunostimulatory function of CRT, I also wanted to confirm that the CRT I had produced in the lab was capable of binding to APCs *in vitro*.

As described in Section 1.2.3, the highly efficient uptake of HSPs and re-presentation of associated peptides led to the belief that APC uptake of HSPs must be receptor mediated. This theory was supported by the ability of HSPs to directly activate APCs. A number of potential HSP receptors were subsequently identified, including CD91, CD40, TLR2/4, LOX-1, SR-A and SREC-F [68-89]. CRT has been demonstrated to bind CD91 [71], SR-A [79] and SREC-F [80], although the role of CD91 has been disputed, as described in section 1.2.3. In order to determine whether my CRT bound APCs, I labelled CRT with a fluorochrome, Alexa-488, to allow direct analysis of binding by FACS and confocal microscopy. I also tested the effects on CRT binding of ligands of CD91 and SRs, the proposed receptors for CRT, to attempt to identify the receptor(s) responsible for any observed binding.

The ability of CRT to chaperone peptides is well documented. Studies by Nair [134] and Golgher [135] have implicated CRT in delivery of peptides for presentation on both MHC class I and II molecules, inducing CD8<sup>+</sup> and CD4<sup>+</sup> T responses, respectively. I decided to utilise the method of complexing peptides to CRT *in vitro*, published by Li [142], a very similar method having also been used successfully by Basu and Srivastava [38].

## 5.2 Results

### 5.2.1 Labelling of CRT with Alexa-Fluor

To evaluate the ability of the purified CRT to bind to APCs, CRT was labelled with Alexa-Fluor 488, as described in materials and methods. This labelled CRT (Alexa-CRT) was then used for *in vitro* binding studies on different types of APCs.

### 5.2.2 CRT specifically binds to APCs

Bone-marrow derived DCs, the DC-like cell line DC2.4 and the macrophage cell line J774 were incubated with increasing concentrations of Alexa-CRT for 1 hour at 4°C, then washed, fixed and analysed by FACS. Binding to fibroblast line K42 was assessed as a control for specificity of binding. In order to identify the receptors involved in any binding, incubations were performed in the presence of the CD91 ligand,  $\alpha 2$ -macroglobulin ( $\alpha 2$ M), and of the scavenger receptor-A (SR-A) ligand maleylated BSA (mBSA). Non-maleylated BSA was used to confirm the specificity of any competition. Incubation of BMDCs and J774 with 25  $\mu$ g/ml Alexa-CRT resulted in a shift in fluorescence, which was abrogated in the presence of mBSA or unlabelled CRT, but not by BSA or  $\alpha 2$ M (Fig. 5.1). A shift in fluorescence was also observed with DC2.4, which was inhibited only by unlabelled CRT. No binding was observed to K42. Binding to BMDCs and J774 is saturable, a further indication of the specificity of binding (Fig. 5.2). Some binding to K42 was observed at high concentrations of CRT, but this was not inhibited by any of the tested ligands, including unlabelled CRT, so could be non-specific. Binding to DC2.4 did not reach saturation, and was poorly inhibited by mBSA and unlabelled CRT, possibly indicating a non-specific binding. Interestingly, binding to BMDCs, but not to any of the cell lines, is partially inhibited by  $\alpha 2$ M. These data indicate that CRT may specifically binds to APC, apparently via SR-A on macrophages and SR-A and CD91 on BMDCs. The lack of binding to K42 indicates that SR-A and CD91 are not expressed on this cell line. In order to exclude the possibility that mBSA is binding to CRT in the supernatant and sequestering it from binding to cells, rather than actually blocking receptor binding, cells were incubated for 1 hour with inhibitors, then washed and incubated for a further hour with Alexa-CRT (Fig.5.3). Although inhibition was decreased compared to when inhibitors and Alexa-CRT were co-incubated with cells, mBSA and unlabelled CRT still effectively inhibit binding of

Alexa-CRT to J774 and BMDCs. The decreased effect is likely to be due to some bound inhibitor being washed off the cells during the wash step, notably inhibition by unlabelled CRT is affected more than that by mBSA, perhaps indicating a weaker binding of CRT.

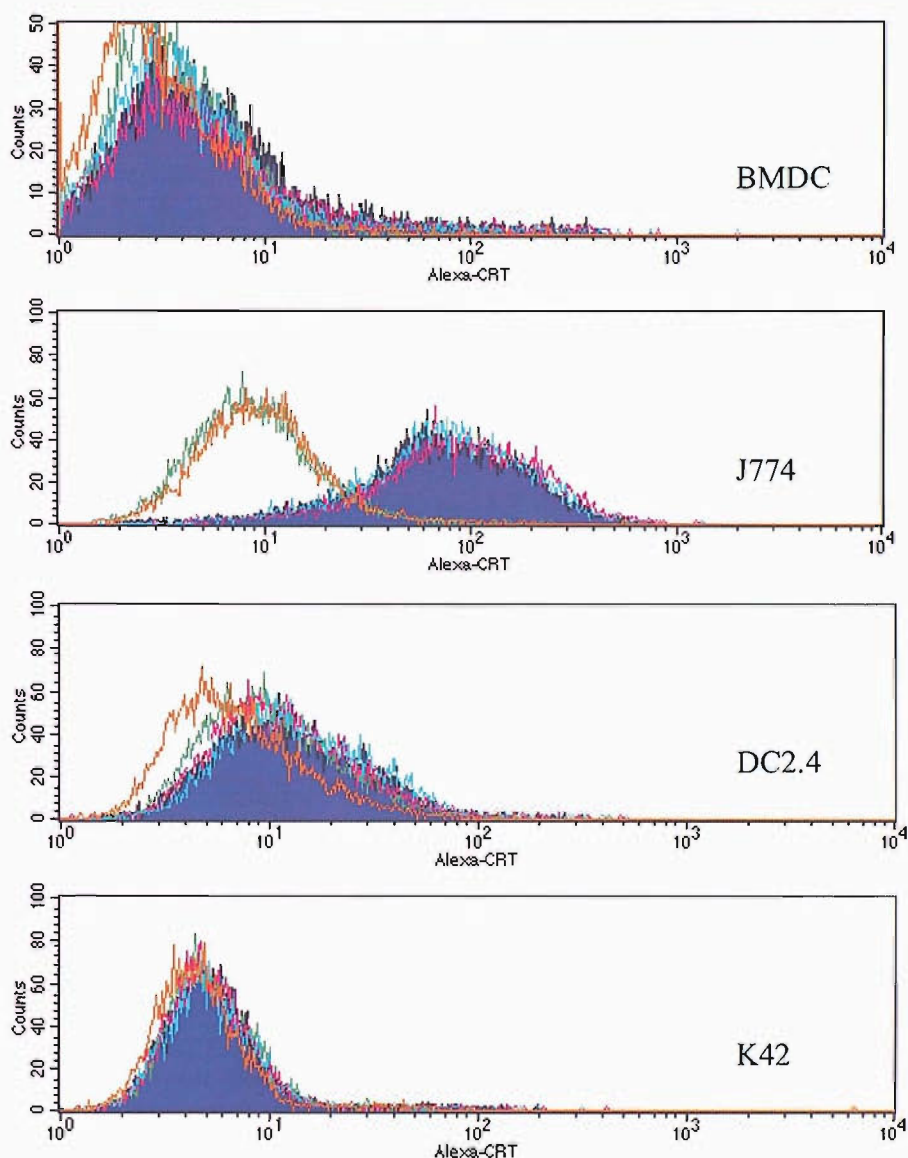


**Figure 5.1** Alexa-CRT binding to APCs. Day 10 BMDCs or indicated cell lines were incubated on ice for 1 hour with 25  $\mu\text{g/ml}$  Alexa-CRT alone (blue filled area) or in the presence of 500  $\mu\text{g/ml}$  mBSA (green line), BSA (pink line),  $\alpha 2\text{M}$  (blue line) or unlabelled CRT (orange line). Cells were washed several times and analysed by FACS. Live cells were gated from the total population.

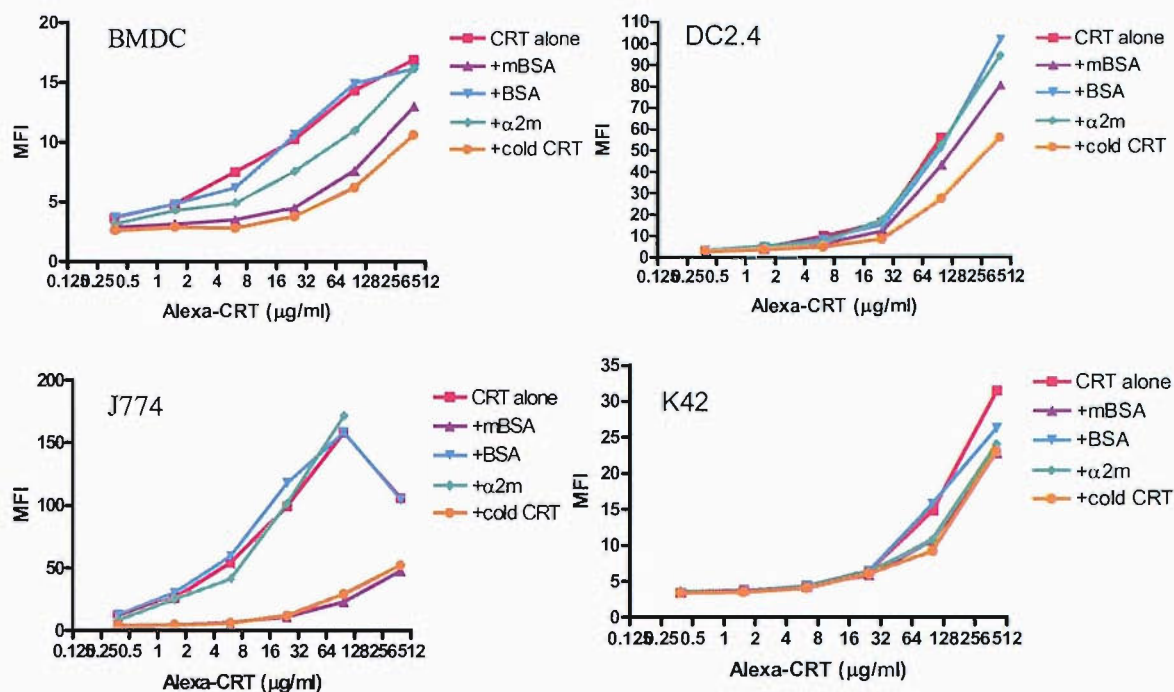


**Figure 5.2** Binding of Alexa-CRT to APCs. Day 10 BMDCs or indicated cell lines were incubated for 1 hour at 4°C with indicated concentrations of Alexa-CRT alone or in presence of 500 $\mu\text{g/ml}$  indicated inhibitors. Points represent mean fluorescence intensity.

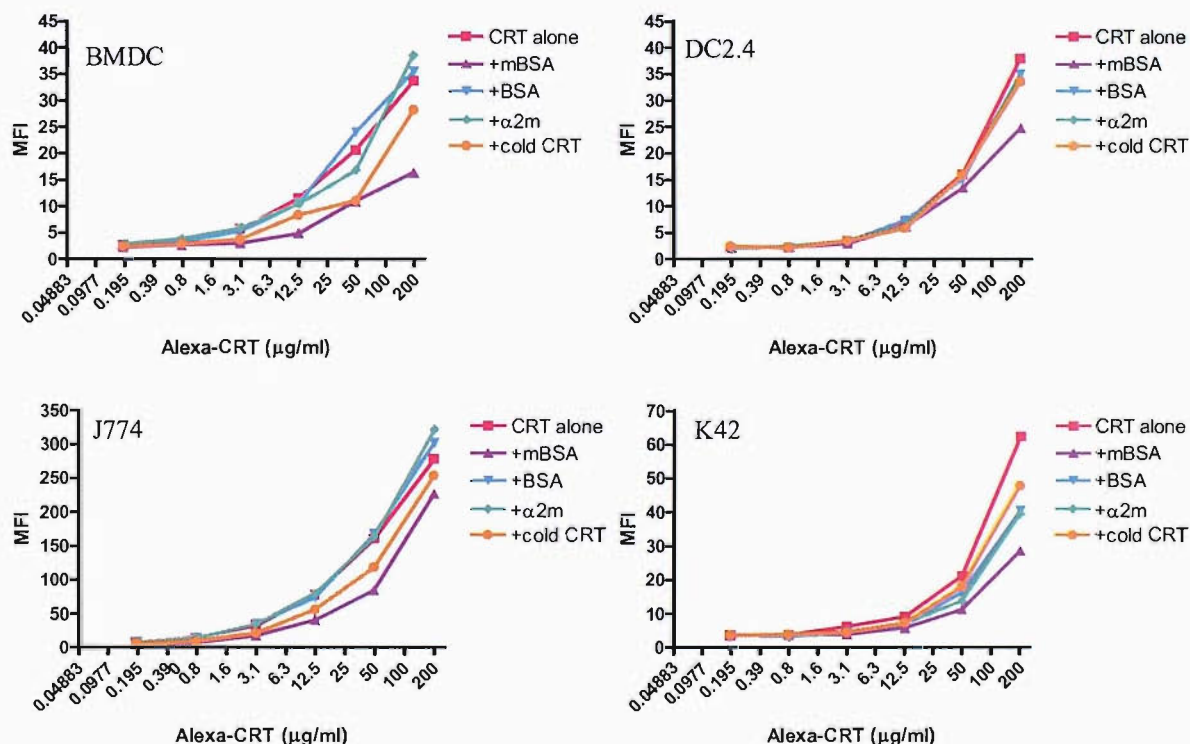


**Figure 5.3** Binding of Alexa-CRT to APCs following pre-incubation with inhibitors. Day 10 BMDCs or indicated cell lines were incubated for 1 hour at 4°C with 500 $\mu\text{g/ml}$  indicated inhibitors then washed and incubated for 1 hour with indicated concentrations of Alexa-CRT. Points represent mean fluorescence intensity.

### 5.2.3 BMDCs internalise CRT *in vitro*

Having demonstrated that CRT binds to a receptor, apparently a scavenger receptor, *in vitro*, confocal microscopy was used to determine whether CRT was internalised by APCs following binding. BMDCs were stained with Alexa-CRT in the presence or absence of mBSA and analysed on confocal microscope as described in materials and methods.

As can be seen in fig 5.4, CRT binds to the surface of BMDC when they are incubated on ice for 15 minutes (5.4a). When incubated at 37°C for 15 minutes, BMDCs display punctate intracellular staining, indicating vesicular localisation (5.4b), and after 2 hours at 37°C staining is more widespread (5.4c). As demonstrated in 5.4d, co-incubation with mBSA led to far fewer cells taking up CRT. Counterstaining cells with anti-CRT and texas-red conjugated secondary demonstrates that there is more co-localisation of internalised and intracellular CRT after 2 hours (5.4f) than 15 minutes (5.4e). These findings indicate that, following receptor binding, CRT is initially internalised into vesicles and subsequently appears to gain access to the ER or early secretory pathway, as assessed by co-localisation with intracellular CRT. The nature of the vesicles entered by CRT is unclear, and further studies are planned to investigate the expression of phagosomal and lysosomal markers in these compartments in order to resolve this. Staining with more ER markers, such as calnexin, may also be useful to confirm the final ER-localisation of CRT. It would also be of interest to study more timepoints in order to gain a more informed view of the intracellular trafficking route followed by CRT following internalisation.

As can be seen from these images CRT does not bind to all of the cells in the BMDC preparation, and this selective binding could be a reason for the lack of observed *in vitro* activation effects. To this end, it would be of interest to repeat these experiments using the J774 cell line, a homogeneous population of cells that should not display such selective binding of CRT.



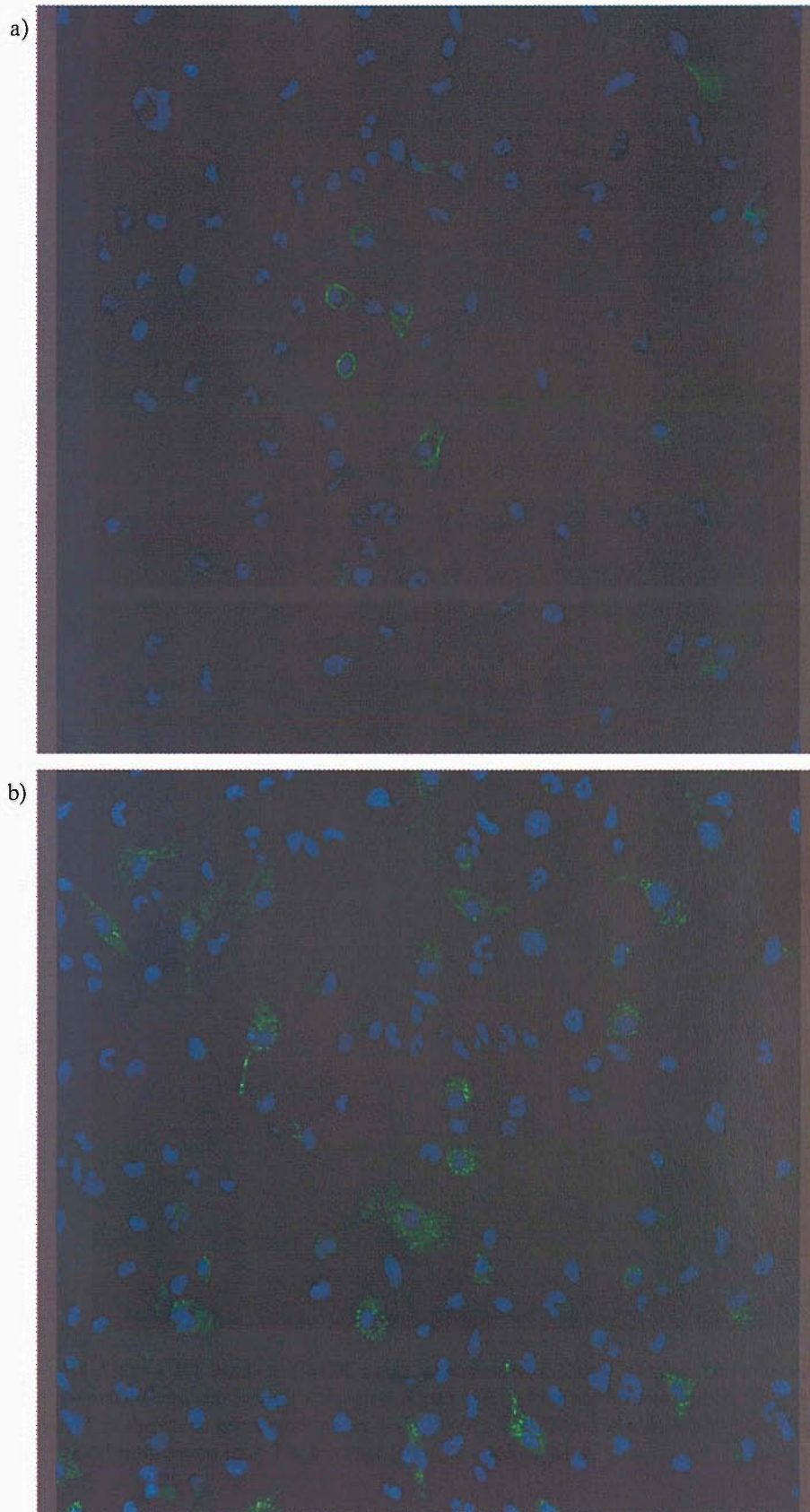


**Figure 5.4** Alexa-CRT binds to BMDCs and is internalised. Day 9 BMDCs were bound to polymer-coated coverslips and stained with 50 $\mu$ g/ml Alexa-CRT alone for 15 min on ice (a) or at 37°C (b). Alexa-CRT is shown in green and nuclei stained with TO-PRO-3 are shown in blue. Images taken under 40x oil immersion lens. Each image is one z-stack or slice.

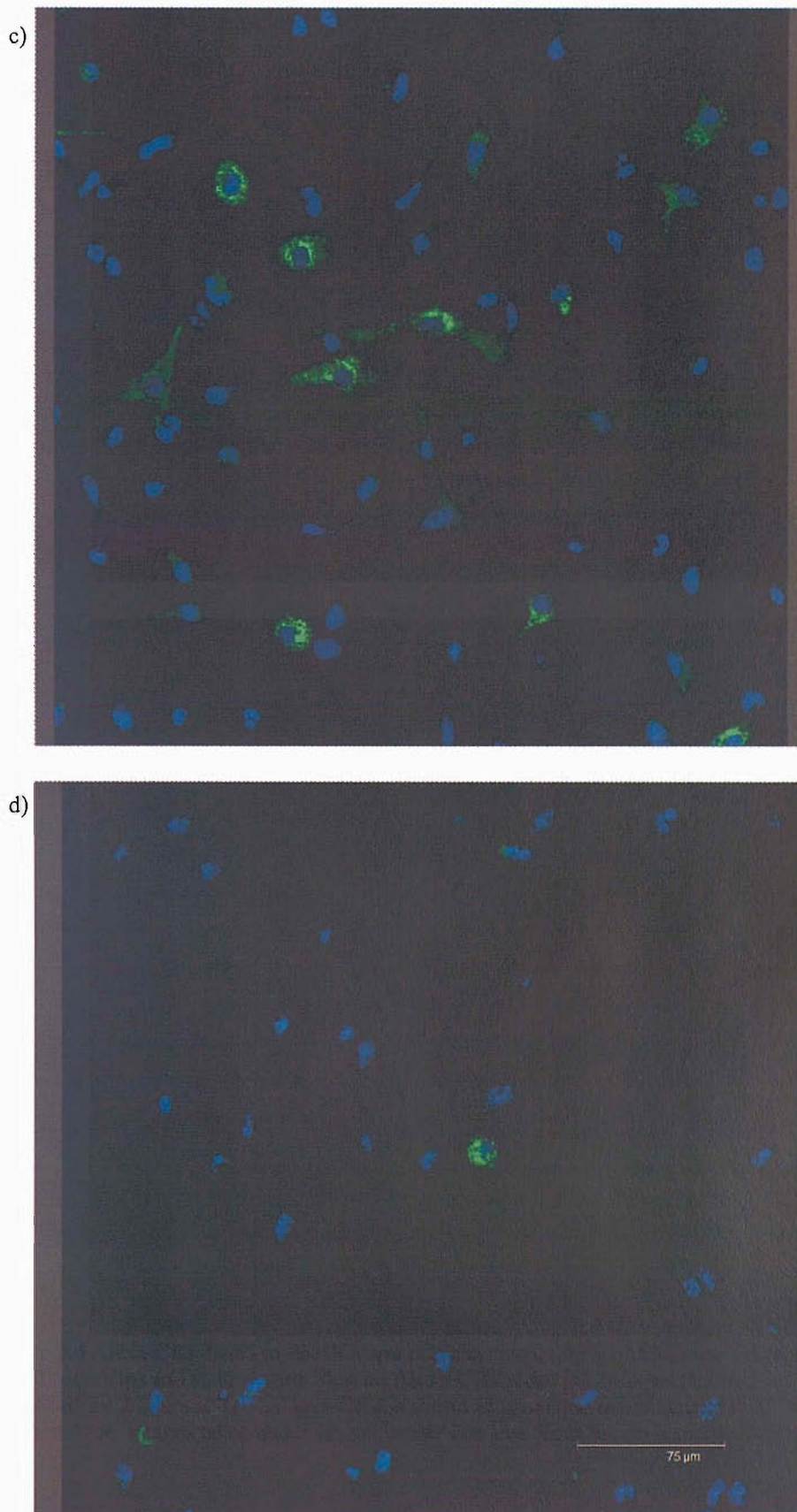


**Figure 5.4** Alexa-CRT binds to BMDCs and is internalised. Day 9 BMDCs were bound to polymer-coated coverslips and stained with 50 $\mu$ g/ml Alexa-CRT alone (c), or in the presence of 400 $\mu$ g/ml mBSA (d) for 2 hours at 37°C. Alexa-CRT is shown in green and nuclei stained with TO-PRO-3 are shown in blue. Images taken under 40x oil immersion lens. Each image is one z-stack or slice.



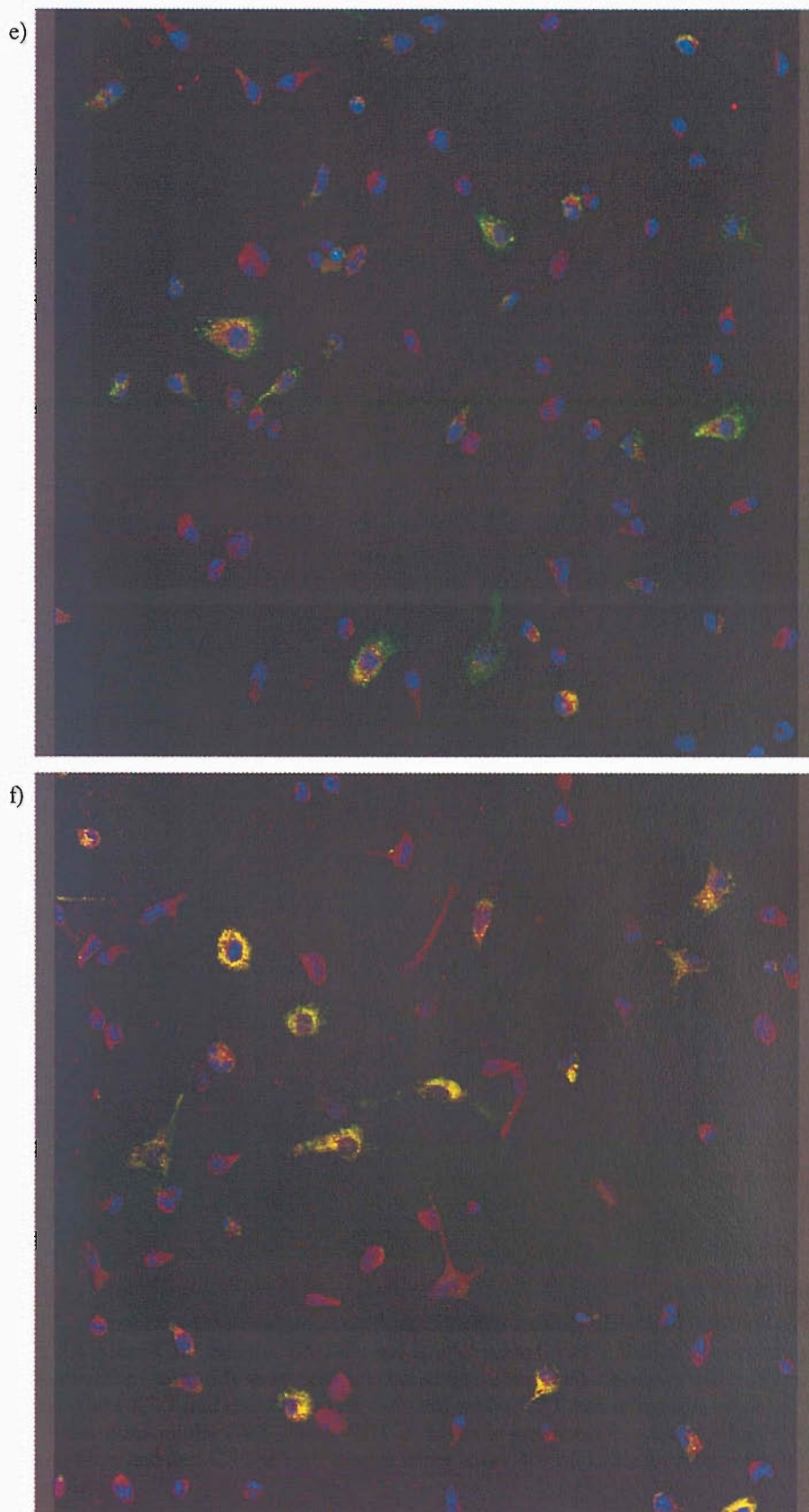


**Figure 5.4** Alexa-CRT binds to BMDCs and is internalised. Day 9 BMDCs were bound to polymer-coated coverslips. e) and f) show cells incubated for 15mins and 2 hours respectively at 37°C with 50 $\mu$ g/ml Alexa-CRT and counterstained with anti-rabbit CRT and anti-rabbit-texas red secondary antibody for intracellular CRT. Alexa-CRT is shown in green, nuclei stained with TO-PRO-3 are shown in blue, and anti-CRT in red. Images taken under 40x oil immersion lens. Each image is one z-stack or slice.

#### 5.2.4 Chaperoning of peptides by CRT for presentation by APCs

My results so far have demonstrated that CRT does not have any immunostimulatory effect on APCs, but that it does bind to APCs in a specific manner and is then internalised. The next step was to assess the antigen delivery function of CRT. In order to do this, the OVA peptide SIINFEKL was complexed to CRT as described in materials and methods. Briefly, CRT and SIINFEKL were mixed at a ratio of 1:10 molar (CRT:SIINFEKL) in binding buffer and the mixture heated to 55°C for 10 minutes, followed by 30 minutes at room temperature. After extensive dialysis to remove free peptide, the complexes were incubated overnight with day 10 BMDCs, in the presence or absence of CpG DNA as an activating stimulus, then CD8<sup>+</sup> T cells from OTI mice were added and incubated with the DCs overnight, after which the culture supernatants were tested for IL-2 production by ELISA. Figure 5.5 shows that SIINFEKL complexed to CRT results in generation of a strong IL-2 response. To confirm that complex formation did in fact occur, CRT mixed with SIINFEKL (CRT + SIINFEKL), and BSA either mixed with SIINFEKL (BSA + SIINFEKL) or “complexed” in the same way as CRT, (i.e. following the same incubations, BSA-SIINFEKL) were used as controls. To assess the removal of free peptide by dialysis, a sample of the same amount of SIINFEKL used in complexes was incubated and dialysed alone (labelled SIINFEKL in graphs). While some element of free SIINFEKL apparently remains in these preparations, as there is a response to the dialysed SIINFEKL alone, the IL-2 response induced is weaker than that induced by CRT-SIINFEKL and less concentration dependent. The response to CRT + SIINFEKL is the same as that to SIINFEKL alone, indicating that here there has been no complexing, and thus the SIINFEKL has been dialysed out to the same extent as free SIINFEKL. While a higher background is seen with BSA either mixed with or “complexed” to SIINFEKL, the response is not concentration dependent, indicating that BSA is not chaperoning the peptide. This slight response may be caused by SIINFEKL simply sticking to BSA in a non-specific manner. It should also be noted that the CRT response was dependent on external stimulation of the DCs with CpG DNA, whereas the response seen with BSA was not, probably due to endotoxin contamination in the BSA, which was not tested prior to use.

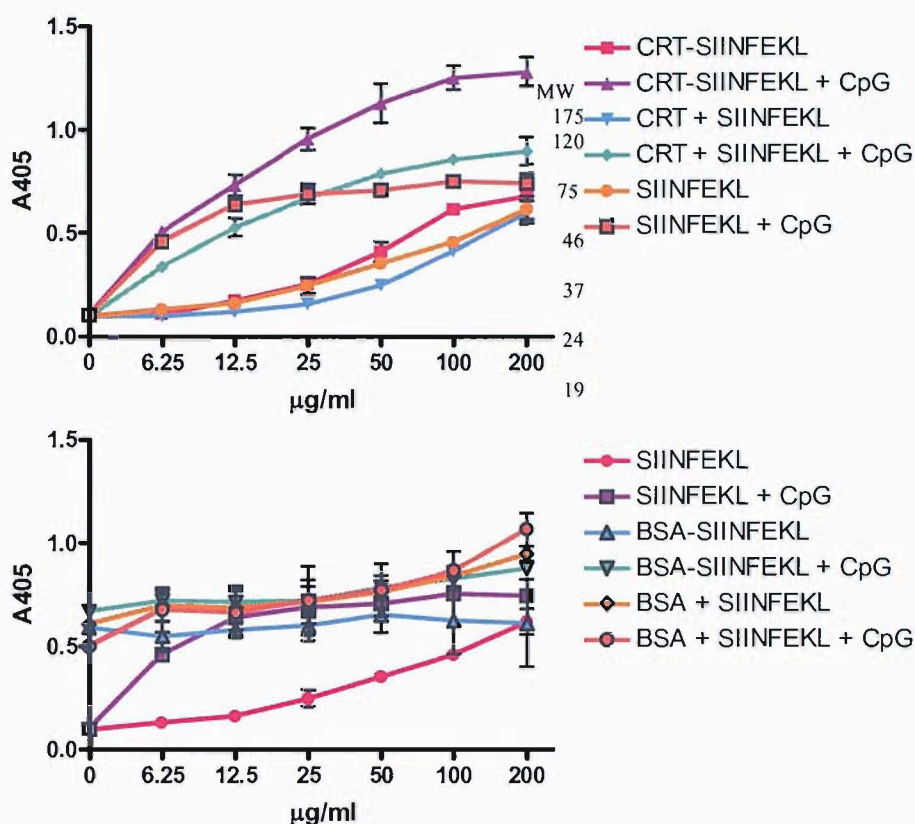


**Figure 5.5** SIINFEKL complexed to CRT induces a stronger response from transgenic T cells than free SIINFEKL. Indicated concentrations of complexes (or same dilution of similarly treated free SIINFEKL as control), were incubated overnight with day 10 DCs in the presence or absence of 10 μg/ml immunostimulatory CpG DNA oligo 1668. CD8<sup>+</sup> T cells from OTI mice were added and incubated overnight with the DCs and the supernatants analysed for IL-2 production by ELISA. Points represent means of 2 replicates, with error bars representing standard deviation.

These results therefore indicate that the method for complexing CRT to SIINFEKL was successful, and that complexation of peptide to CRT was an effective way of delivering it for presentation. I was unable to quantitate peptide binding to CRT, which would allow comparison with the response to the same amount of free SIINFEKL. Without these data, it cannot be concluded whether or not CRT is chaperoning SIINFEKL to DCs for more efficient presentation than would occur for free peptide, but it does show that peptide can be chaperoned for class I presentation by CRT and not BSA. Further work to establish the binding affinity of CRT for SIINFEKL will help to answer this question.

## 5.3 Discussion

The data presented in chapters 3 and 4 of this thesis have indicated that, while CRT has some protective anti-tumour effect *in vivo* and induces bystander proliferation of CD8<sup>+</sup> T cells *in vivo* and some IL-2 production by these T cells *in vitro*, it has no effects on DC expression of activation markers or pro-inflammatory cytokine production. In light of this lack of effect on DCs, I wanted to establish whether the CRT I had produced was capable of binding to these cells, and if so if it was internalised. Related to this, I also investigated the ability of CRT to chaperone an OVA peptide for presentation to OVA-specific T cells.

### 5.3.1 CRT binding to APCs

FACS analysis of various cells that had been incubated with Alexa-labelled CRT indicated that CRT binds to both BMDCs and the macrophage cell line J774 in a saturable manner. Binding to both cell types was inhibited by an excess of unlabelled CRT and by the SR-A ligand mBSA, but not by BSA. In the case of BMDCs, binding was also partially inhibited, to a much lesser extent than by mBSA, by the CD91 ligand  $\alpha$ 2M. These data indicate that CRT binds to macrophages via SR-A, and to BMDCs via both SR-A and CD91, although SR-A appears to be the main receptor. These data are in keeping with previously published reports of CRT binding to both of these receptors [71,79]. CD91 was initially identified as a receptor for gp96 [70], and subsequently as a common receptor for other HSPs, including CRT [71]. However, the role of CD91 has been disputed by other groups, and Berwin and colleagues have carried out studies demonstrating that CRT binding, uptake and trafficking are all CD91-independent [72,75], and have also identified both SR-A and SREC-1 as receptors for CRT [79,80]. My data indicate a role for both SR-A and CD-91, depending on cell type. As yet, I have not directly studied expression of these and other receptors by the cells used in these experiments, however this would be a useful piece of future work to establish whether there is a difference in expression of CD91 that could account for the lack of inhibition by  $\alpha$ 2M on J774. This would also be of use in determining the reasons behind the lack of binding to K42 and the apparently non-specific binding to DC2.4. It is also possible that another receptor is mediating binding to DC2.4.

### 5.3.2 CRT internalisation and trafficking

Confocal microscopy analysis of BMDCs incubated over a timecourse with Alexa-CRT has provided some interesting preliminary data on the uptake and trafficking of CRT by BMDCs. At 4°C, CRT binds to the cell surface, and when the temperature is increased to 37°C the CRT is internalised into vesicles after 15 minutes. After 2 hours incubation, the Alexa-CRT is found largely colocalised with intracellular CRT, indicating that it traffics eventually to the ER compartment. The fact that Alexa-CRT is observed to enter the ER also indicates that the CRT is not degraded when it is internalised. At the moment, the precise nature of the vesicles entered by CRT is unclear, as is the trafficking route by which it enters the ER. Future work to investigate the nature of the endocytic vesicles and also more detailed timecourse studies with staining for a broad range of intracellular markers would be useful to further elucidate these pathways. Berwin and colleagues have demonstrated that CRT co-localises with FcγR and gp96 on uptake in a peripheral endosomal population in macrophages, but that vesicular trafficking does not parallel that of a CD91 ligand [75]. At this time, there are no further, detailed studies on the intracellular trafficking of externally acquired CRT, and no data on these pathways in primary BMDCs. Thus a more detailed study of CRT uptake and trafficking would also greatly enhance our knowledge of the interaction of HSPs with primary DCs.

### 5.3.3 Chaperoning function of CRT

Initial studies on the chaperoning function of CRT have not been highly informative as yet, but have provided evidence that it is possible to complex the OVA peptide SIINFEKL to CRT *in vitro* following an established protocol [134,142]. Initial experiments with these complexes indicate that SIINFEKL complexed to CRT is presented on MHC class I and, in the presence of additional DC stimulation, results in generation of a specific T cell response as assessed by IL-2 production. However, I have not yet ascertained the kinetics of CRT-SIINFEKL binding, so it is not possible to determine the amount of peptide delivered in the complexes. This makes it impossible to determine whether CRT-chaperoned SIINFEKL is presented more efficiently than free SIINFEKL. It has previously been demonstrated that CRT-bound peptides are re-presented on DC MHC class I and induce CTL responses *in vivo* [38,134]. Thus we would expect to also see a peptide-chaperoning effect *in vitro*.

Although the peptide chaperoning functions of CRT and other HSPs have been well documented and studied, their ability to chaperone whole proteins has not. Previous studies have demonstrated that CRT can interact with both glycosylated and non-glycosylated proteins *in vitro* [143,144], but it has also been demonstrated that CRT interacts better with unfolded proteins than with native proteins. None of these studies have attempted to complex protein to CRT *in vitro*, and investigate the processing of these proteins by APCs. Creation of such complexes would be an interesting area for future work, allowing direct comparison of the effects of free vs. complexed OVA, and of the amounts of each type of OVA required to induce the same level of response. This would also allow direct comparison of induction of MHC class I- and II-restricted responses, another under-investigated area of HSP immunology. It would also be of interest to investigate the *in vivo* response to such complexes, given that co-administration of CRT with OVA induces proliferation of OTI CD8<sup>+</sup> T cells.

## 6. General Discussion

### 6.1 Summary of findings

The aim of this thesis was to investigate the immunostimulatory and Ag-chaperoning functions of autologous CRT on antigen presenting cells. CRT was purified from a murine mastocytoma cell line, P815. CRT, along with the model Ag OVA and all components of the model system were made endotoxin free ( $<0.5\text{EU/mg}$ ). This ensured that all subsequent findings could be interpreted without fear of artefact caused by endotoxin contamination.

In the first part of this thesis, I demonstrated that CRT appears to have no immunostimulatory effect on murine bone marrow-derived DCs. Incubation of DCs with CRT (at concentrations from  $0.39\text{-}200\mu\text{g/ml}$ ) did not result in upregulation of surface levels of CD80, CD86 or MHC class II, nor in production of pro-inflammatory cytokines IL-2 or IL-12. The DCs were functional and capable of responding by upregulation of costimulation and production of cytokines in response to LPS, CpG DNA or  $\text{TNF}\alpha$ . DCs incubated with CRT were incapable of priming naïve OVA-specific transgenic  $\text{CD4}^+$  T cells when pulsed with OVA, although all the stimulatory compounds mentioned above were capable of inducing this. Some stimulation of  $\text{CD8}^+$  T cells was observed when DCs were incubated with CRT and OVA, although this was much less than that induced by LPS. I also found that addition of extracellular CRT had no effect on the ability of the dendritic cell-like line DC2.4 to phagocytose OVA- or FCS-coated latex beads, nor on the ability of DC2.4 to process and present bead-associated OVA to the T cell hybridoma B3Z.

In the second part of this thesis, I investigated the ability of CRT to bind to APCs and chaperone peptides and proteins. Fluorescently labelled CRT bound to bone marrow-derived DCs and the macrophage cell line J774 in a concentration-dependent, saturable manner, and this binding was inhibited by the SR-A ligand maleylated BSA. The CD91 ligand  $\alpha 2$ -macroglobulin also partially inhibited binding of CRT to bone marrow-derived DCs. These findings indicate a primary role for SR-A in binding of CRT to APCs, with some role for CD91 in primary BMDCs, and also



suggest that the lack of immunostimulatory function observed is not simply due to a failure of CRT to interact with DCs. Confocal microscopy timecourse experiments demonstrated that, following binding, CRT is internalised by BMDCs, initially into vesicles, and that over time internalised CRT co-localises with resident CRT within the cell, although further studies are required to confirm the intracellular trafficking of internalised CRT. Binding was again observed to be inhibited by maleylated BSA.

I also generated complexes of CRT with OVA peptide (CRT-SIINFEKL) *in vitro*, and observed that peptide complexed to CRT was processed and presented to T cells by DCs. These results are preliminary, and more detailed studies of the binding kinetics of CRT to SIINFEKL, and of complex formation and trafficking are required to determine the efficiency of delivery of complexed peptides in comparison to free peptide and to fully elucidate the significance of these data.

## 6.2 Discussion and Future Work

The main findings in this thesis have been discussed at the end of each chapter. Here I will discuss how these findings relate to the wider field of HSP immunology, and how future work could further expand and elucidate our knowledge of the role of CRT in the immune response.

### 6.2.1 Effects of CRT on different cell types

The immunogenic properties of CRT *in vivo* are well documented, as described in chapter 1. In chapter 4 of this thesis I observed that co-administration of CRT with OVA led to enhanced proliferation of adoptively transferred CD8<sup>+</sup>, but not CD4<sup>+</sup> T cells *in vivo*. When the ability of CRT to activate DCs and induce priming of T cells *in vitro* was investigated, some activation of CD8<sup>+</sup>, but not CD4<sup>+</sup> T cells was observed, although there was no evidence of DC activation. This raises the question of how T cell proliferation and IL-2 production are induced in the absence of detectable DC activation. It may be that a cell type other than the CD11c<sup>+</sup> cells studied by FACS analysis, such as a particular DC subtype or other innate immune cells such as NK cells or  $\gamma\delta$ -T cells, is involved. A more extensive phenotyping of the BMDC preparations would be beneficial in addressing this question – so far I have classified DCs only by their expression of CD11c. This means that plasmacytoid DCs are not being considered at all, as these are low CD11c expressers, and it is unknown which of the other DC subtypes described in section 1.1.2 are present. The observed effects on CD8<sup>+</sup> T cells indicate that cross-priming is taking place, and CD8 DCs are believed to be the main DC subtype involved in this process [5], therefore establishing whether these DCs are present in my BMDCs would be of use. It would also be interesting to attempt isolation of the different DC subtypes from mice and to compare the effects of CRT on individual subsets or combinations of subsets. Plasmacytoid DCs may play an important role in the activation of other DC subtypes. Cross-talk between DCs and other innate immune cells, such as NK cells, is also emerging as a key factor in sustained DC activation. Colombo and colleagues [145] have reported that bystander effects of hsp70 on phagocytosis and cross-priming are dependent on NK cells, so it would be useful to study the effects of CRT on these cells directly, and also to look for them in my *in vitro* DC cultures. Further studies on

the interaction of CRT with various cell types may also be useful in determining why there appears to be preferential CD8<sup>+</sup> T cell activation.

### **6.2.2 A separate danger signal *in vivo*?**

Another possibility is that the danger signal *in vivo* does not come from CRT, and that my *in vitro* observations of IL-2 production by OTI T cells in response to CRT + OVA are a result of some artefact. It is also possible that this weak response could be boosted *in vivo* in the presence of other cell types or stimuli. This is supported by my findings that CRT has no immunostimulatory effect on DCs *in vitro*. In this scenario, where could the danger signal come from? One possibility that has been suggested is endotoxin contamination, however, as described fully earlier in this thesis, this is not always likely where HSPs are engineered to be secreted *in vivo* or are demonstrated to contain very low levels of endotoxin. Rigorous controls are also usually used to rule out an effect of endotoxin. It is possible that there may be other contaminants in the preparations that have an effect *in vivo*, Nicchitta's group have demonstrated that even apparently "pure" gp96 preparations contain enzymologically significant levels of "bystander" proteins, which may play a role in induction of immune responses [146]. As shown in chapter 3, while the CRT used in this project has been extensively purified, there are still detectable levels of protein contaminants. This can be resolved by gel filtration of CRT although, as described earlier, this results in significant protein loss and endotoxin contamination.

### **6.2.3 CRT as an immune suppressor?**

At this point, it is worth considering a possible immunostimulatory role for CRT in the physiological context. Although CRT is released, along with other HSPs, by damaged or necrotic cells, it also plays a physiological role in the uptake of apoptotic cells – a situation in which induction of an immune response would be undesirable as it could lead to generation of autoimmunity. In light of this function of CRT, it may be supposed that CRT is more likely either to have no effect on the induction of immune responses, or even to be actively suppressive. This is supported by my observations of inhibition of upregulation of costimulatory markers by DCs in response to LPS or TNF $\alpha$ . HSPs, including CRT, hsp70 and hsp60, have all been demonstrated to be sources of Ag in various autoimmune diseases including systemic lupus erythematosus (SLE), rheumatoid arthritis (RA) and type I diabetes [147].

However, it has also been reported that hsp60 and hsp70 can in fact function in inducing responses to suppress these diseases. This is proposed to occur by the generation of hsp-specific regulatory T cells (Tregs), for example in juvenile idiopathic arthritis (JIA) patients, activation with human hsp60 or hsp60-derived peptides results in generation of CD4<sup>+</sup>25<sup>+</sup> T cells with high levels of surface CD25 expression and expression of Treg markers such as glucocorticoid-induced TNF-receptor-related protein (GITR), CTLA4 and CD30 as well as the transcription factor FOXP3. These cells were also found to be capable of suppressing immune responses *in vitro*. While no such effect has been looked for with CRT, this is an interesting aspect of HSP immunology, and further studies on the role of CRT in autoimmune diseases would provide valuable information on this potential role for CRT.

#### **6.2.4 Differential effects of autologous vs foreign HSPs**

Another interesting point to arise from studies on HSPs in autoimmunity and in inflammation is whether there are differences in the responses to autologous and foreign HSPs. As discussed in chapter 4, Paul Lehner's group have found that human hsp70 is less efficient than microbial hsp70 at inducing human CTL responses (Babak Javid, PhD thesis, University of Cambridge). This group also has preliminary data suggesting that there are differences in the signalling responses induced by autologous and foreign hsp70. Studies on the suppressive effects of hsp60 and hsp70 have shown that only epitopes from these HSPs that induce self-HSP-cross reactive T cells protect against disease, a further indication that there is a distinction between foreign and self HSPs [147]. Further investigations directly comparing the effects of host-derived and foreign CRT (and other HSPs) on DC activation and T cell priming both *in vitro* and *in vivo* would be extremely useful, as this is an area that has not been investigated in detail in the published literature. These differences do call into question the physiological relevance of any effect of CRT. Due to the abundance of HSPs, it is understandable that bacterial HSPs would become targets of the mammalian immune system during evolution. Thus, responses against mammalian HSPs such as hsp70 may be a result of immune cross-reactivity between bacterial and mammalian HSPs. However, unlike hsp70, CRT is not found in prokaryotes, but is found only in eukaryotes, including pathogens such as yeast, nematodes and helminths – immunity to all of which is less dependent on CTL. Thus it seems less

likely that CRT would become a target of the immune system, particularly for generation of CTL.

#### **6.2.5 CRT and Ag delivery**

Our studies on the effects of CRT on phagocytosis by the DC-like cell line DC2.4 have indicated that exogenous CRT has no effect on the phagocytic activity of these cells. Whereas stimulation with LPS resulted in an increase both in the percentage of cells taking up protein-coated latex beads and in the number of beads taken up per cell, CRT had no effect on either. At first glance, this may appear to contradict the published data on the role for CRT in uptake of apoptotic cells, however these studies relate to the role of CRT as a ligand or receptor for phagocytosis, rather than as an exogenous stimulus. We have not yet investigated this function of CRT, but future experiments to study the uptake of latex beads coated with CRT and with a combination of CRT and OVA are planned to study the effects of CRT on phagocytosis and Ag processing and presentation. A recent study by Wang et al. demonstrated that exogenous autologous hsp70 does enhance phagocytosis by macrophages in an almost identical system [148]. These authors observed that, while doses of  $<20\mu\text{g/ml}$  hsp70 enhanced phagocytosis, the peak effect occurred at  $40\mu\text{g/ml}$  and reached a plateau at  $100\mu\text{g/ml}$ . Our studies on phagocytosis were performed with only  $5\mu\text{g/ml}$  CRT, so it may be worth studying a wider range of concentrations, as we have done with other functional assays. However these data may simply reflect a difference in the immunostimulatory effects of hsp70 and CRT – interestingly, gp96 and hsp90 had a much lesser effect on phagocytosis than hsp70 in this study.

Preliminary experiments to determine the ability of CRT to chaperone Ag for T cell priming have indicated that it is possible to generate complexes of CRT with the OVA peptide SIINFEKL *in vitro*, and that such complexed peptide is processed and presented by DCs to T cells. However, as discussed in chapter 5, it is unclear whether delivery is enhanced compared to that of free peptide, and this is a question that we aim to resolve with future work to determine the kinetics of CRT binding to peptides and to attempt generation of CRT-OVA complexes.

My observations in chapter 5 that CRT binds specifically to SR-A on macrophages and to SR-A and CD91 on BMDCs and is subsequently internalised would suggest that bound Ags should be delivered more efficiently for processing and presentation than free Ag. Further investigations into the trafficking pathway followed by internalised CRT would help to clarify this issue, as the internal compartments accessed by CRT and bound Ag will influence the fate of these Ags. My data on T cell responses indicate that CRT promotes cross-presentation, and particular pathways must be followed in order for cross-presentation to occur, as described in chapter 1. Further investigation of the trafficking of CRT and associated Ag would also, therefore, be useful for the elucidation of the cross-presentation pathways in general, and particularly their utilisation by HSPs. As discussed in chapter 5, these studies could involve more detailed timecourse experiments utilising confocal microscopy and also more detailed counterstaining with markers for various intracellular compartments, such as DC-LAMP 1 and 2.

In conclusion, this study has confirmed previous reports of the *in vivo* immunostimulatory effects of CRT, and has also provided novel data on the mechanisms underlying these effects. This is a useful addition to the field of HSP immunology, and has also indicated several possible future areas for research in order to further elucidate the effects exerted by extracellular CRT on the immune system and their underlying mechanisms.

## References

1. Shortman, K. and Y.J. Liu, *Mouse and human dendritic cell subtypes*. Nat Rev Immunol, 2002. **2**(3): p. 151-61.
2. Banchereau, J. and R.M. Steinman, *Dendritic cells and the control of immunity*. Nature, 1998. **392**(6673): p. 245-52.
3. Banchereau, J., et al., *Immunobiology of dendritic cells*. Annu Rev Immunol, 2000. **18**: p. 767-811.
4. Heath, W.R., et al., *Cross-presentation, dendritic cell subsets, and the generation of immunity to cellular antigens*. Immunol Rev, 2004. **199**: p. 9-26.
5. Colonna, M., G. Trinchieri, and Y.J. Liu, *Plasmacytoid dendritic cells in immunity*. Nat Immunol, 2004. **5**(12): p. 1219-26.
6. Villadangos, J.A. and W.R. Heath, *Life cycle, migration and antigen presenting functions of spleen and lymph node dendritic cells: limitations of the Langerhans cells paradigm*. Semin Immunol, 2005. **17**(4): p. 262-72.
7. Guernonprez, P., et al., *Antigen presentation and T cell stimulation by dendritic cells*. Annu Rev Immunol, 2002. **20**: p. 621-67.
8. Desjardins, M., M. Houde, and E. Gagnon, *Phagocytosis: the convoluted way from nutrition to adaptive immunity*. Immunol Rev, 2005. **207**: p. 158-65.
9. Jutras, I. and M. Desjardins, *Phagocytosis: At the Crossroads of Innate and Adaptive Immunity*. Annu Rev Cell Dev Biol, 2005.
10. Villadangos, J.A., P. Schnorrer, and N.S. Wilson, *Control of MHC class II antigen presentation in dendritic cells: a balance between creative and destructive forces*. Immunol Rev, 2005. **207**: p. 191-205.
11. Ackerman, A.L. and P. Cresswell, *Cellular mechanisms governing cross-presentation of exogenous antigens*. Nat Immunol, 2004. **5**(7): p. 678-84.
12. Rock, K.L. and L. Shen, *Cross-presentation: underlying mechanisms and role in immune surveillance*. Immunol Rev, 2005. **207**: p. 166-83.
13. Pierre, P., *Dendritic cells, DRiPs, and DALIS in the control of antigen processing*. Immunol Rev, 2005. **207**: p. 184-90.
14. Cresswell, P., et al., *Mechanisms of MHC class I-restricted antigen processing and cross-presentation*. Immunol Rev, 2005. **207**: p. 145-57.



15. Bevan, M.J., *Cross-priming for a secondary cytotoxic response to minor H antigens with H-2 congenic cells which do not cross-react in the cytotoxic assay*. J Exp Med, 1976. **143**(5): p. 1283-8.
16. Faló, L.D., Jr., et al., *Targeting antigen into the phagocytic pathway in vivo induces protective tumour immunity*. Nat Med, 1995. **1**(7): p. 649-53.
17. Kovacsóvics-Bankowski, M., et al., *Efficient major histocompatibility complex class I presentation of exogenous antigen upon phagocytosis by macrophages*. Proc Natl Acad Sci U S A, 1993. **90**(11): p. 4942-6.
18. Li, M., et al., *Cell-associated ovalbumin is cross-presented much more efficiently than soluble ovalbumin in vivo*. J Immunol, 2001. **166**(10): p. 6099-103.
19. Garin, J., et al., *The phagosome proteome: insight into phagosome functions*. J Cell Biol, 2001. **152**(1): p. 165-80.
20. Medzhitov, R., *Toll-like receptors and innate immunity*. Nat Rev Immunol, 2001. **1**(2): p. 135-45.
21. Akira, S. and K. Takeda, *Toll-like receptor signalling*. Nat Rev Immunol, 2004. **4**(7): p. 499-511.
22. Fujii, S., et al., *The linkage of innate to adaptive immunity via maturing dendritic cells in vivo requires CD40 ligation in addition to antigen presentation and CD80/86 costimulation*. J Exp Med, 2004. **199**(12): p. 1607-18.
23. Munz, C., R.M. Steinman, and S. Fujii, *Dendritic cell maturation by innate lymphocytes: coordinated stimulation of innate and adaptive immunity*. J Exp Med, 2005. **202**(2): p. 203-7.
24. Ritossa, F., *A new puffing pattern induced by temperature shock and DNP in Drosophila*. experientia, 1962. **18**: p. 571-573.
25. Ritossa, F., *Discovery of the heat shock response*. Cell Stress Chaperones, 1996. **1**(2): p. 97-8.
26. Lindquist, S., *The heat-shock response*. Annu Rev Biochem, 1986. **55**: p. 1151-91.
27. Srivastava, P., *Roles of heat-shock proteins in innate and adaptive immunity*. Nat Rev Immunol, 2002. **2**(3): p. 185-94.
28. Lindquist, S. and E.A. Craig, *The heat-shock proteins*. Annu Rev Genet, 1988. **22**: p. 631-77.

29. Gething, M.J. and J. Sambrook, *Protein folding in the cell*. Nature, 1992. **355**(6355): p. 33-45.
30. Parsell, D.A. and S. Lindquist, *The function of heat-shock proteins in stress tolerance: degradation and reactivation of damaged proteins*. Annu Rev Genet, 1993. **27**: p. 437-96.
31. Haas, I.G., *BiP--a heat shock protein involved in immunoglobulin chain assembly*. Curr Top Microbiol Immunol, 1991. **167**: p. 71-82.
32. Rutherford, S.L. and S. Lindquist, *Hsp90 as a capacitor for morphological evolution*. Nature, 1998. **396**(6709): p. 336-42.
33. Srivastava, P.K. and M.R. Das, *The serologically unique cell surface antigen of Zajdela ascitic hepatoma is also its tumor-associated transplantation antigen*. Int J Cancer, 1984. **33**(3): p. 417-22.
34. Srivastava, P.K., A.B. DeLeo, and L.J. Old, *Tumor rejection antigens of chemically induced sarcomas of inbred mice*. Proc Natl Acad Sci U S A, 1986. **83**(10): p. 3407-11.
35. Ullrich, S.J., et al., *A mouse tumor-specific transplantation antigen is a heat shock-related protein*. Proc Natl Acad Sci U S A, 1986. **83**(10): p. 3121-5.
36. Udono, H. and P.K. Srivastava, *Heat shock protein 70-associated peptides elicit specific cancer immunity*. J Exp Med, 1993. **178**(4): p. 1391-6.
37. Tamura, Y., et al., *Immunotherapy of tumors with autologous tumor-derived heat shock protein preparations*. Science, 1997. **278**(5335): p. 117-20.
38. Basu, S. and P.K. Srivastava, *Calreticulin, a peptide-binding chaperone of the endoplasmic reticulum, elicits tumor- and peptide-specific immunity*. J Exp Med, 1999. **189**(5): p. 797-802.
39. Wang, X.Y., et al., *Characterization of heat shock protein 110 and glucose-regulated protein 170 as cancer vaccines and the effect of fever-range hyperthermia on vaccine activity*. J Immunol, 2001. **166**(1): p. 490-7.
40. Srivastava, P.K. and R.J. Amato, *Heat shock proteins: the 'Swiss Army Knife' vaccines against cancers and infectious agents*. Vaccine, 2001. **19**(17-19): p. 2590-7.
41. Srivastava, P., *Interaction of heat shock proteins with peptides and antigen presenting cells: chaperoning of the innate and adaptive immune responses*. Annu Rev Immunol, 2002. **20**: p. 395-425.

42. Zhu, X., et al., *Structural analysis of substrate binding by the molecular chaperone DnaK*. Science, 1996. **272**(5268): p. 1606-14.
43. Prodromou, C., et al., *Identification and structural characterization of the ATP/ADP-binding site in the Hsp90 molecular chaperone*. Cell, 1997. **90**(1): p. 65-75.
44. Linderoth, N.A., A. Popowicz, and S. Sastry, *Identification of the peptide-binding site in the heat shock chaperone/tumor rejection antigen gp96 (Grp94)*. J Biol Chem, 2000. **275**(8): p. 5472-7.
45. Arnold, D., et al., *Cross-priming of minor histocompatibility antigen-specific cytotoxic T cells upon immunization with the heat shock protein gp96*. J Exp Med, 1995. **182**(3): p. 885-9.
46. Arnold, D., et al., *Influences of transporter associated with antigen processing (TAP) on the repertoire of peptides associated with the endoplasmic reticulum-resident stress protein gp96*. J Exp Med, 1997. **186**(3): p. 461-6.
47. Blachere, N.E., et al., *Heat shock protein-peptide complexes, reconstituted in vitro, elicit peptide-specific cytotoxic T lymphocyte response and tumor immunity*. J Exp Med, 1997. **186**(8): p. 1315-22.
48. Binder, R.J., N.E. Blachere, and P.K. Srivastava, *Heat shock protein-chaperoned peptides but not free peptides introduced into the cytosol are presented efficiently by major histocompatibility complex I molecules*. J Biol Chem, 2001. **276**(20): p. 17163-71.
49. Binder, R.J. and P.K. Srivastava, *Peptides chaperoned by heat-shock proteins are a necessary and sufficient source of antigen in the cross-priming of CD8+ T cells*. Nat Immunol, 2005. **6**(6): p. 593-9.
50. Doody, A.D., et al., *Glycoprotein 96 can chaperone both MHC class I- and class II-restricted epitopes for in vivo presentation, but selectively primes CD8+ T cell effector function*. J Immunol, 2004. **172**(10): p. 6087-92.
51. Palliser, D., et al., *Multiple intracellular routes in the cross-presentation of a soluble protein by murine dendritic cells*. J Immunol, 2005. **174**(4): p. 1879-87.
52. Asea, A., et al., *HSP70 stimulates cytokine production through a CD14-dependant pathway, demonstrating its dual role as a chaperone and cytokine*. Nat Med, 2000. **6**(4): p. 435-42.

53. Basu, S., et al., *Necrotic but not apoptotic cell death releases heat shock proteins, which deliver a partial maturation signal to dendritic cells and activate the NF-kappa B pathway*. Int Immunol, 2000. **12**(11): p. 1539-46.
54. Panjwani, N.N., L. Popova, and P.K. Srivastava, *Heat shock proteins gp96 and hsp70 activate the release of nitric oxide by APCs*. J Immunol, 2002. **168**(6): p. 2997-3003.
55. More, S.H., M. Breloer, and A. von Bonin, *Eukaryotic heat shock proteins as molecular links in innate and adaptive immune responses: Hsp60-mediated activation of cytotoxic T cells*. Int Immunol, 2001. **13**(9): p. 1121-7.
56. Lehner, T., et al., *Heat shock proteins generate beta-chemokines which function as innate adjuvants enhancing adaptive immunity*. Eur J Immunol, 2000. **30**(2): p. 594-603.
57. Zheng, H., et al., *Cell surface targeting of heat shock protein gp96 induces dendritic cell maturation and antitumor immunity*. J Immunol, 2001. **167**(12): p. 6731-5.
58. Singh-Jasuja, H., et al., *The heat shock protein gp96 induces maturation of dendritic cells and down-regulation of its receptor*. Eur J Immunol, 2000. **30**(8): p. 2211-5.
59. Somersan, S., et al., *Primary tumor tissue lysates are enriched in heat shock proteins and induce the maturation of human dendritic cells*. J Immunol, 2001. **167**(9): p. 4844-52.
60. Binder, R.J., et al., *Cutting edge: heat shock protein gp96 induces maturation and migration of CD11c<sup>+</sup> cells in vivo*. J Immunol, 2000. **165**(11): p. 6029-35.
61. Casey, D.G., et al., *Heat shock protein derived from a non-autologous tumour can be used as an anti-tumour vaccine*. Immunology, 2003. **110**(1): p. 105-11.
62. Zeng, Y., et al., *Induction of BCR-ABL-specific immunity following vaccination with chaperone-rich cell lysates derived from BCR-ABL<sup>+</sup> tumor cells*. Blood, 2005. **105**(5): p. 2016-22.
63. Feng, H., et al., *Stressed apoptotic tumor cells stimulate dendritic cells and induce specific cytotoxic T cells*. Blood, 2002. **100**(12): p. 4108-15.
64. Feng, H., et al., *Exogenous stress proteins enhance the immunogenicity of apoptotic tumor cells and stimulate antitumor immunity*. Blood, 2003. **101**(1): p. 245-52.

65. MacAry, P.A., et al., *HSP70 peptide binding mutants separate antigen delivery from dendritic cell stimulation*. Immunity, 2004. **20**(1): p. 95-106.
66. Tsan, M.F. and B. Gao, *Cytokine function of heat shock proteins*. Am J Physiol Cell Physiol, 2004. **286**(4): p. C739-44.
67. Wallin, R.P., et al., *Heat-shock proteins as activators of the innate immune system*. Trends Immunol, 2002. **23**(3): p. 130-5.
68. Binder, R.J., R. Vatner, and P. Srivastava, *The heat-shock protein receptors: some answers and more questions*. Tissue Antigens, 2004. **64**(4): p. 442-51.
69. Arnold-Schild, D., et al., *Cutting edge: receptor-mediated endocytosis of heat shock proteins by professional antigen-presenting cells*. J Immunol, 1999. **162**(7): p. 3757-60.
70. Binder, R.J., D.K. Han, and P.K. Srivastava, *CD91: a receptor for heat shock protein gp96*. Nat Immunol, 2000. **1**(2): p. 151-5.
71. Basu, S., et al., *CD91 is a common receptor for heat shock proteins gp96, hsp90, hsp70, and calreticulin*. Immunity, 2001. **14**(3): p. 303-13.
72. Berwin, B., et al., *Cutting edge: CD91-independent cross-presentation of GRP94(gp96)-associated peptides*. J Immunol, 2002. **168**(9): p. 4282-6.
73. Binder, R.J. and P.K. Srivastava, *Essential role of CD91 in re-presentation of gp96-chaperoned peptides*. Proc Natl Acad Sci U S A, 2004. **101**(16): p. 6128-33.
74. Tobian, A.A., et al., *Bacterial heat shock proteins promote CD91-dependent class I MHC cross-presentation of chaperoned peptide to CD8+ T cells by cytosolic mechanisms in dendritic cells versus vacuolar mechanisms in macrophages*. J Immunol, 2004. **172**(9): p. 5277-86.
75. Walters, J.J. and B. Berwin, *Differential CD91 Dependence for Calreticulin and Pseudomonas Exotoxin-A Endocytosis*. Traffic, 2005. **6**(12): p. 1173-82.
76. Wang, Y., et al., *CD40 is a cellular receptor mediating mycobacterial heat shock protein 70 stimulation of CC-chemokines*. Immunity, 2001. **15**(6): p. 971-83.
77. Becker, T., F.U. Hartl, and F. Wieland, *CD40, an extracellular receptor for binding and uptake of Hsp70-peptide complexes*. J Cell Biol, 2002. **158**(7): p. 1277-85.
78. Delneste, Y., et al., *Involvement of LOX-1 in dendritic cell-mediated antigen cross-presentation*. Immunity, 2002. **17**(3): p. 353-62.

79. Berwin, B., et al., *Scavenger receptor-A mediates gp96/GRP94 and calreticulin internalization by antigen-presenting cells*. *Embo J*, 2003. **22**(22): p. 6127-36.
80. Berwin, B., et al., *SREC-I, a Type F Scavenger Receptor, Is an Endocytic Receptor for Calreticulin*. *J. Biol. Chem.*, 2004. **279**(49): p. 51250-51257.
81. Asea, A., et al., *HSP70 peptide bearing and peptide-negative preparations act as chaperokines*. *Cell Stress Chaperones*, 2000. **5**(5): p. 425-31.
82. Asea, A., et al., *Novel signal transduction pathway utilized by extracellular HSP70: role of toll-like receptor (TLR) 2 and TLR4*. *J Biol Chem*, 2002. **277**(17): p. 15028-34.
83. Vabulas, R.M., et al., *HSP70 as endogenous stimulus of the Toll/interleukin-1 receptor signal pathway*. *J Biol Chem*, 2002. **277**(17): p. 15107-12.
84. Vabulas, R.M., et al., *The endoplasmic reticulum-resident heat shock protein Gp96 activates dendritic cells via the Toll-like receptor 2/4 pathway*. *J Biol Chem*, 2002. **277**(23): p. 20847-53.
85. Dybdahl, B., et al., *Inflammatory response after open heart surgery: release of heat-shock protein 70 and signaling through toll-like receptor-4*. *Circulation*, 2002. **105**(6): p. 685-90.
86. Vabulas, R.M., et al., *Endocytosed HSP60s use toll-like receptor 2 (TLR2) and TLR4 to activate the toll/interleukin-1 receptor signaling pathway in innate immune cells*. *J Biol Chem*, 2001. **276**(33): p. 31332-9.
87. Ohashi, K., et al., *Cutting edge: heat shock protein 60 is a putative endogenous ligand of the toll-like receptor-4 complex*. *J Immunol*, 2000. **164**(2): p. 558-61.
88. Stebbing, J., et al., *Disease-associated dendritic cells respond to disease-specific antigens through the common heat shock protein receptor*. *Blood*, 2003. **102**(5): p. 1806-14.
89. Panjwani, N.N., Popova, L., Febbraio, M. and Srivastava, P.K., *The CD36 scavenger receptor as a receptor for gp96*. *Cell Stress Chaperones*, 2000. **5**(5): p. 391.
90. Chen, W., et al., *Human 60-kDa heat-shock protein: a danger signal to the innate immune system*. *J Immunol*, 1999. **162**(6): p. 3212-9.
91. Gao, B. and M.F. Tsan, *Endotoxin contamination in recombinant human heat shock protein 70 (Hsp70) preparation is responsible for the induction of*

- tumor necrosis factor alpha release by murine macrophages.* J Biol Chem, 2003. **278**(1): p. 174-9.
92. Bausinger, H., et al., *Endotoxin-free heat-shock protein 70 fails to induce APC activation.* Eur J Immunol, 2002. **32**(12): p. 3708-13.
  93. Reed, R.C., et al., *GRP94/gp96 elicits ERK activation in murine macrophages. A role for endotoxin contamination in NF-kappa B activation and nitric oxide production.* J Biol Chem, 2003. **278**(34): p. 31853-60.
  94. Suto, R. and P.K. Srivastava, *A mechanism for the specific immunogenicity of heat shock protein-chaperoned peptides.* Science, 1995. **269**(5230): p. 1585-8.
  95. Castellino, F., et al., *Receptor-mediated uptake of antigen/heat shock protein complexes results in major histocompatibility complex class I antigen presentation via two distinct processing pathways.* J Exp Med, 2000. **191**(11): p. 1957-64.
  96. Michalak, M., et al., *Calreticulin: one protein, one gene, many functions.* Biochem J, 1999. **344 Pt 2**: p. 281-92.
  97. Coppelino, M.G. and S. Dedhar, *Calreticulin.* Int J Biochem Cell Biol, 1998. **30**(5): p. 553-8.
  98. Gelebart, P., M. Opas, and M. Michalak, *Calreticulin, a Ca<sup>2+</sup>-binding chaperone of the endoplasmic reticulum.* Int J Biochem Cell Biol, 2005. **37**(2): p. 260-6.
  99. Sadasivan, B., et al., *Roles for calreticulin and a novel glycoprotein, tapasin, in the interaction of MHC class I molecules with TAP.* Immunity, 1996. **5**(2): p. 103-14.
  100. Guo, L., et al., *Identification of an N-domain histidine essential for chaperone function in calreticulin.* J Biol Chem, 2003. **278**(50): p. 50645-53.
  101. Johnson, S., et al., *The ins and outs of calreticulin: from the ER lumen to the extracellular space.* Trends Cell Biol, 2001. **11**(3): p. 122-9.
  102. Groenendyk, J. and M. Michalak, *Endoplasmic reticulum quality control and apoptosis.* Acta Biochim Pol, 2005. **52**(2): p. 381-95.
  103. Spee, P. and J. Neefjes, *TAP-translocated peptides specifically bind proteins in the endoplasmic reticulum, including gp96, protein disulfide isomerase and calreticulin.* Eur J Immunol, 1997. **27**(9): p. 2441-9.



104. Gao, B., et al., *Assembly and antigen-presenting function of MHC class I molecules in cells lacking the ER chaperone calreticulin*. Immunity, 2002. **16**(1): p. 99-109.
105. Wearsch, P.A., et al., *Major histocompatibility complex class I molecules expressed with monoglucosylated N-linked glycans bind calreticulin independently of their assembly status*. J Biol Chem, 2004. **279**(24): p. 25112-21.
106. Dedhar, S., *Novel functions for calreticulin: interaction with integrins and modulation of gene expression?* Trends Biochem Sci, 1994. **19**(7): p. 269-71.
107. Coppolino, M., et al., *Inducible interaction of integrin alpha 2 beta 1 with calreticulin. Dependence on the activation state of the integrin*. J Biol Chem, 1995. **270**(39): p. 23132-8.
108. Coppolino, M.G., et al., *Calreticulin is essential for integrin-mediated calcium signalling and cell adhesion*. Nature, 1997. **386**(6627): p. 843-7.
109. Fadel, M.P., et al., *Calreticulin affects focal contact-dependent but not close contact-dependent cell-substratum adhesion*. J Biol Chem, 1999. **274**(21): p. 15085-94.
110. Opas, M., et al., *Calreticulin modulates cell adhesiveness via regulation of vinculin expression*. J Cell Biol, 1996. **135**(6 Pt 2): p. 1913-23.
111. Goicoechea, S., et al., *Thrombospondin mediates focal adhesion disassembly through interactions with cell surface calreticulin*. J Biol Chem, 2000. **275**(46): p. 36358-68.
112. Goicoechea, S., et al., *The anti-adhesive activity of thrombospondin is mediated by the N-terminal domain of cell surface calreticulin*. J Biol Chem, 2002. **277**(40): p. 37219-28.
113. Orr, A.W., et al., *Low density lipoprotein receptor-related protein is a calreticulin coreceptor that signals focal adhesion disassembly*. J Cell Biol, 2003. **161**(6): p. 1179-89.
114. Orr, A.W., et al., *Thrombospondin signaling through the calreticulin/LDL receptor-related protein co-complex stimulates random and directed cell migration*. J Cell Sci, 2003. **116**(Pt 14): p. 2917-27.
115. Li, S.S., A. Forslow, and K.G. Sundqvist, *Autocrine regulation of T cell motility by calreticulin-thrombospondin-1 interaction*. J Immunol, 2005. **174**(2): p. 654-61.

116. Pike, S.E., et al., *Vasostatin, a calreticulin fragment, inhibits angiogenesis and suppresses tumor growth*. J Exp Med, 1998. **188**(12): p. 2349-56.
117. Cheng, W.F., et al., *Tumor-specific immunity and antiangiogenesis generated by a DNA vaccine encoding calreticulin linked to a tumor antigen*. J Clin Invest, 2001. **108**(5): p. 669-78.
118. Pike, S.E., et al., *Calreticulin and calreticulin fragments are endothelial cell inhibitors that suppress tumor growth*. Blood, 1999. **94**(7): p. 2461-8.
119. Yao, L., et al., *Anti-tumor activities of the angiogenesis inhibitors interferon-inducible protein-10 and the calreticulin fragment vasostatin*. Cancer Immunol Immunother, 2002. **51**(7): p. 358-66.
120. Yao, L., et al., *Effective targeting of tumor vasculature by the angiogenesis inhibitors vasostatin and interleukin-12*. Blood, 2000. **96**(5): p. 1900-5.
121. Cheng, W.F., et al., *Characterization of DNA vaccines encoding the domains of calreticulin for their ability to elicit tumor-specific immunity and antiangiogenesis*. Vaccine, 2005. **23**(29): p. 3864-74.
122. Molina, M.C., et al., *An in vivo role for Trypanosoma cruzi calreticulin in antiangiogenesis*. Mol Biochem Parasitol, 2005. **140**(2): p. 133-40.
123. Sim, R.B., et al., *Interaction of C1q and the collectins with the potential receptors calreticulin (cC1qR/collectin receptor) and megalin*. Immunobiology, 1998. **199**(2): p. 208-24.
124. Stuart, G.R., et al., *The C1q and collectin binding site within C1q receptor (cell surface calreticulin)*. Immunopharmacology, 1997. **38**(1-2): p. 73-80.
125. Stuart, G.R., et al., *Localisation of the C1q binding site within C1q receptor/calreticulin*. FEBS Lett, 1996. **397**(2-3): p. 245-9.
126. Ogden, C.A., et al., *C1q and mannose binding lectin engagement of cell surface calreticulin and CD91 initiates macropinocytosis and uptake of apoptotic cells*. J Exp Med, 2001. **194**(6): p. 781-95.
127. Gardai, S.J., et al., *Cell-surface calreticulin initiates clearance of viable or apoptotic cells through trans-activation of LRP on the phagocyte*. Cell, 2005. **123**(2): p. 321-34.
128. Chen, D., et al., *Surface calreticulin mediates muramyl dipeptide-induced apoptosis in RK13 cells*. J Biol Chem, 2005. **280**(23): p. 22425-36.
129. Asgari, S. and O. Schmidt, *Is cell surface calreticulin involved in phagocytosis by insect hemocytes?* J Insect Physiol, 2003. **49**(6): p. 545-50.

130. Fajardo, M., et al., *Calnexin, calreticulin and cytoskeleton-associated proteins modulate uptake and growth of Legionella pneumophila in Dictyostelium discoideum*. Microbiology, 2004. **150**(Pt 9): p. 2825-35.
131. Muller-Taubenberger, A., et al., *Calreticulin and calnexin in the endoplasmic reticulum are important for phagocytosis*. Embo J, 2001. **20**(23): p. 6772-82.
132. Afshar, N., B.E. Black, and B.M. Paschal, *Retrotranslocation of the chaperone calreticulin from the endoplasmic reticulum lumen to the cytosol*. Mol Cell Biol, 2005. **25**(20): p. 8844-53.
133. Corbett, E.F., et al., *The conformation of calreticulin is influenced by the endoplasmic reticulum luminal environment*. J Biol Chem, 2000. **275**(35): p. 27177-85.
134. Nair, S., et al., *Calreticulin displays in vivo peptide-binding activity and can elicit CTL responses against bound peptides*. J Immunol, 1999. **162**(11): p. 6426-32.
135. Golgher, D., et al., *An immunodominant MHC class II-restricted tumor antigen is conformation dependent and binds to the endoplasmic reticulum chaperone, calreticulin*. J Immunol, 2001. **167**(1): p. 147-55.
136. Lutz, M.B., et al., *An advanced culture method for generating large quantities of highly pure dendritic cells from mouse bone marrow*. J Immunol Methods, 1999. **223**(1): p. 77-92.
137. Paquet, M.E., M.R. Leach, and D.B. Williams, *In vitro and in vivo assays to assess the functions of calnexin and calreticulin in ER protein folding and quality control*. Methods, 2005. **35**(4): p. 338-47.
138. Chandawarkar, R.Y., M.S. Wagh, and P.K. Srivastava, *The dual nature of specific immunological activity of tumor-derived gp96 preparations*. J Exp Med, 1999. **189**(9): p. 1437-42.
139. Chandawarkar, R.Y., et al., *Immune modulation with high-dose heat-shock protein gp96: therapy of murine autoimmune diabetes and encephalomyelitis*. Int Immunol, 2004. **16**(4): p. 615-24.
140. Hojrup, P., P. Roepstorff, and G. Houen, *Human placental calreticulin characterization of domain structure and post-translational modifications*. Eur J Biochem, 2001. **268**(9): p. 2558-65.
141. West, M.A., et al., *Enhanced Dendritic Cell Antigen Capture via Toll-Like Receptor-Induced Actin Remodeling*. Science, 2004. **305**(5687): p. 1153-1157.

142. Li, Z., *In vitro* reconstitution of heat shock protein-peptide complexes for generating peptide-specific vaccines against cancers and infectious diseases. *Methods*, 2004. **32**(1): p. 25-8.
143. Saito, Y., et al., *Calreticulin functions in vitro as a molecular chaperone for both glycosylated and non-glycosylated proteins*. *Embo J*, 1999. **18**(23): p. 6718-29.
144. Jorgensen, C.S., et al., *Polypeptide binding properties of the chaperone calreticulin*. *Eur J Biochem*, 2000. **267**(10): p. 2945-54.
145. Massa, C., C. Melani, and M.P. Colombo, *Chaperon and adjuvant activity of hsp70: different natural killer requirement for cross-priming of chaperoned and bystander antigens*. *Cancer Res*, 2005. **65**(17): p. 7942-9.
146. Baker-LePain, J.C., R.C. Reed, and C.V. Nicchitta, *ISO: a critical evaluation of the role of peptides in heat shock/chaperone protein-mediated tumor rejection*. *Curr Opin Immunol*, 2003. **15**(1): p. 89-94.
147. van Eden, W., R. van der Zee, and B. Prakken, *Heat-shock proteins induce T-cell regulation of chronic inflammation*. *Nat Rev Immunol*, 2005. **5**(4): p. 318-30.
148. Wang, R., et al., *Exogenous Heat Shock Protein-70 binds macrophage-lipid raft-microdomain and stimulates phagocytosis, processing and MHC-II presentation of antigens*. *Blood*, 2005.